Effect of Platelet-Rich Fibrin on Composite Graft of Autogenous Bone and Deproteinized Bovine Bone in New Bone Formation in Rabbit Calvarial Defect

Kingkaew Phurisat

A Thesis Submitted in Partial Fulfillment of the Requirements for the Degree of

Master of Science in Oral and Maxillofacial Surgery

Prince of Songkla University

2008

ชื่อวิทยานิพนธ์	ผลของเพลตเลท-ริช-ไฟบรินต่อการสร้างกระดูกใหม่ในกะโหลกศีรษะกระต่ายเมื่อใช้ร่วมกับกระดูกอาตมันและกระดูกวัวสังเคราะห์
ผู้เขียน	นางสาวกิ่งแก้ว ภูริสัตย์
สาขาวิชา	ศัลยศาสตร์ช่องปากและแม็กซิลโลเฟเชียล
ปีการศึกษา	2551

บทคัดย่อ

เพลตเลท-ริช-ไฟบรินเป็นแหล่งของสารเหนี่ยวนำการสร้างกระดูกซึ่งผลิตจากตัวผู้-ป่วยเอง ได้แก่ PDGF, TGF-β และ IGF ซึ่งมีผลส่งเสริมการสร้างกระดูกได้ อย่างไรก็ตามปัจจุบันยังไม่มีผลการศึกษายืนยันเกี่ยวกับการใช้เพลตเลท-ริช-ไฟบรินร่วมกับกระดูกอาตมัน กระดูกปลูกข้ามคน และกระดูกปลูกจากสัตว์ในงานศัลยศาสตร์ช่องปากใบหน้าและขากรรไกร

วัตถุประสงค์: เพื่อศึกษาผลการสร้างกระดูกของเพลตเลท-ริช-ไฟบรินในรอยวิการกะโหลกศีรษะของกระต่ายโดยเปรียบเทียบการสร้างกระดูกใหม่ของกระดูกอาตมัน กระดูกวัวสังเคราะห์ และ กระดูกปลูกผสมระหว่างกระดูกอาตมันกับกระดูกวัวสังเคราะห์

วิธีการ: ทำการทดลองในกระต่ายพันธุ์นิวซีแลนด์ไวท์จำนวน 20 ตัว แต่ละตัวทำรอยวิการบนกระดูกกะโหลกศีรษะเป็นรูปสี่เหลี่ยมจัตุรัสจำนวน 2 ตำแหน่งแต่ละตำแหน่งมีขนาด 10x10มม. แบ่งกระต่าย 10 ตัวเป็นกลุ่มควบคุมซึ่งเปรียบเทียบรอยวิการว่างเปล่า กระดูกอาตมัน กระดูกปลูกผสมระหว่างกระดูกอาตมันกับกระดูกวัวสังเคราะห์ (อัตราส่วน 1:1) และกระดูกวัวสังเคราห์ะเพียงอย่างเดียว กระต่ายที่เหลือ 10 ตัวในกลุ่มทดลองได้แก่ เพลตเลท-ริช-ไฟบริน กระดูกอาตมันผสมกับเพลตเลท-ริช-ไฟบริน กระดูกปลูกผสมระหว่างกระดูกอาตมันกับกระดูกวัวสังเคราะห์ (อัตราส่วน 1:1) และเพลตเลท-ริช-ไฟบริน กระดูกวัวสังเคราะห์ผสมกับเพลตเลท-ริช-ไฟบริน จากนั้นทำการฆ่าสัตว์ทดลองที่ 8 สัปดาห์หลังการผ่าตัดเพื่อนำชิ้นกระดูกมาศึกษาผลการสร้างกระดูกใหม่ด้วยวิธีทางจุลพยาธิวิทยาและทางภาพถ่ายรังสี

ผลการทดลอง: จากการตรวจทางภาพถ่ายรังสีของตัวอย่างชิ้นกระดูกพบว่า ค่าความทึบแสงกลุ่มรอยวิการว่างเปล่ามีค่าน้อยที่สุด (0.114±0.062) โดยมีความแตกต่างกับทุกกลุ่มอย่างมีนัยสำคัญ โดยแต่ละกลุ่มมีค่าความทึบแสงดังนี้ กลุ่มกระดูกอาตมัน (0.356±0.027) กลุ่มกระดูกปลูกผสมระหว่างกระดูกอาตมันกับกระดูกวัวสังเคราะห์ (อัตราส่วน 1:1) (0.906±0.046) กลุ่มกระดูกวัวสังเคราห์ะเพียงอย่างเดียว (1.066±0.052) กลุ่มเพลตเลท-ริช-ไฟบริน (0.294±0.062) กลุ่มกระดูกอาตมันผสมกับเพลตเลท-

ริช-ไฟบริน (0.596±0.189) กระดูกปลูกผสมระหว่างกระดูกอาตมันกับกระดูกวัวสังเคราะห์(อัตราส่วน 1:1)และเพลตเลท-ริช-ไฟบริน(0.810±0.154) กระดูกวัวสังเคราะห์ผสมกับเพลตเลท-ริช-ไฟบริน (1.178±0.167) จากการตรวจด้วยวิธีทางจุลพยาธิวิทยาพบว่ากลุ่มกระดูกอาตมันผสมกับเพลตเลท-ริช-ไฟบรินมีปริมาณการสร้างกระดูกใหม่มากที่สุด (38.031± 4.231) ซึ่งมีความแตกต่างอย่างมีนัยสำคัญกับกลุ่มรอยวิการว่างเปล่า (7.155±5.860) และมีค่ามากกว่ากลุ่มกระดูกอาตมัน (30.223±16.722) กลุ่มกระดูกปลูกผสมระหว่างกระดูกอาตมันกับกระดูกวัวสังเคราะห์ (อัตราส่วน 1:1) และเพลตเลท-ริช-ไฟบริน (22.633±3.605) กลุ่มกระดูกปลูกผสมระหว่างกระดูกอาตมันกับกระดูกวัวสังเคราะห์ (อัตราส่วน 1:1) (20.929±6.169) กลุ่มเพลตเลท-ริช-ไฟบริน (18.807±9.272) กลุ่มกระดูกวัวสังเคราะห์ผสมกับเพลตเลท-ริช-ไฟบริน (13.067±3.643) กระดูกวัวสังเคราะห์เพียงอย่างเดียว (14.441±2.741)

สรุป: การใช้เพลตเลท-ริช-ไฟบรินส่งเสริมการสร้างกระดูกใหม่โดยเฉพาะเมื่อใช้ร่วมกับกระดูกอาตมัน แต่ไม่ส่งเสริมการสร้างกระดูกใหม่เมื่อใช้ร่วมกับกระดูกวัวสังเคราะห์

Thesis Title	Effect of Platelet-Rich Fibrin on Composite Graft of Autogenous Bone and Deproteinized Bovine Bone in New Bone Formation in Rabbit Calvarial Defect
Author	Miss Kingkaew Phurisat
Major Program	Oral and Maxillofacial Surgery
Academic Year	2008

Abstract

Platelet-rich fibrin (PRF), an autologous source of growth factors, were used as an autologous source of PDGF, TGF-β and IGF. Therefore it may be beneficial for enhance bone regeneration. However there is no clear evidence to support the clinical use of PRF, when added to grafting material such as autogenous, allograft and xenografts materials in oral and maxillofacial region.

Objective: This study aimed to investigate the effect of platelet-rich fibrin on autogenous bone chip, deproteinized bovine bone and the composite of deproteinized bovine bone and autogenous bone chips in new bone formation in rabbit calvarial defects.

Materials and methods: Two bicortical skull defects were prepared in 20 New Zealand white rabbits. Ten rabbits were used as controls: filled with autogenous bone chips, defect was left empty for the critical size defect (CSD), Composite DBB and autogenous bone chips (proportion 1:1) and DBB alone. The other 10 rabbits were used as test groups; filled with PRF alone, autogenous bone chips and PRF, DBB and PRF, Composite DBB and autogenous bone chips (proportion 1:1) and PRF. The animals were sacrificed at 8 weeks. New bone formation was assessed by radiographic densitometry and histomorphometric analysis.

Results: Mean OD of the CSD was the lowest (0.114±0.062). There was a statistically significant difference between CSD and all other groups; autogenous bone chip (0.356±0.027), the composite DBB+autogenous bone chips proportion 1:1 (0.906±0.046), DBB alone (1.066±0.052), CSD+PRF (0.294±0.062), autogenous bone chips+PRF (0.596±0.189), the composite DBB+autogenous bone chips proportion 1:1+PRF (0.810±0.154), DBB+PRF (1.178±0.167). The histomorphometric analysis

demonstrated that the percentage new bone area of autogenous bone chips+PRF was the highest (38.031± 4.231) and significantly different from the CSD (7.155±5.860) and higher than the autogenous bone chips (30.223±16.722), the composite DBB+autogenous bone chips+PRF (22.633±3.605), the composite DBB+autogenous bone chips (20.929±6.169), CSD+PRF (18.807±9.272), DBB alone (14.441±2.741) and DBB+PRF (13.067±3.643) groups.

Conclusions: The addition of PRF enhances bone formation in the critical size defect of the rabbit's calvarial defect particularly with autogenous bone chips. There is no improvement when added PRF to DBB.

Acknowledgement

This thesis is the end of my long journey in obtaining my degree in Msc. in oral and maxillofacial surgery. In the first place I would like to express my deep and sincere gratitude to my supervisor, Associate Professor Prisana Pripatnanont, Head of the Department of Oral and Maxillofacial Surgery, Faculty of Dentistry, Prince of Songkla University. Her wide knowledge and her logical way of thinking have been of great value for me. Her understanding, encouraging and personal guidance have provided a good basis for the present thesis.

I am deeply grateful to my supervisors, Associate Professor Thongchai Nuntanaranont, Associate dean for Research and International relations, Faculty of Dentistry and Assistant Professor Surapong Vongvacharanont, Associate dean for dental hospital affairs, Faculty of Dentistry, Prince of Songkla University, for their teaching, supervision and important support throughout this work.

Next, thanks to Mr.Jakchai Jantaramano and Mr.Ruj Rojasvasathian for their technical assistance. I also would like to thank the staff of the oral surgery clinic, operating theater, department of stomatology of Faculty of Dentistry for their help and assistance during my time of study.

Finally, I wish to express my love and gratitude to all my friends. I would particularly like to thank my parents for their years of endless support and constant inspiration in my life.

Kingkaew Phurisat

Contents

List of Tables

List of Figures

List of Figures (continued)

List of Figures (continued)

List of Figures (continued)

List of Figures (continued)

List of Figures (continued)

List of Figures (continued)

List of Figures (continued)

List of Figures (continued)

List of Figures (continued)

List of Figures (continued)

List of Figures (continued)

List of Figures (continued)

List of Abbreviations and Symbols

α_2M	= Alpha2-macroglobulin
µm	= Micrometer
ºC	= Degree celcius
ANOVA	= One-way analysis of variance
bFGF	= Basic fibroblast growth factor
BMP	= Bone Morphogenic protein
cm	= Centimeter
CSD	= Critical size defect
cu.mm.	= Cubic millimeter
DBB	= Deproteinized bovine bone
EGF	= Epithelial Growth Factor
FDBA	= Freeze-dried bone allograft
g	= Gravitation force
g.	= Gram
HA	= Hydroxyapatite
HCL	= Hydrochloric acid
H&E	= Hematoxylin and eosin
hr	= Hour, Hours
IL-1	= Interleukin-1
IGF	= Insulin-like growth factor
IGF-1	= Insulin-like growth factor-1
kd	= Kilo Daltons
keV	= Kiloelectron volt
kvp	= Kilovolt peak
mA	= Miliampere
mg	= Milligram

List of Abbreviations and Symbols (continued)

min = Minutes

ml = Milliter

mm = Millimeter

mm Hg = Millimeters of mercury

MTEC = The National Metal and Materials Technology Center

N = Number

OD = Optical density

PAF-4 = Platelet activating factor-4

PDEGF = Platelet-derived endothelial cell growth factor

PDGF = Platelet-derived growth factors

PGS = Penicillin G sodium

PO_2 = Partial pressure of oxygen

PPP = Platelet-poor plasma

PRF = Platelet-rich fibrin

PRP = Platelet-rich plasma

rpm = Round per minute

SD = Standard deviation

SE = Standard error

SEM = Scanning electron microscope

TCP = Tricalcium phosphate

TGF- α = Transforming growth factor alpha

TGF-β = Transforming growth factor-beta

TGF-β1 = Transforming growth factor-beta 1

TGF-β2 = Transforming growth factor-beta 2

VEGF = Vascular endothelial growth factor

XCP = Extension cone paralleling

Chapter 1

Introduction

Bone reconstruction in oral and maxillofacial region permits the recovery of the esthetics and function of the craniofacial skeleton. For this purpose, various surgical techniques are used. An autogenous bone grafting is the gold standard method to stimulate bone healing and fill bone defects. Autogenous bone provides 3 elements necessary to generate and maintain bone: scaffold for osteoconduction, growth factors for osteoinduction, and progenitor cells for osteogenesis.[1] While these sources produce excellent results, autogenous bone grafts are subject to limitations of an available amount of bone, secondary donor site defects, increased operative time, blood loss, postoperative pain, infection, unpredictable resorption, length of hospital stay and cost. These limitations increase interest in bone substitute material, including allogenic, xenogenic and alloplastic bone materials. A bone graft substitute should be osteoconductive, osteoinductive, biocompatible, bio-resorbable, structurally similar to bone, easy to use, and cost-effective.[2] A bone substitute material can be used instead of or in combination with an autograft to increase graft volume.

Deproteinized bovine bone (DBB) is one of bone substituted materials that has the structure like human bone and has the properties of osteoconduction and biocompatibility.[3-5] Animal and clinical human researches have demonstrated that DBB is biocompatible and promotes growth of bone into its natural cavities which is well integrated by the host bone.[4,6-12] DBB has been used successfully to fill bone defects particularly for maxillary sinus floor grafting to facilitate implant. However it has slow resorption rate[3, 12] and leads to long time taking for complete bone formation. The composite of autogenous bone and bone substitute are widely used clinically because it combines the osteogenesis property of autogenous bone and osteoconductive property of DBB. Combination of autogenous and DBB in proper proportion would be an effective choice for bone grafting.[13]

At present, the proportion of the autogenous bone and the bone substitute are varied. Our previous study in Prince of Songkla University[13] assessed the quality and quantity of new bone formation from the 3 different proportions (1:1, 1:2, 1:4) of the autogenous bone and

DBB in rabbit calvarial defects and showed that proportion 1:1 and 1:2 enhancing greater bone formations than the proportion 1:4, DBB alone and the critical size defect. The proportion 1:1 and 1:2 are preferable to be used in clinical application. However this composite graft poses only two properties by bone regeneration, osteogenesis from autografts and osteoconductive from DBB.

Numerous studies have demonstrated that osteoinductive growth factor or gene delivery significantly improves bone repair. The considerable attention has focused on the potential application of growth factors to enhance wound healing. Several polypeptide growth factors, e.g. fibroblast growth factor, insulin-like growth factor-I (IGF-I), platelet-derived growth factors (PDGF), transforming growth factor- β (TGF-β) and bone morphogenic proteins (BMP) alone or in combination have been demonstrated effective on cell proliferation, chemotaxis, differentiation and extracellular matrix synthesis and consequence facilitating bone regeneration in animal and human studies.[14-18] These growth factors except BMP are found in nature, therefore using platelet products raise the attractive for an adjuvant to bone grafting.

There are 3 generations of fibrin technologies from platelet regarding the biochemical properties of surgical additives as fibrin adhesives, platelet-rich plasma (PRP) and platelet-rich fibrin (PRF) (Table 1). The use of fibrin adhesives in many field-related protocols is well documented from the past 30 years.[19] However, controversy still remains to the complexity of the production protocols (for autologous adhesives) and risk of cross-infection (for commercial adhesives).[20] Since the early 1990s, platelet-rich plasma has been introduced, the concentration of autologous platelets in plasma, for clinical application by Marx et al.[21] The growth factors contained within platelets in relation to their biological enhancement of continuity bone grafts to the mandible have been explored. A new family of platelet concentrate, which is neither a fibrin glue nor a classical platelet concentrate, was called platelet-rich fibrin (PRF), it looks like an autologous cicatricial matrix and was introduced by Dohan in 2006. [20] PRF belongs to a new generation of platelet concentrates geared to simplified preparation without biochemical blood handling, one centrifugation, and natural fibrin clot polymerization.[20, 22-25]

PRP has been explored in various aspects, but there is no sufficient data upon PRF. Quantitative platelet counts verified that the platelet-rich plasma used in the previous studies[21, 45-48] consisted of 595,000 to 1,100,000 platelets in the concentrate. These reviews on PRP were as the basic understanding of the nature PRF characteristics. These values confirmed

the platelet sequestration ability of the process and quantified the concentration as 338% of baseline platelet counts[21], but there is a discrepancy between theses values due to a variation of the procedures for centrifugation of the original plasma samples such as force, time, ect (Table 2).

Table 1. Conclusion of the 3 generations of fibrin technologies.

Detail	**3 Generation of fibrin technologies**		
	Fibrin adhesive	**PRP**	**PRF**
Protocol	Many different protocols	Many different protocols	1 Protocol
Volume of blood sample required	400 ml[26, 27] 200 ml[28] 50 ml[29]	400-500 ml[21, 30-32] 200ml[33] 55-60 ml[34-36] 40 ml[37]	10 ml[20, 22-25]
Blood collection with anticoagulant	Yes	Yes	No
Preparation with biochemical blood handling	Yes	Yes	No
Fibrin polymerization	Artificial way	Artificial way	Natural way
Equipments or tools	Kit	- Platelet Concentration Collection System kit - Cell separator - Centrifuge	Centrifuge
Centrifugation	A self-mixing syringe	2 Steps of centrifugation	1 Step of centrifugation
Risk of life threatening	Cross infection[20, 38] Coagulopathies[39, 40] (for commercial adhesive)	Coagulopathies[38, 41-43] (from bovine thrombin)	No
Instruments cost	2,500$[44]	4,000-9,000$[31]	1,000$

Table 2. The level of platelets in PRP.

Author	Year	% Increase
Marx et al.[21]	1998	338 %
Landesberg et al.[45]	2000	205.7%
Kim et al.[46]	2001	287%
Okuda et al.[47]	2003	283.4 %
Gerard et al.[48]	2006	388%

There are many studies[21, 30, 47] suggested significant correlations between number of platelet counts and levels of growth factors such as PDGF, TGF-β, VEGF and IGF. However no statistically significant correlation was found between these 2 parameters in the unconcentrated plasma. This result implies that the platelet is the major source of these growth factors in the PRP. The additional amounts of growth factors obtained by adding platelet-rich plasma to grafts was evident from a radiographic maturation rate 1.62 to 2.16 times of grafts without platelet-rich plasma. As assessed by histomorphometry, there was also a greater bone density in grafts in which platelet-rich plasma was added than in grafts in which platelet-rich plasma was not added.[21] Treatment with PRP to support osseointegration of dental implants has also been described suggesting that PRP may be useful in accelerating the osseointegration of titanium implants.[49] There are very few studies in refereed journals in which PRP was used and added to autogenous, allograft, xenograft or alloplast bone. The application of PRP has been investigated in several clinical and animal studies (Table 3 and 4). These articles described the PRP techniques used and reported the formation of some osteoid material or the osteogenesis of bone grafting.[21, 37, 46, 49, 50] However, the results are conflicting or equivocal. In many of these studies, few cases are to be evaluated and no statistical testing was performed to confirm the validity of the results.[48, 51-53]

Table 3. The applications of PRP investigated in clinical trials.

Author	Year	No. of patients	Method of investigation	Conclusion
Marx et al.[21]	1998	88 Cancellous cellular marrow bone graft reconstructions of mandibular continuity defects	- Radiographic graft maturity (Panoramic radiographs)	- The adding of platelet-rich plasma to grafts showed a radiographic maturation rate 1.62 to 2.16 times than that of grafts without platelet-rich plasma.
			- Histomorphometry	- Bone grafts with PRP demonstrated even greater trabecular bone density than did bone grafts without PRP.
Froum et al.[30]	2002	3 Patients undergoing bilateral sinus augmentation	- Histomorphometry	- The addition of PRP to the grafts of anorganic bovine bone was not different either in vital bone production or in interfacial bone contact on the test implants.
Oyama et al.[37]	2004	12 Cleft patients	- 3-dimensional computed tomography (CT)	- The average of the volume ratio of regenerated bone to alveolar cleft in cases with PRP was higher than in controls.
Raghoeba et al.[35]	2005	5 Edentulous patients, undergoing bilateral sinus augmentation	- Microradiographic - Histomorphometry	- No beneficial effect of PRP on wound healing and bone remodeling of autologous bone grafts.

Table 4. The applications of PRP investigated in animal models.

Author	Year	Animals and No.	Methods of investigation	Conclusion
Kim et al.[46]	2001	Rabbits (N=20)	- Soft x-ray imaging	- Greater bone densities were obtained in grafts combined with PRP
			- Computer tomography	
Kim et al.[49]	2002	Dogs (N=10)	- Histomorphometry	- A higher percentage of bone contact with particulate dentin-plaster of Paris and PRP than the control and particulate dentin-plaster of Paris.
Aghaloo et al.[50]	2004	Rabbits (N=15)	- Radiographs	- Significantly greater bone density at the Bio-Oss, autogenous bone, and Bio-Oss + PRP sites than at control sites
			- Histomorphometry	-Increase in bone formation with the addition of PRP to Bio-Oss in non-critical-sized defects.
Wiltfang et al.[54]	2004	Mini-pigs (N=24)	- Microradiography	- PRP did not add additional benefit on xenogenic bone substitutes.
			- Histological examination	- But had a significant effect on bone regeneration in the autogenous group initially.
Gerard et al.[48]	2006	Dogs (N=13)	- Digitized radiographs	- PRP enhanced early autologous graft healing. But, after 2 months this effect is no longer significant
			- Histomorphometry	
Miranda et al.[53]	2006	Rabbits (N=16)	- Histological and histomorphometry evaluation.	- The addition of PRP in between autogenous bone blocks and the receptor bed did not confer significant benefit for the new bone formation and healing.
Mooren et al.[55]	2007	Goats (N=20)	- Histological and histomorphometry evaluation.	- The early and late bone healing was not enhanced when PRP was used.
Schlegel et al.[56]	2007	Mini-pigs (N=24)	- Microradiographic examination	- No positive effect of enhancement of bone implant contact in the PRP group could be detected.

Currently, the autogenous bone grafting is the gold standard method to stimulate bone healing. However, autogenous bone grafting has drawbacks such as donor site morbidity, limited source and increased operative time. Bone substitute materials are appealing alternative such as deproteinized bovine bone (DBB). But most bone substitute materials provide only osteoconduction property and are expensive. The use of bone substitute materials alone or in combination with autogenous bone does not achieve the osteogenesis perfectly. It is hypothesized that bone regeneration could be enhanced by adding growth factors to bone grafting materials in skeletal reconstruction in the maxillofacial area.

In our study, platelet-rich fibrin was used as an autologous source of PDGF, TGF-β and IGF.[20, 22-25] PRF poses many advantages such as easy preparation, low cost and no harmful to patient. Therefore it may be beneficial for enhancing bone regeneration. However there is no clear evidence to support the clinical use of PRF, when adding to grafting material such as autogenous, allograft and xenografts materials in oral and maxillofacial region. A possible role of PRF as a source of growth factor to stimulate bone regeneration is expected. The present study aimed to assess the quality and quantity of new bone formation from the adjuvant of PRF to autogenous bone chips, deproteinized bovine bone and the composite of deproteinized bovine bone and autogenous bone chips in rabbit calvarial defects. A conceptual framework is presented in Figure 1.

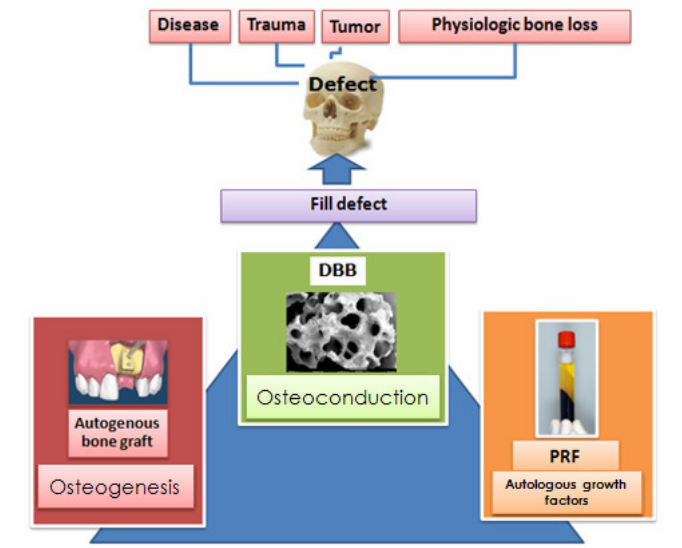

Figure 1. Conceptual Framework shows a role of the major components of osteogenesis (autogenous bone graft), osteoconduction (scaffold from DBB) and osteoinduction (growth factor from PRF) to fill the defect from various causes.

Review of Literatures

Platelet-rich fibrin (PRF)

Platelet-rich fibrin was first developed in France by Dohan et al[20] for a specific use in oral and maxillofacial surgery. The protocol is as follows. A blood sample is taken without anticoagulant in a 10 ml tube. It is immediately centrifuged at 3000 rpm (approximately 400g) for 10 minutes (Figure 2). The absence of anticoagulant implies the activation in a few minutes of most platelets of the blood sample in contact with the glass tube walls and the release of the coagulation cascades. Fibrinogen is initially concentrated in the high part of the tube, before the circulating thrombin transforms it into fibrin. A fibrin clot is then obtained in the middle part of the tube, just between the red corpuscles at the bottom and acellular plasma at the top (Figure 3, 4 and 5).

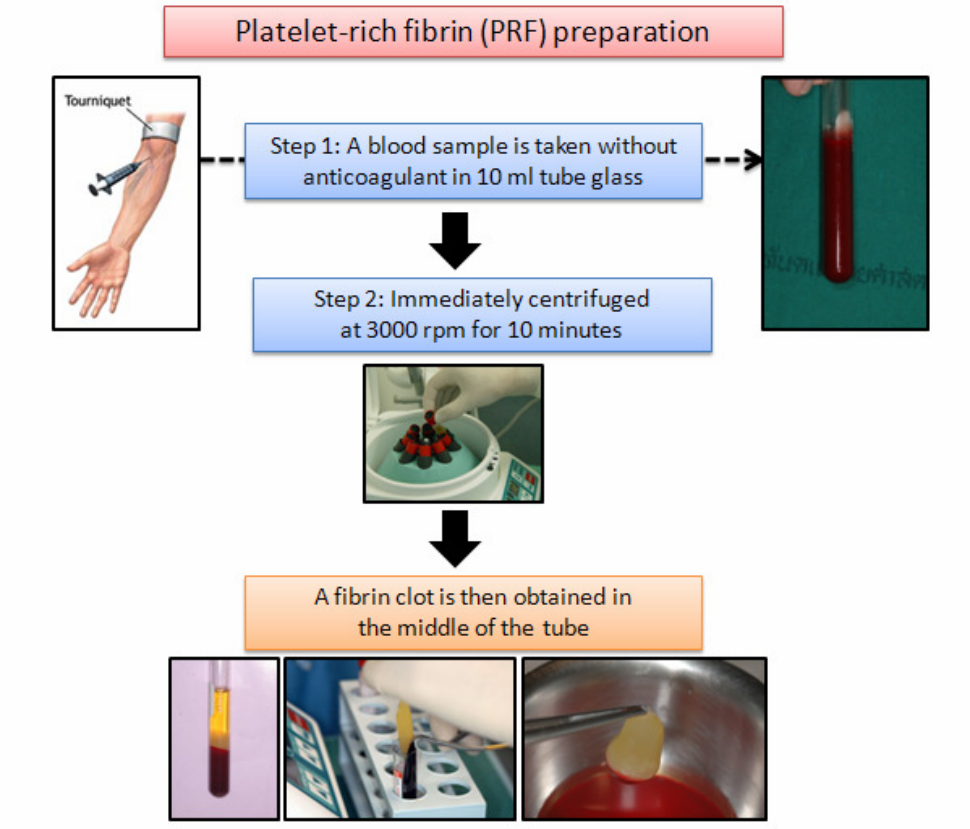

Figure 2. Flow chart of preparation of PRF following the PRF protocol.[20]

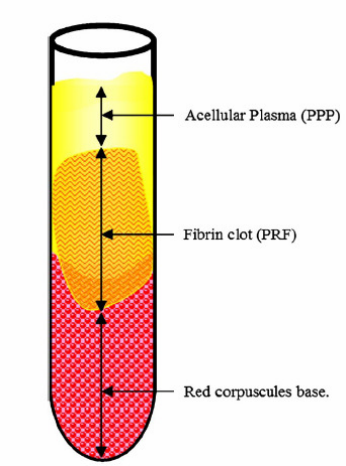

Figure 3. Diagram of blood centrifugation shows a structured fibrin clot in the middle part of the tube, between the red corpuscles at the bottom and acellular plasma at the top.[20]

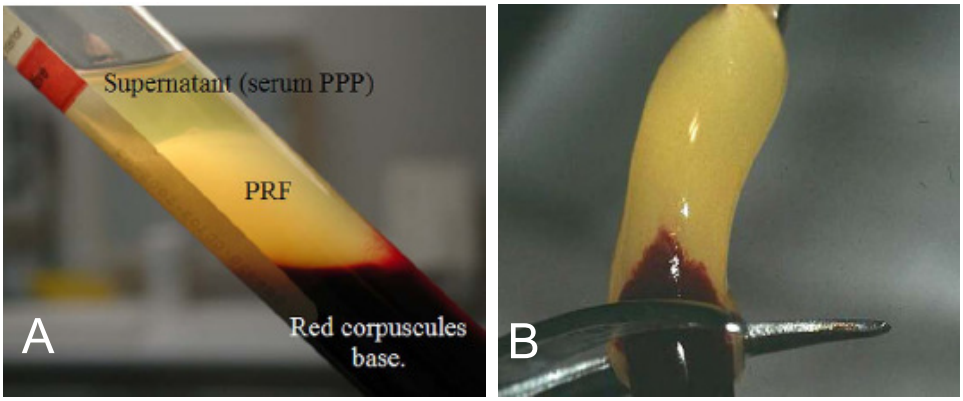

Figure 4. Blood processing with a centrifuge for PRF allows the composition of a structured fibrin clot in the middle of the tube (A). Collection of the PRF (B).[20]

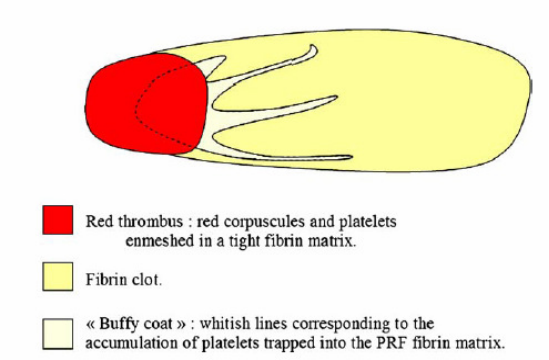

Figure 5. The PRF fibrin clot is composed of 3 parts: a red thrombus in contact with the red blood corpuscle base, an acellular fibrin gel, and a network of buffy columns corresponding to platelet accumulation.[22]

The success of this technique entirely depends on the speed of blood collection and transfer to the centrifuge. Indeed, without anticoagulant, the blood samples start to coagulate almost immediately upon contact with the tube glass, and it takes a minimum of a few minutes of centrifugation to concentrate fibrinogen in the middle and upper part of the tube. Quick handling is the only way to obtain a clinically usable PRF clot. If the duration required to collect blood and launch centrifugation is overly long, failure will occur: The fibrin will polymerize in a diffuse way in the tube and only a small blood clot without consistency will be obtained.[20]

Dohan et al[22] investigated the platelet-associated features of PRF. Preliminary hematologic studies revealed that platelet in the acellular supernatant (platelet-poor plasma (PPP)) or in the red blood corpuscles base, did not remain. A few histologic analyses were sufficient enough to determine the platelet distribution within the various layers of the centrifuged collection tube. They accumulate in the lower part of the fibrin clot, mainly at the junction between the red corpuscles (red thrombus) and the PRF clot itself (Figure 6). During PRF processing by centrifugation, platelets are activated and their massive degranulation implies a very significant cytokine release. These initial analyses revealed that slow fibrin polymerization during PRF processing leads to the intrinsic incorporation of platelet cytokines and glycanic chains in the fibrin meshes. This result would imply that PRF, unlike the simple fibrin adhesives (Figure 7) or platelet-rich plasma (Figure 8), would be able to progressively release cytokines during fibrin matrix remodeling. It is possible to consider that on the whole, PRF platelet cytokines remain trapped in the fibrin meshes, and probably even in the fibrin polymers (Figure 9).

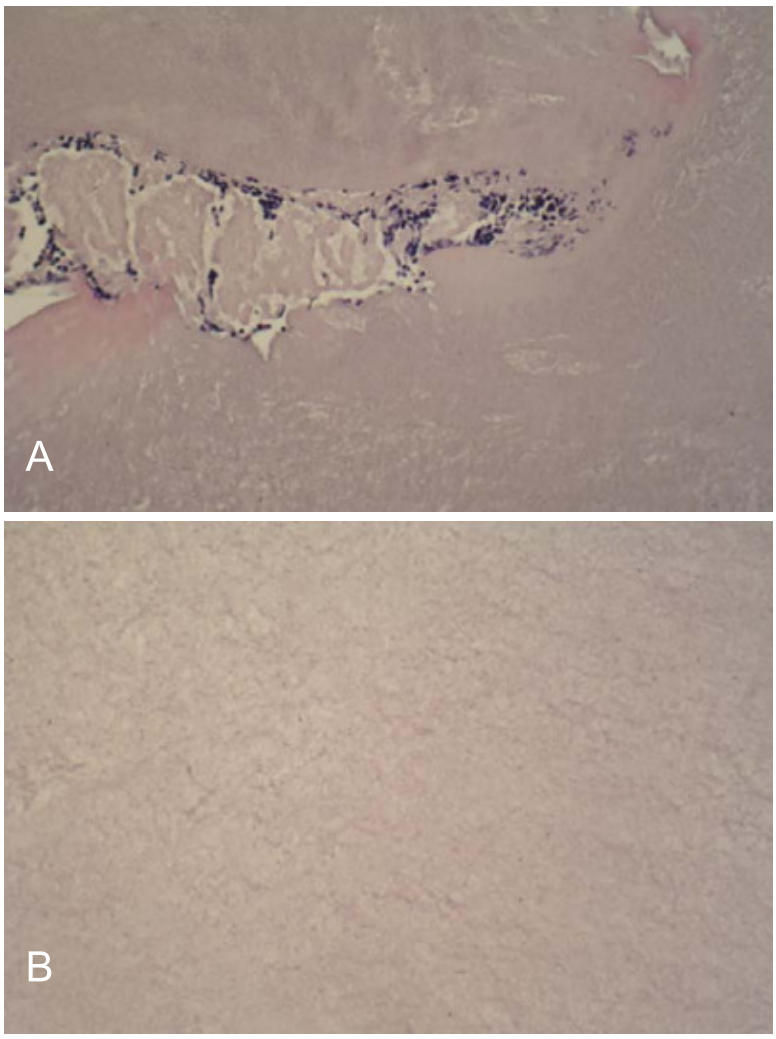

Figure 6. The lower part of the PRF fibrin matrix is occupied by whitish streaks looking like cell fragment aggregates on histological sections. These are the platelet accumulations and constitute a ‘‘buffy coat’’ (A). But there is no platelet or any other cellular body in the upper part of the PRF fibrin clot (B). Hemalun-eosin staining, 52X.[22]

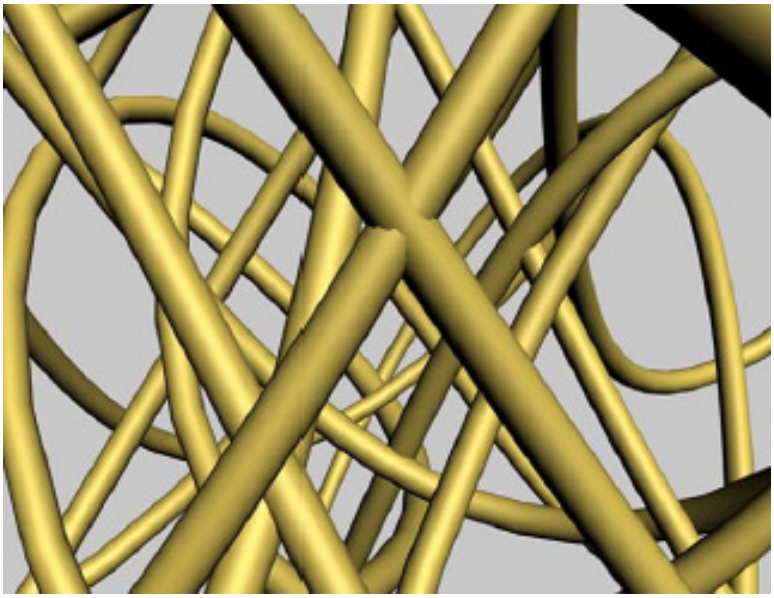

Figure 7. Theoretical computer modeling of a fibrin network resulting from fibrin glue polymerization.[22]

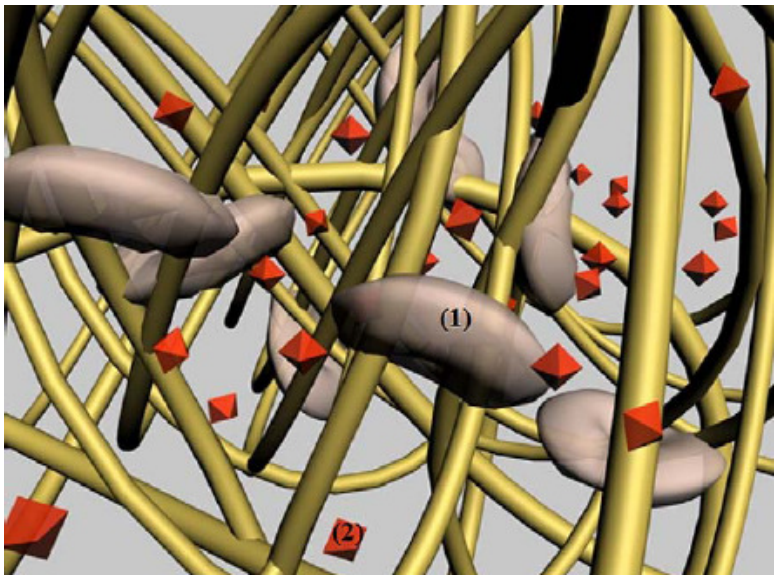

Figure 8. Theoretical computer modeling of PRP, the activated platelets are trapped in the fibrin meshes and release a significant quantity of cytokines extrinsically retained in the fibrin architecture. (1) Platelet trapped in the fibrin gel. (2) Platelet cytokine in solution (extrinsic).[22]

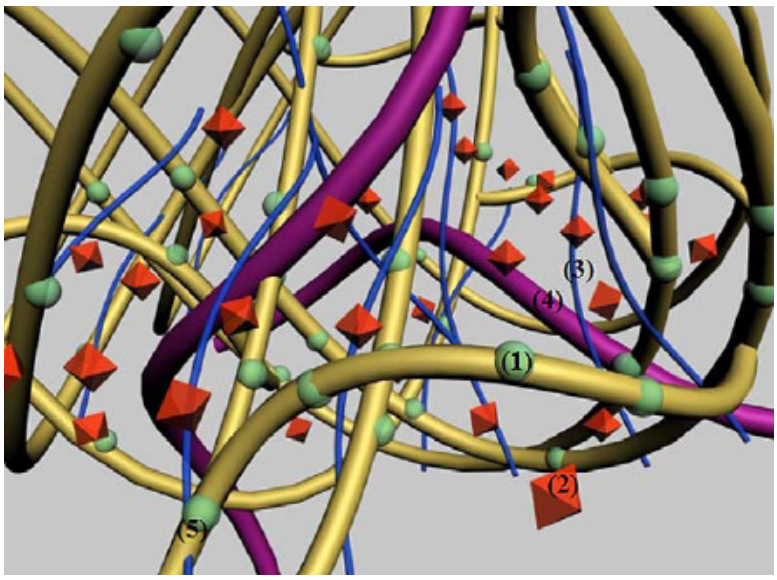

Figure 9. Theoretical computer modeling of a PRF clot, the presence of structural glycoproteins (fibronectin) and extrinsic cytokines (in solution) enmeshed in the fibrin matrix. The PRF slow polymerization process would also allow the intrinsic retaining of glycanic chains and cytokines within fibrin polymers. PRF would be thus very close to a natural fibrin thrombus. (1) Cytokine intrinsically retained within fibrin fibrillae. (2) Platelet cytokine in solution (extrinsically associated with fibrin polymers). (3) Fibrin-associated glycanic chains. (4) Circulating glycoproteins (fibronectin). (5) Fibrin fibrilla associated with glycanic chains and intrinsic cytokines.[22]

Choukroun et al[24] confirmed that PRF can be considered as a healing biomaterial. Clinical example dealed with the filling of a tooth socket by PRF. Rapid healing of the wound was observed without pain, dryness, or purulent complications. Sinus floor augmentation was performed with freeze-dried bone allograft (FDBA) and PRF leaded to a reduction of healing time prior to implant placement. From a histologic point of view, this healing time could be reduced to 4 months. After complete maxillary cystic ablation, a cystic cavity filled with PRF were totally healed in two and a half months later, the osseous defect was replaced by a dense and cortical bone. This physiologic healing phenomenon is accelerated, because physiologic healing time of this cystic cavity lies between 6 months and 1 year.

The autogenous growth factors in platelet-rich fibrin

Researchers in oral and maxillofacial surgery continuously strive to improve on current bone-grafting techniques and provide a faster and denser bony regenerate. Growth factors are a realistic way to improve and expedite both soft tissue and bony wound healing.

Platelets are small, irregularly shaped anuclear cells and 2-4 μm in diameter. They are derived from fragmentation of precursor megakaryocytes. Platelets contain angiogenic, mitogenic, and vascular growth factors in their granules.[35, 57] Platelets are very important in the wound healing process. They arrive quickly at the wound site and begin coagulation. They release multiple wound-healing growth factors and cytokines, including platelet-derived growth factor (PDGF), transforming growth factors (TGF-β1 and TGF-β2, vascular endothelial growth factor (VEGF), platelet-derived endothelial cell growth factor (PDEGF), interleukin-1 (IL-1), basic fibroblast growth factor (bFGF), and platelet activating factor-4 (PAF-4). One of the highest concentrations of PDGF and TGF-β in the body is found within blood platelet (Table 5.)

Among those growth factors, both PDGF and TGF-β have been studied extensively and these growth factors are thought to contribute to bone regeneration and increased vascularity, vital features of a healing bone graft.[57]

Table 5. Platelet: A principle source of growth factors at wound sites.

Growth factor	Major sources at the wound site
PDGF	Platelets, macrophages, bone matrix, epithelial cells, endothelial cells, smooth muscle cells
TGF-β	Platelets, macrophages, osteoblasts, bone matrix-activated T-lymphocytes, immature chondrocytes
EGF/TGF-α	Platelets, macrophages, epithelial cells, eosinophils
IGF-1	Plasma, epithelial cells, endothelial cells, fibroblast, smooth muscle cells, osteoblasts, bone matrix
bFGF	Macrophages, endothelial cells, osteoblasts, immature and mature chondrocytes, bone matrix

Platelet-derived growth factor (PDGF)

PDGF is a glycoprotein with a molecular weight of approximately 30 kd. Although it was first described in the alpha granules of platelets, it is also synthesized and secreted by other cells, such as macrophages and endothelium (Table 5). It seems to be the first growth factor present in a wound, and it initiates connective tissue healing, including bone regeneration and repair. In humans, it exists mostly as a heterodimer of two chains--termed A and B chains-- of about equal size and molecular weight (approximately 14 kd to 17 kd). Homodimers of A-A and B-B chains are also present in human platelets and have the same effects on bone regeneration.

PDGF is known to emerge from degranulating platelets at the time of injury. Its mechanism is to activate cell membrane receptors on target cells, which in turn are thought to develop high-energy phosphate bonds on internal cytoplasmic signal proteins. The bonds then activate the signal proteins to initiate a specific activity within the target cell.[58] The important specific activities of PDGF include mitogenesis (increase in the cell populations of healing cells), angiogenesis (endothelial mitoses into functioning capillaries), and macrophage activation (debridement of the wound site and a second phase source of growth factors for continued repair and bone regeneration). There are approximately 0.06 ng of PDGF per one million platelets, a fact that underscores this molecule's great potency.

At the higher concentrations of PDGF, it is believed to be present more proximally in wounded areas where cell migrations, neutrophil activation, collagenase release of fibroblast, and cell division have occurred. PDGF thus may play a pivotal role in wound healing (Figure 10).[59] PDGF is stored in the bone matrix and is released upon activation of osteoblast, resulting in an increase of new bone formation.[60] In support of these findings, in vitro studies demonstrated that PDGF initially stimulates bone resorption and also stimulates the proliferation and chemotaxis of osteoblast.[61] Therefore a greater concentration of platelets can be expected to have a profound effect on wound healing enhancement and bone regeneration.

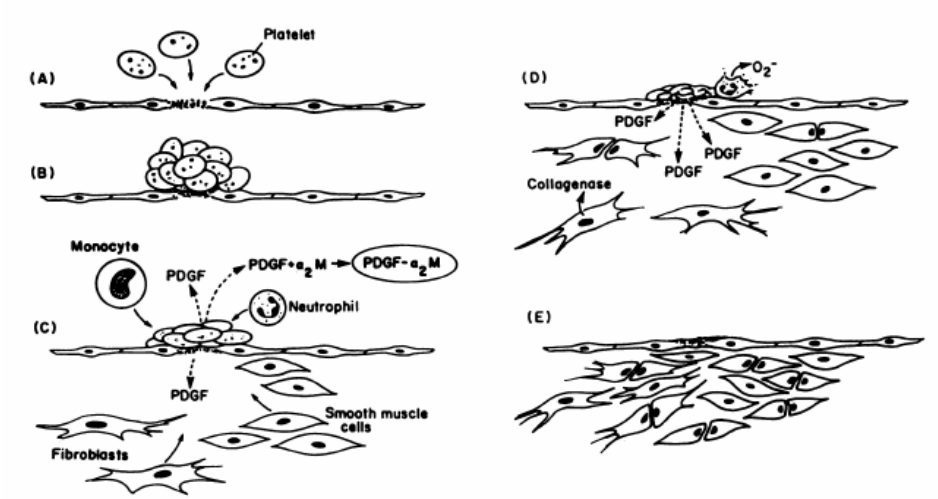

Figure 10. Potential roles of PDGF in wound healing. PDGF is released after injury (A) and platelet adherence and aggregation at injured sites (B). The PDGF released locally stimulates the migration of neutrophils, monocytes, fibroblasts, and smooth muscle cells (in vessel wall injury) into the wounded sites; PDGF released into the systemic circulation is complexed to alpha2-macroglobulin (α_2M) (C). At the higher concentrations of PDGF proximal in the wound, PDGF activates neutrophils to generate and release superoxide and stimulates fibroblasts to synthesize and release collagenase. PDGF also stimulates cellular proliferation of fibroblasts and smooth muscle cells (D). Remodeling and reorganization follow (E).[59]

Transforming growth factors (TGF)

TGF-β is applied to the superfamily of growth and differentiating factors of which the bone morphogenetic protein (BMP) family, containing at least 13 described BMPs, is a member.[62] The TGF-βs referred to and studied in previous article[21] are the TGF-β1 and TGF-β 2 proteins, which are protein and generic growth factors involved with general connective tissue repair and bone regeneration. TGF-β1 and TGF-β2 are proteins that have molecular weights of approximately 25 kd. Like PDGF, they are synthesized and found in platelets and macrophages, as well as in some other cell types (Table 5). When released by platelet degranulation or actively secreted by macrophages, they act as paracrine growth factors (ie, growth factors secreted by one cell exerting its effect on an adjacent second cell), affecting mainly fibroblasts, marrow stem

cells, and the preosteoblasts. However, each of these target cells has the ability to synthesize and secrete its own TGF-β proteins to act on adjacent cells in a paracrine fashion or act on itself as an autocrine growth factor (ie, a growth factor which is secreted by a cell and acts on its own cell membrane to continue its activity). TGF-βs therefore represent a mechanism for sustaining a long-term healing and bone regeneration module and even evolve into a bone remodeling factor over time.

The important functions of TGF-β1and TGF-β2 seem to be the chemotaxis and mitogenesis of fibroblasts, marrow stem cells, endothelial cells, epithelial cells, and pre-osteoblastic cells[52], and they also have the ability to stimulate osteoblast deposition of the collagen matrix of wound healing and of bone. In addition, TGF-βs inhibit osteoclast formation and bone resorption by stimulating chemotactic migration of osteoblasts to the site of injury[52], thus favoring bone formation over resorption by two different mechanisms.[21] TGF-β is also found at higher levels in bone matrix and upon activation facilitates wound healing under inflammation conditions.[63]

Previous in vivo study[64] showed that TGF-β1, when coated on to β-tricalcium phosphate pellets, substantially stimulated cell proliferation and differentiation of osteoblast-lineage cells, and eventually induced new bone formation in experimental rat calvarial osseous defect. In addition, in association with gingival wound healing after flap surgery in rats, the topical applied TGF-β1 was demonstrated that it stimulated the proliferation of gingival fibroblastic cells, the formation of blood vessels, and the remodeling of extracellular matrix molecules, which resulted in increased formation of granulation tissue of the periodontal tissue.[65]

The role of growth factors in bone regeneration

Growth factors are proteins that serve as signaling agents for cells. They function as part of a vast cellular communications network that influences such critical functions as cell division, matrix synthesis, and tissue differentiation. The results of experimental studies have been established that growth factors play an important role in bone and cartilage formation, fracture healing, and the repair of other musculoskeletal tissues. Recently, with the advent of recombinant proteins, there has been considerable interest in the use of growth factors as

therapeutic agents in the treatment of skeletal injuries.[65] A cancellous cellular marrow graft, whether for a mandibular continuity defect, an alveolar cleft, or a sinus lift surgery, is placed into a dead space filled with clotted blood. The wound dead space is hypoxic (PO2, 5-10 mm Hg) and acidotic (pH, 4-6) and contains platelets, leukocytes, red blood cells, and fibrin in a complex clot adjacent to the transferred osteocytes, endosteal osteoblasts, and marrow stem cells21 (Figure 11). The marrow stem cells, which are the primary bone-regenerating cells, normally exist in very small numbers (approximately 1 per 400,000 structural cells in a 50-year-old human being).[21] Just outside periosteal level, the tissue is physiologically normal. The tissue is normoxic (PO2, 45-55 mm Hg) and at physiologic pH (pH, 7.42), and contains a population of structural cells, healing-capable stem cells (also in very small numbers), and cut capillaries with clots and exposed endothelial cells.

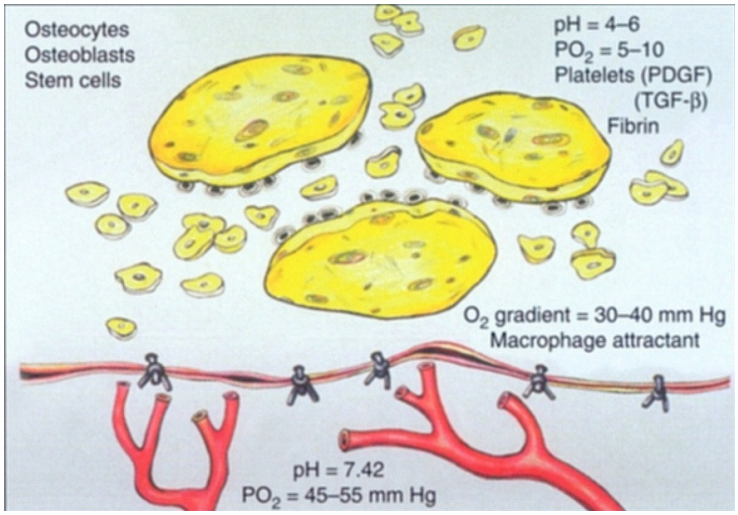

Figure 11. Physiologic of a bone graft at the time it is placed. Basic cells, biochemistry, and growth factors associated inside and outside wound space of cancellous marrow graft.[21]

The initiation of bone regeneration starts with the release of PDGF and TGF-β from the degranulation of platelets in the graft (Table 6). The PDGF stimulates mitogenesis of the marrow stem cells and endosteal osteoblasts transferred in the graft to increase their numbers by several orders of magnitude. It also begins an angiogenesis of capillary budding into the graft by inducing endothelial cell mitosis. The TGF-β initially activates fibroblasts and preosteoblasts to

mitose and increases their numbers, as well as promoting their differentiation toward mature functioning osteoblasts. Continued TGF-β secretion influences the osteoblasts to lay down bone matrix and the fibroblast to lay down collagen matrix to support capillary ingrowth. These activities begin immediately on wound closure. By the third day capillaries can be seen to penetrate the graft. Complete capillary permeation of the graft is seen by day 14 to day 17 [21] (Figure 12 and 13).

Table 6. The role of growth factors in bone regeneration.

Growth factor	Role in bone regeneration
PDGF	- Mitogenesis (increase in the cell populations of healing cells) - Angiogenesis - Macrophage activation
TGF-β	- Chemotaxis and mitogenesis of fibroblasts, marrow stem cells, endothelial cells, epithelial cells, and pre-osteoblastic cells - Inhibit osteoclast formation and bone resorption by stimulating chemotactic migration of osteoblasts to the site of injury - Osteoblasts lay down bone matrix and the fibroblasts lay down collagen matrix to support capillary ingrowth

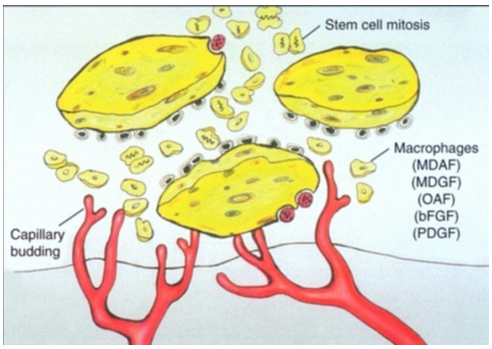

Figure 12. Physiologic of a bone graft at approximately 3 days. By day 3 capillary ingrowth begins in response to PDGF and TGF-β. Stem cells and endosteal osteoblasts mitose in response to these growth factors to create a cell population capable of producing functional quantity of new bone. Macrophage becomes main growth factor elaborating cell, inasmuch as platelets have completely degranulated by now.[21]

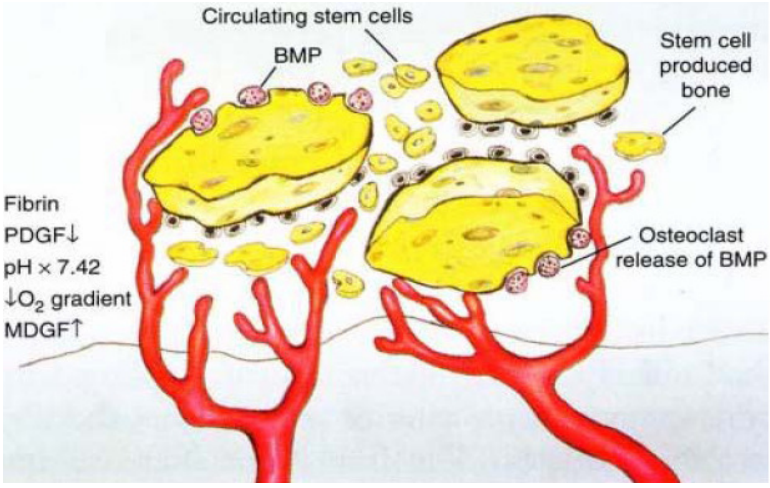

Figure 13. Physiologic of a bone graft at approximately 14 to 17 days. By day 14 capillary ingrowth is nearly complete. Bone-forming cells are now sustaining themselves with their own autocrine production of TGF-β. With physiologic normalization of wound by capillary perfusion, macrophage function begins to dissipate.[21]

Deproteinized bovine bone (DBB)

Deproteinized bovine (DBB) bone has a long history of being successfully used to fill in bone defects and for maxillary sinus floor grafting to facilitate implantations.[6, 66-70] DBB granules provide an ideal scaffold for new bone formation in animal studies.[6, 8, 71, 72] Application of DBB has shown that this material can be utilized to elevate the sinus floor, eventually leading to the formation of lamellar bone[11, 73] and increase bone density. In human sinus floor elevation, DBB alone or mixed with other materials (autogenous bone or demineralized freeze-dried bone allografts) has strong osteoconductive properties, and allows the formation of bone bridges between and around the granules.[3]

The various chemical treatments have been developed to remove the antigenic proteins and cellular elements of xenogeneic bone. The results show that the chemically deproteinated materials retain some antigenicity, which could evoke immunological response.[74] Heat treatment is as an alternative to obtain protein-free xenogeneic bone. The heat treated bone maintains the morphological structure of natural bone, which has an interconnective porous structure of 70% volume porosity and allows bone in-growth.[75] When bovine bone is treated by

chemical agents or heat to remove organic components, the microstructure is affected. Antigenic organic matter of bovine bone can be 100% removed by heat treatment at 500 °C.[74] High temperatures of 800-1000°C can induce carbonate decomposition and high crystallinity, or transform the material into a crystalline phase of bovine hydroxyapatite.[74, 76] When heated further to 1,300°C, the material will transform into hydroxyapatite and calcium phosphate.[77] Therefore, heating temperature should be below 1300°C to keep the structure of the material to be in the hydroxyapatite phase. The National Metal and Materials Technology Center (MTEC) produced bovine hydroxyapatite at three sintering temperatures. The material was produced from bovine bone, and completely deproteinized by heat treatment at 800°C, 1,200°C, and 1,350°C. The sintering temperature in synthetic hydroxyapatite influences strength, density, decomposition, dehydroxylation, and microstructure.[78] Pripatnanont et al[78] indicated that heat-treated bovine hydroxyapatite enhances bone formation by osteoconductive manner and sintering temperature at 1,200°C could provide the material that enhanced more bone than that the temperature at 800°C and 1350°C. This finding supported Wang et al[79] that hydroxyapatite sintered at 1,200°C could enhance osteoblast proliferation and induce the expression of all bone-related proteins more than hydroxyapatite sintered at 1,000°C or 800°C.

For this study the material was produced by MTEC from bovine bone which are completely deproteinized by heat treatment at 1200 °C (Figure 14). The particle size of DBB is in the range of 0.25-1mm. The porous structure and surface morphology were investigated with a scanning electron microscope (JSM-5800 LV, JEOL, Japan) at magnifications of 40X and 6500X using acceleration potentials at 10 keV. The observation revealed that DBB had a porous, well-interconnected pore structure. The pore size of the particle was in the range of 200-500 μm, which can provide a scaffold for vascular and osteogenic cell ingrowth[78] (Figure 15).

The pore size and the pore distribution are quite important parameters for cell growth inside the tissue engineered scaffolds or matrices. Since osteoblasts need cell-to-cell contact for proliferation, an average pore should be at least 3 times (>100 μm) as large as an osteoblast cell (~ 30 μm) so that a single cell could establish contact with the others.[80] Osteoblasts have a preferred pore size (200-400 μm diameter) for encouraging migration, attachment and proliferation. This may be because the curvature of these pores provides optimum compression and tension on the cell's mechanoreceptars.[81]

Figure 14. Deproteinized bovine (DBB), the particle size is 0.25-1 mm.

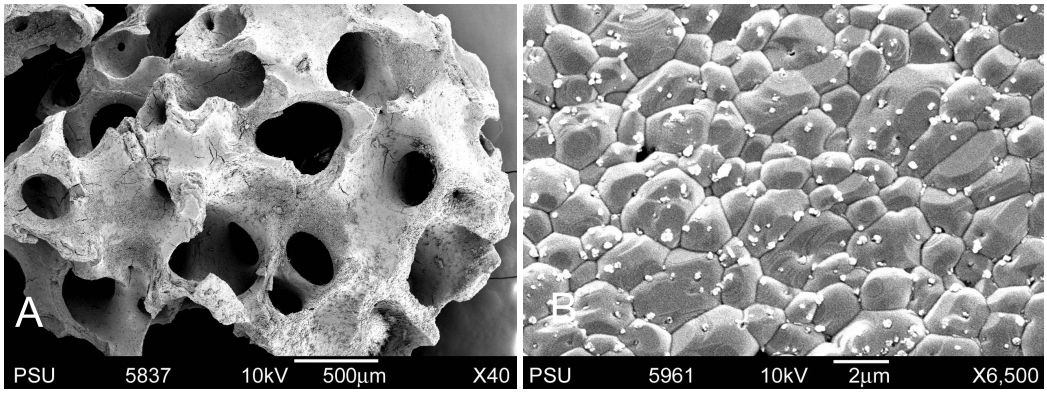

Figure 15. SEM photographs of DBB granules showing the pore structure, original magnification, x 40 (A) Microstructure of HA1200, original magnification, x 6500 (B).[78]

Objective of the study

General Objective

- To investigate the effect of PRF when combine with different graft materials on bone formation in the rabbit's calvarial defect

Specific objectives

1. To compare the amount of new bone formation of all different graft materials by using histomorphometry.
2. To compare the bone density of all different graft materials

Expected outcome

1. To provide a scientific knowledge to verify benefit of using PRF when combine with different graft materials and be possible to improve its clinical application.
2. To develop knowledge and experience in preparing and using autogenous growth factors for repairing skeletal defect or enhancing bone regeneration.
3. To obtain the best choice of composite graft among autogenous bone graft, xenograft and PRF.

Hypothesis

- The addition of PRF to bone graft materials (autogenous bone chip and DBB) enhances increasing in new bone formation.

Chapter 2

Materials and methods

1. Scope of study

This study is an *in vivo* study using male New Zealand White rabbits. The study was performed to investigate the effect of PRF on bone formation by assessing the quality and quantity of new bone formation from the adjuvant of PRF to autogenous bone chip, DBB alone, composite DBB and autogenous bone chip in rabbit calvarial defects.

1.1 Sample size

Estimate sample size for two-sample comparison of means was computed by using data from Marx's study[21] in the Table 7.

Table 7. Histomorphometric findings at 6 months.[21]

Trabecular bone area (TBA)		P
Native mandible (10)	38.9% ±6%	-
Bone grafts (44)	55.1% ± 8%	0.005
Bone grafts with PRP (44)	74.0%±11%	0.005

Estimated power for two-sample comparison of means

We used the formula:

$$n/group = \frac{2(Z_{\alpha/2} + Z\beta)^2 \sigma^2}{(\Delta)^2}$$

n/group = Sample size per group

α = α error

β = β error

Δ = Mean difference

σ^2 = Pooled variance

$$= \frac{(n_1-1)\, sd_1^2 + (n_2-1)\, sd_2^2}{n_1 + n_2 - 2}$$

Assumptions:

$\alpha = 0.05$ (Two-sided) $\beta = 0.2$

$Z_{\alpha//2} = Z_{0.05/2} = 1.96$ $Z\beta = Z_{0.2} = 0.84$

$n_1 = 44$ $n_2 = 44$

$sd_1 = 11$ $sd_2 = 8$

$\sigma^2 = 92.5$ $\Delta = 74.0 - 55.1 = 18.9$

$$n/group = \frac{2\,(1.96 + 0.84)^2\,(90.5)}{18.9^2} = 3.97$$

Sample size for each group**:** 5 rabbits (Estimated power: Power = 0.8743)

1.2 Groups of study

The animals were randomly allocated into 4 groups with simple random sampling (SRS). Control groups (non-PRF groups) comprised of Group 1 and Group 2. Group 1 comprised of a CSD (critical size defect) versus autogenous bone chips, Group 2 comprised of the composited of DBB with autogenous bone chips versus DBB alone. Experimental groups (PRF groups) comprised of Group 3 and Group 4. Group 3 comprised of critical size defect with PRF versus autogenous bone chips with PRF. Group 4 comprised of the composite of DBB, and autogenous bone chips with PRF versus DBB with PRF (Table 8) (Figure 16).

Table 8. Groups of study

Groups	Descriptions	Number of rabbits
1	Critical size defect, empty defect Vs. Autogenous bone chips	5
2	Composite DBB + autogenous bone chips Vs. DBB alone	5
3	Critical size defect + PRF Vs. autogenous bone chips + PRF	5
4	DBB + PRF Vs. Composite DBB + autogenous bone chips + PRF	5
Total		20

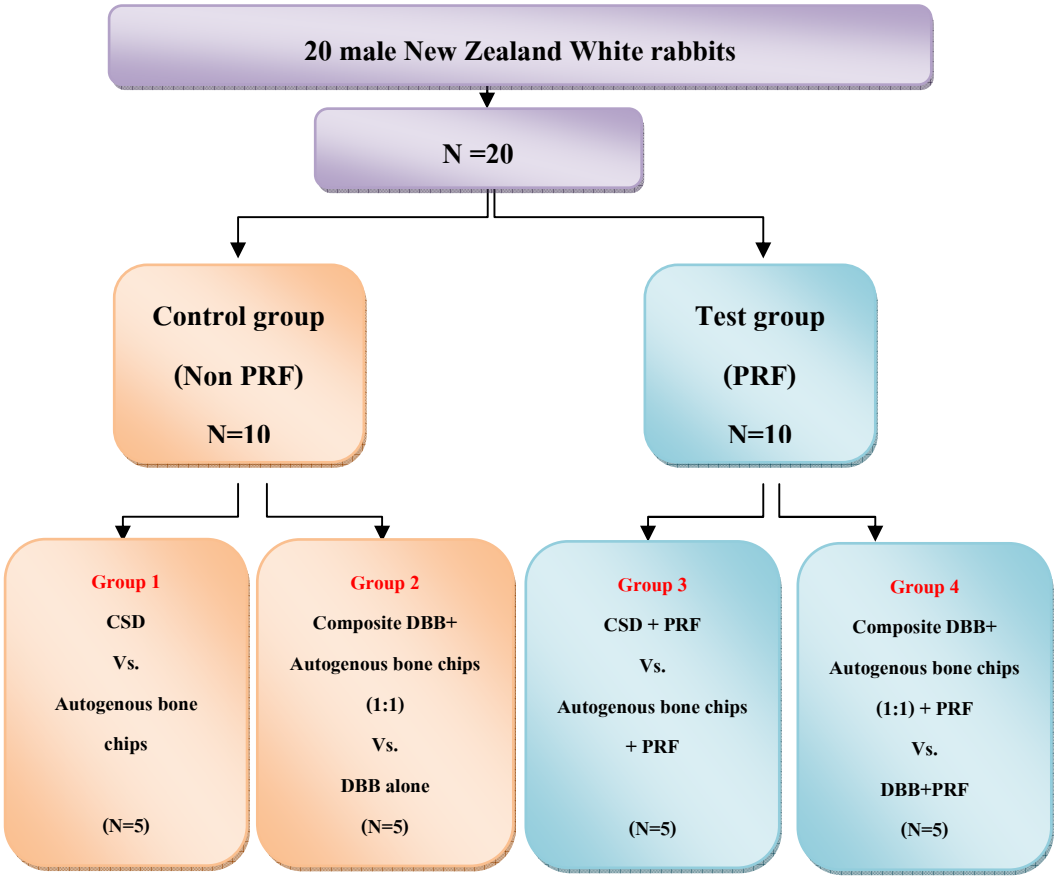

Figure 16. Groups of study

2. Materials

2.1 Animals

This study was performed in accordance with the regulations and approval of the animal experiment ethic committee of Prince of Songkla University. The study was performed on 20 male New Zealand White rabbits aged 5-7 months, weighing 3-4 kilograms. The animals were fed standard rabbit diet, given water ad libitum and kept separately in cages at the animal house, Faculty of Science, Prince of Songkla University (Figure 17).

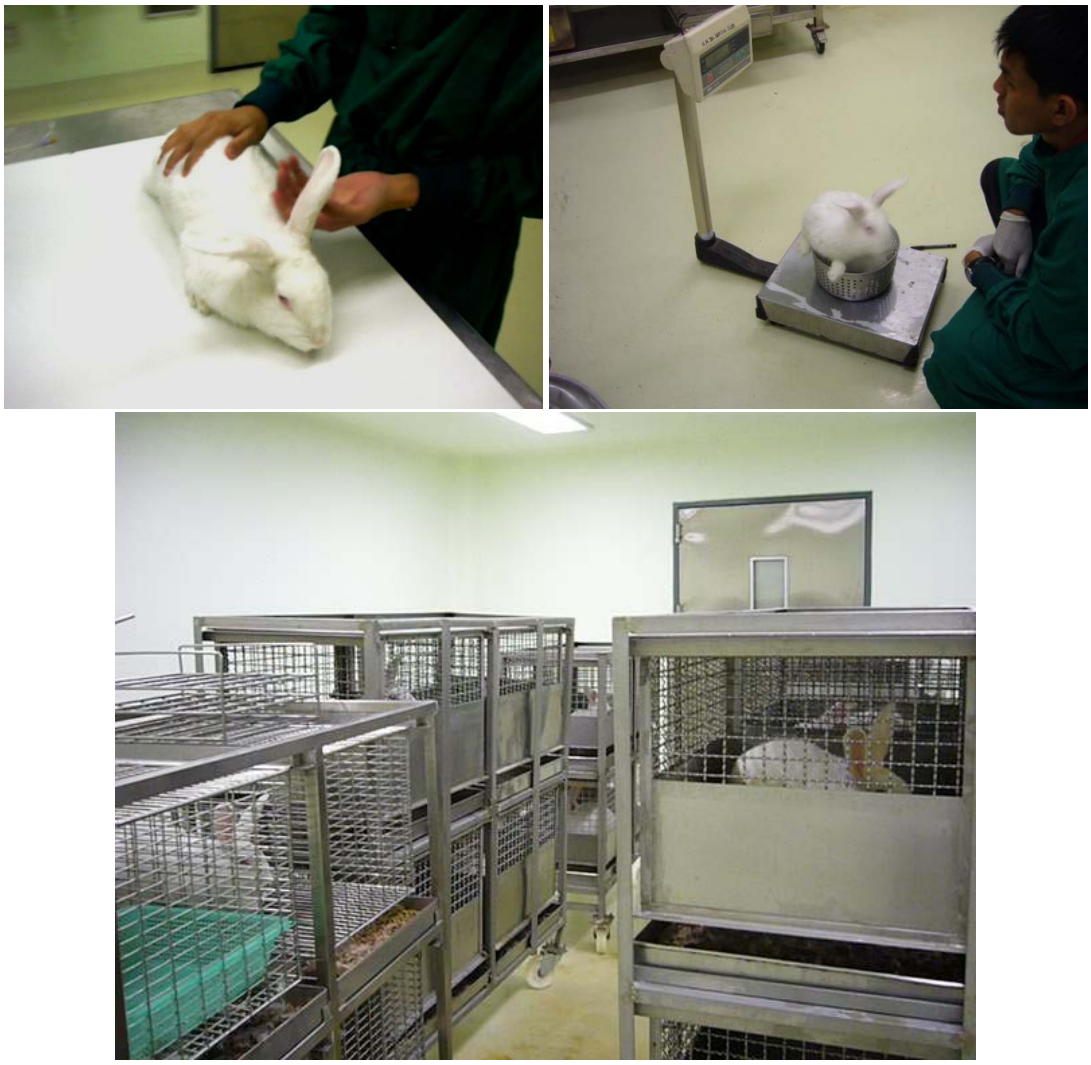

Figure 17. Adult male New Zealand White rabbits, weighing 3-4 kilograms were placed in separate cages.

2.2 Deproteinized bovine bone

Deproteinized bovine bone (DBB) derived from heat treatment at 1,200°C with grain size 0.25-1 mm, was obtained from the Metal and Material Technology Center Thailand (Figure 18).

Figure 18. Sterilized deproteinized bovine bone (DBB) from heat treatment at 1,200°C.

3. Methods

3.1 Platelet-rich fibrin (PRF) preparation

The animal, New Zealand White rabbit, was placed into a restraining box (Figure 19) to perform blood collection before anesthetized. The preparation of platelet-rich fibrin (PRF) is shown in Figure 20. Blood samples were treated according to the PRF protocol.[20] The preparation method is shown in a flow chart (Figure 20). The fur on the ear was shaved, and the skin was disinfected with 70% alcohol. Eight mL of autologous whole blood (Group 3 and 4) was collected from central ear artery (Figure 21) by needle gauge No.20 connected with 10 ml. sterile syringe without anticoagulant. It is best to insert the needle into the artery as distally (toward the tip of the ear) as possible. If another needle insertion is required, the needle

can be moved proximally about 1 inch from the insertion site. The needle gauge No.20 was inserted into the artery (about 2/3 the way up the central ear artery, with the tip of the needle pointing toward the base of the ear). The blood should flow immediately through the tube, and then the drawn syringe was to collect the blood. After 8 ml. of autologous whole blood has been collected, removed the needle from the artery, and hold off the artery with gauze until bleeding stopped. Then the whole blood was transferred into 10 ml. glass tube and placed immediately into the swinging bucket rotor (Labofuge 400R® centrifuge, Hereus, Hanau, Germany) for centrifugation at 3000 rpm for 10 minutes (Figure 22). A fibrin clot was then obtained in the middle of the tube, just between the red corpuscles at the bottom and acellular plasma at the top. The part of PPP was discarded with a syringe. After that the fibrin clot was collected with straight non-toothed forceps and cut the PRF clot into two halves with an iris stitch scissor (Figure 23-24).

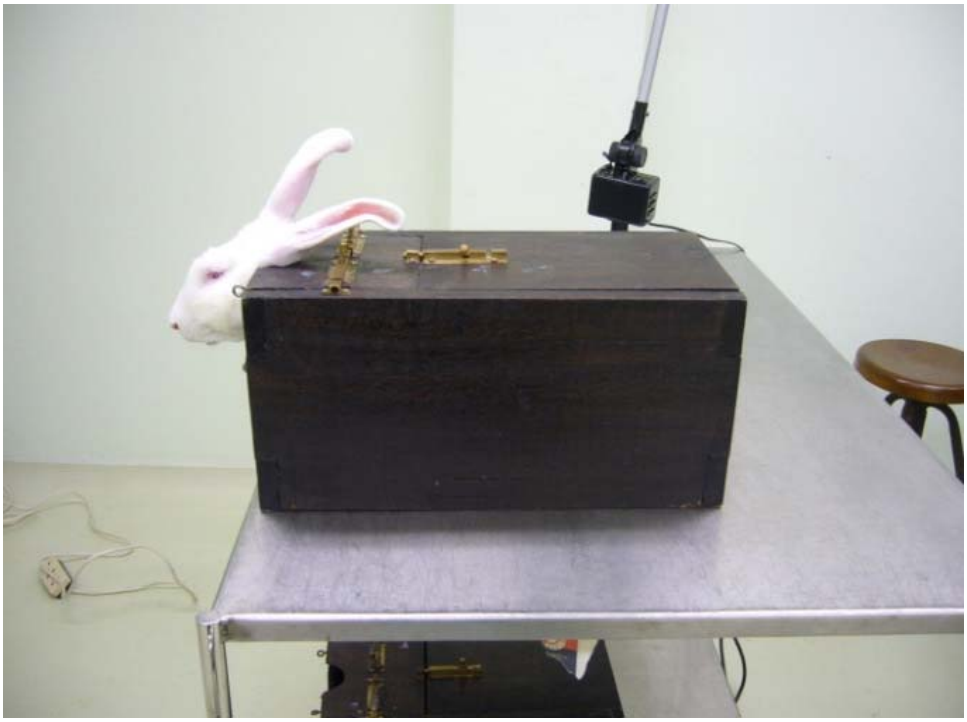

Figure 19. The rabbit was controlled in the restrain box.

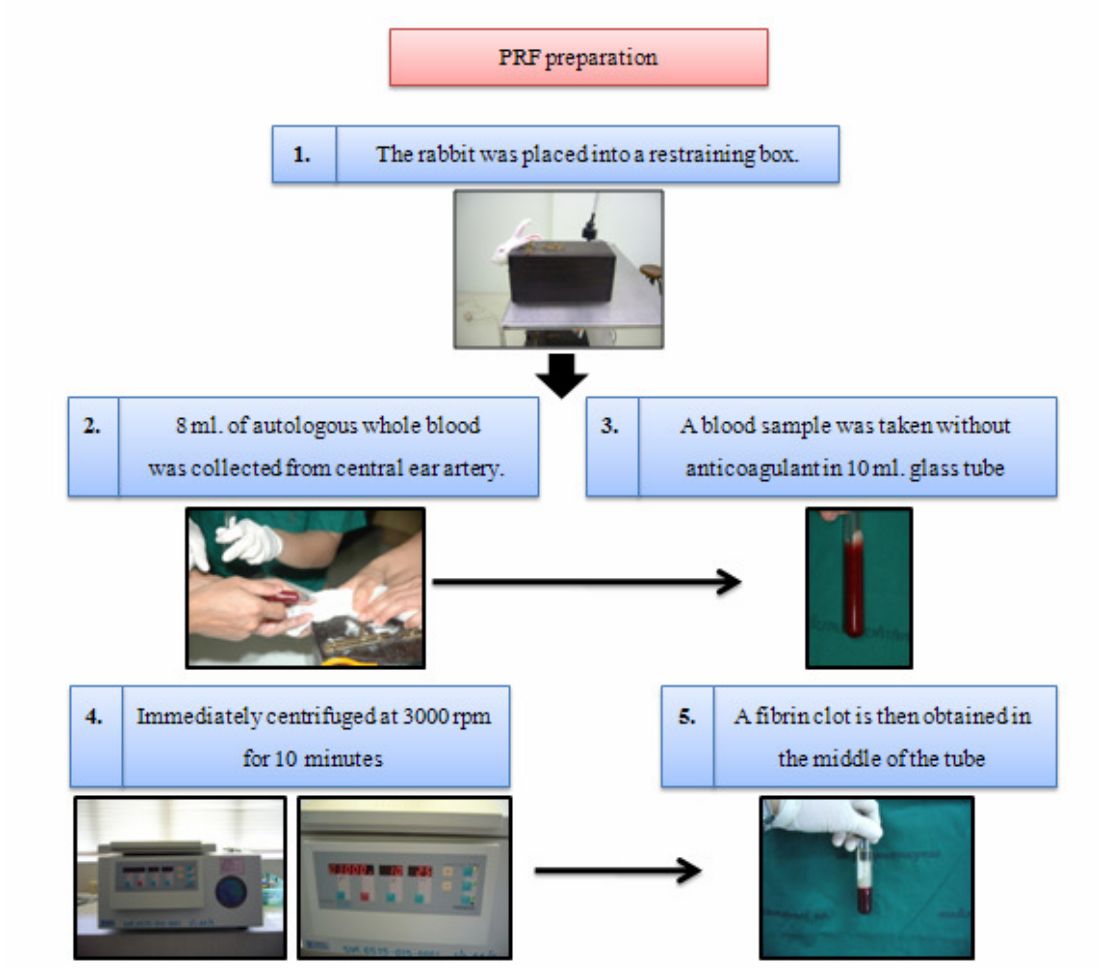

Figure 20. Flow chart of PRF preparation protocol.

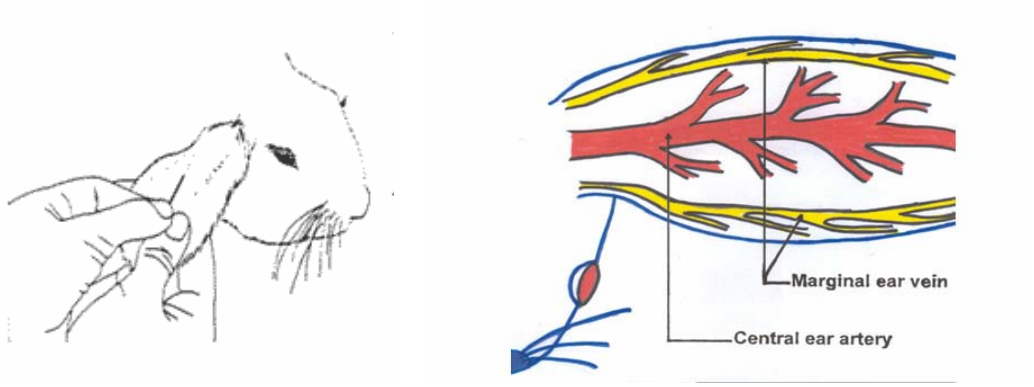

Figure 21. Illustration of the rabbit's ear artery that was used to collect the blood sampling.

Figure 22. Labofuge 400R® centrifuge was used for preparation of PRF.

Figure 23. Blood processing with a centrifuge for PRF allowed the composition of a structured fibrin clot in the middle of the tube (arrow), just between the red corpuscles at the bottom and acellular plasma at the top.

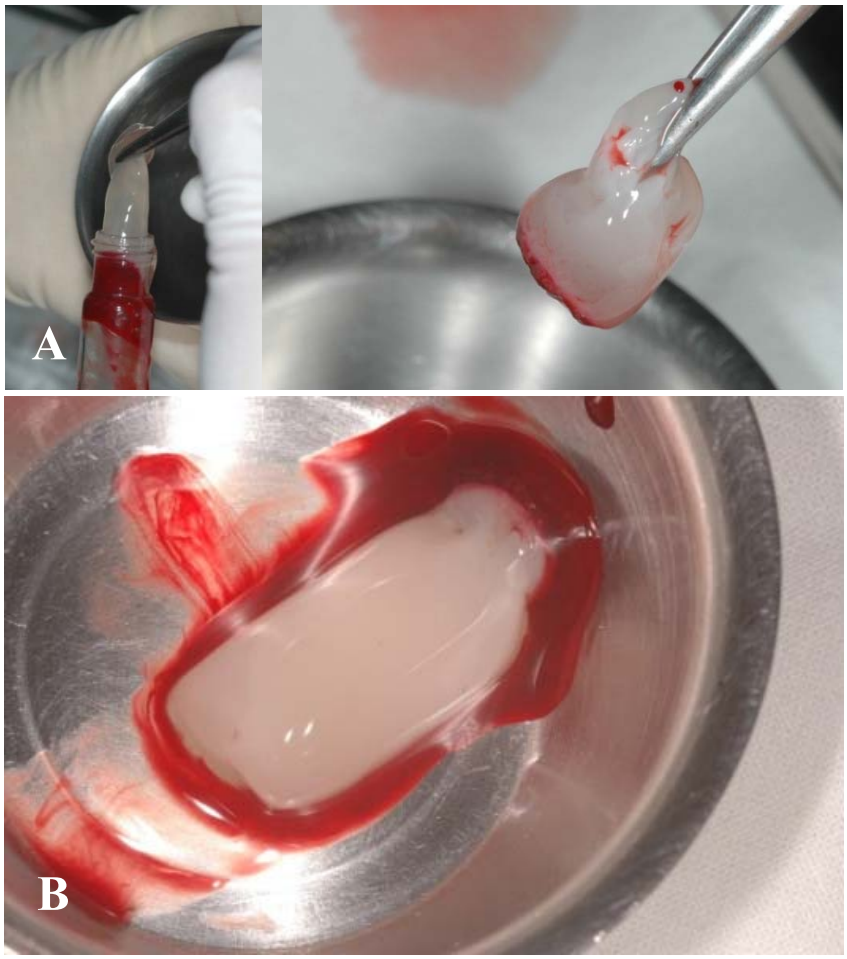

Figure 24. The PRF was collected with straight non-toothed forceps (A). A collection of the PRF itself (B).

3.2 Anesthesia in surgical procedure the experimental rabbit

The rabbit was placed on the surgical table in a prone position. Anesthesia was induced by ketamine 25 mg/kg and diazepam 5 mg/kg intramuscularly into the gluteal region. Three minutes later, an intravenous catheter was placed into the marginal ear vein for intravenous anesthesia (Figure 25). Thiopental 5 mg/kg was administered intravenously and then titrated at the rate of 2 mg/kg every 15 minutes (maximum dose not more than 30 mg/kg)[82] until achieving the level of unconsciousness. The intravenous fluid, Dextrose 5% in ¼ Sterile saline (D5 ¼ S) at the rate of 4 ml/kg/hr was given throughout the operation.

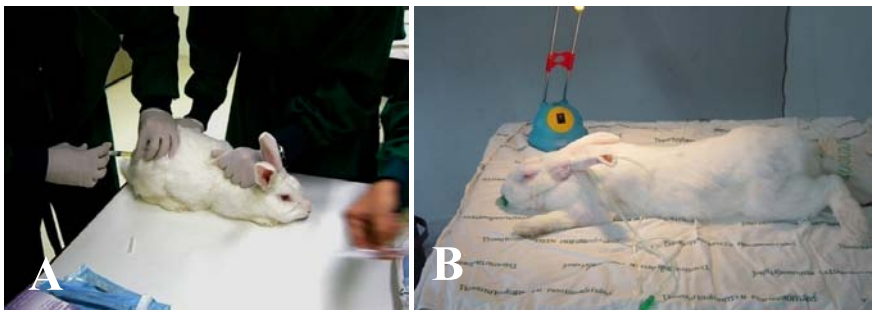

Figure 25. The animal was anesthetized by ketamine 25mg/kg and diazepam 5 mg/kg intramuscularly into the gluteal region (A). Then intravenous anesthesia was administered with thiopental (B).

All surgical procedures were performed under aseptic conditions by the same surgical team. The surgical method is shown in a flow chart (Figure 26). When the animal was in the level of anesthesia, the calvarial region was shaved and disinfected with Providone-Iodine 10%, and then draped to allow aseptic access to an operation field (Figure 27). Mid-sagittal incision from the nasal to the occipital region was performed after local infiltration of 2% lidocaine HCL with 1:100,000 epinephrine 1.8 ml (Figure 28). The subperiosteal dissection was carried out (Figure 29), and 2 bicortical bone defects sized 10 X 10 mm. were created in the left and the right parietal bone with a small round bur and a fissure bur which activated by a micro motor. A sterilized aluminum size 10X10 mm was used as a surgical template (Figure 30). A square bone plug was gently removed and avoided injury to the dura mater. A 1 mm deep circular marking was made with a small round bur and filled with preheated gutta percha for later identification of the defect edges on the histological sections (Figure 31). **In group 1,** a defect was left empty for a negative control of critical size defect in one side and the other side was filled with minced autogenous bone from the removed calvarium as a positive control. Autogenous bone was cut with side-cutting rongeur forceps then minced with bone morselizer (total weight of 0.24 mg) and placed in the contra lateral side as mentioned above (Figure 32-33). **In group 2**, DBB was soaked with normal saline and mixed with minced autogenous bone from the removed calvarium (autogenous:DBB at 1:1 ratio by weight to achieve total weight of 0.24 mg.) and placed in one side and the contra lateral side was placed with DBB alone (Figure 34). **In group 3**, PRF clot was divided into 2 halves. Iris scissors was used to cut the PRF clot

through a long axis. Then one half of PRF was placed into the critical size defect in one side and the other half was mixed with autogenous bone chips (0.24 mg) and placed in the contra lateral side (Figure 35). **In group 4,** PRF clot was also divided into 2 halves. DBB was soaked with normal saline and mixed with minced autogenous bone chips and one half of PRF (autogenous: DBB at 1:1 ratio by weight to achieve total weight of 0.24 mg) was placed in one side and the contra lateral side was placed with the DBB (0.24 mg) and the other half of PRF (Figure 36). Subsequently, the periosteal, the muscle and the skin were sutured with Vicryl® 4-0, and Providone-Iodine 10% was applied to the wound. After surgery, each rabbit was returned to its cage and it could ambulate within 2 or 3 hours after surgery. The single dose of pethidine (10 mg/kg) was administered intramuscularly for post-operative analgesic. For the post-operative antibiotic, PGS 1,000,000 units were injected intramuscular once daily for the first week. All animals were fed a standard diet and water ad libitum until the date of sacrifice.

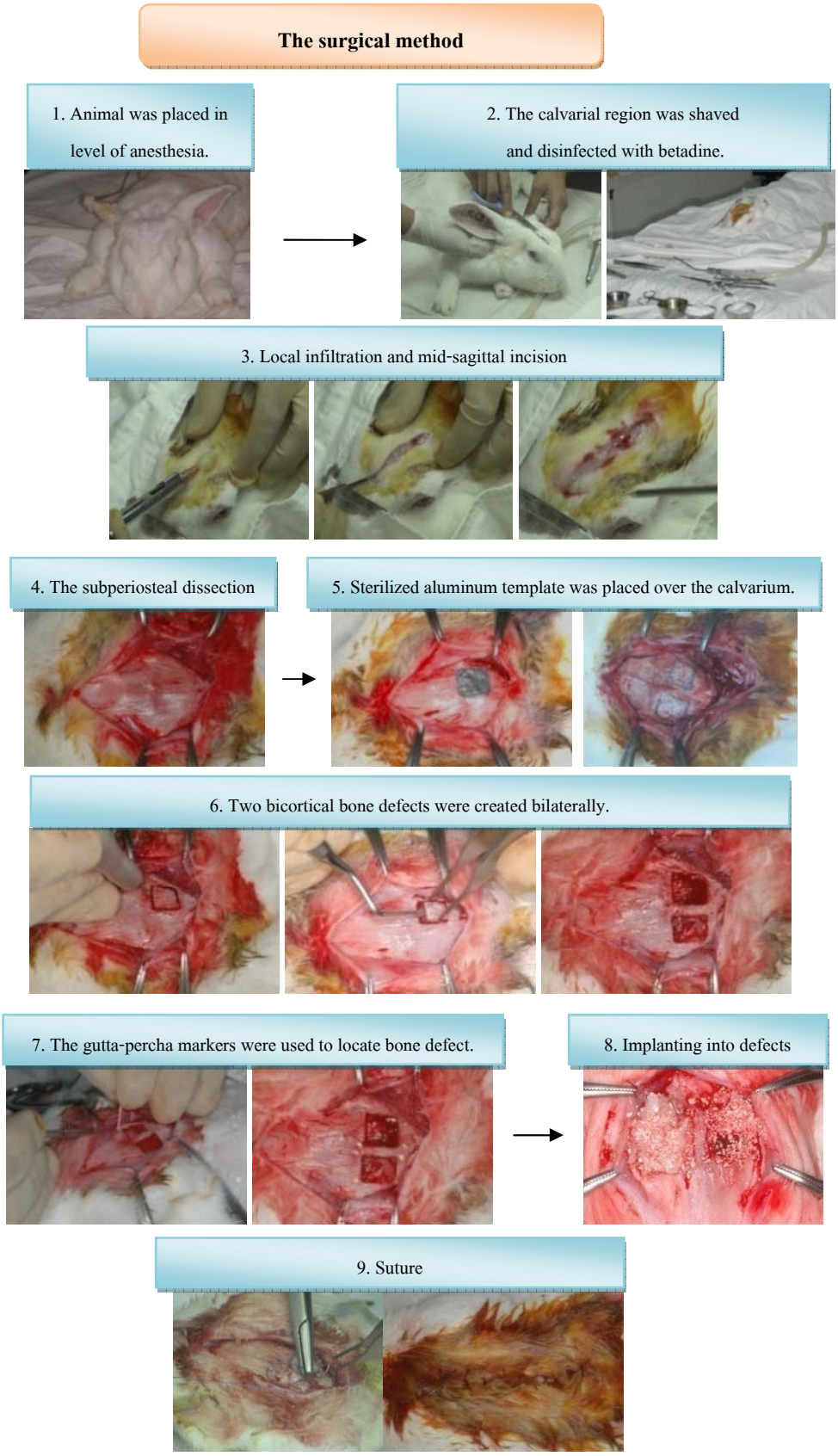

Figure 26. Flow chart of surgical method

Figure 27. Position of the animal on the table (A). The incision site was carefully draped to create a sterile area (B).

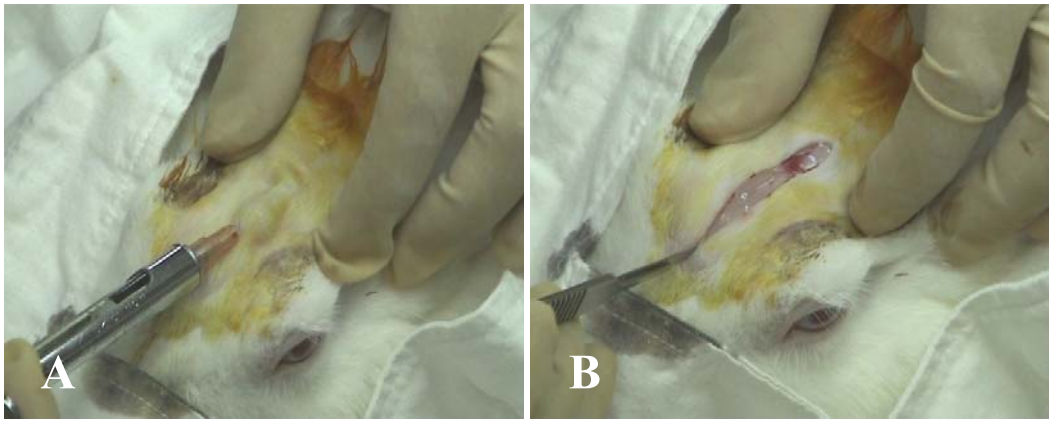

Figure 28. The incision line was infiltrated with 1.8 ml of 2% lidocaine HCL with 1:100,000 epinephrine (A). The sagittal incision was made from a nasal to an occipital part of a rabbit (B).

Figure 29. A skin-periosteal flap was raised to expose the calvarial surface on both sides of the midline.

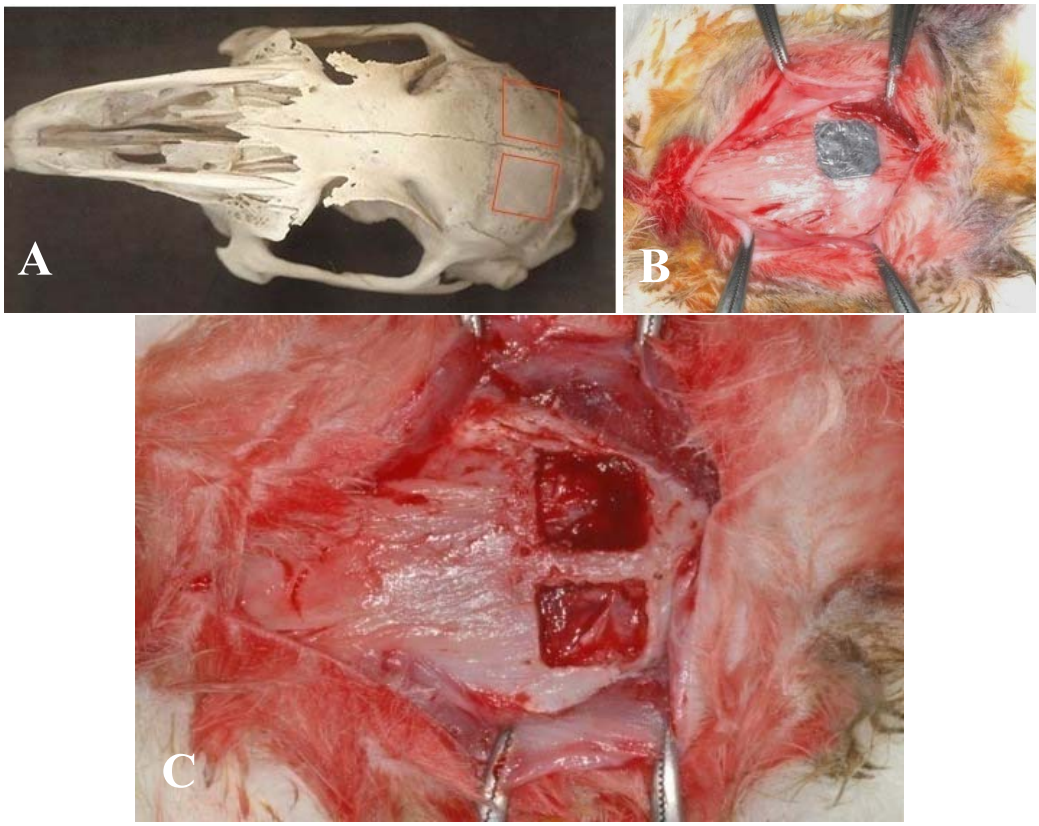

Figure 30. Schematic presentation of the critical size defects in rabbit calvarial (A). Two bicortical bone defects with 10x10 mm were prepared according to a sterilized aluminum template (B). Two rectangular critical-sized defects 10X10 mm. were created in the parietal bones (C).

Figure 31. The gutta-percha markers were used to locate bone defect (arrows).

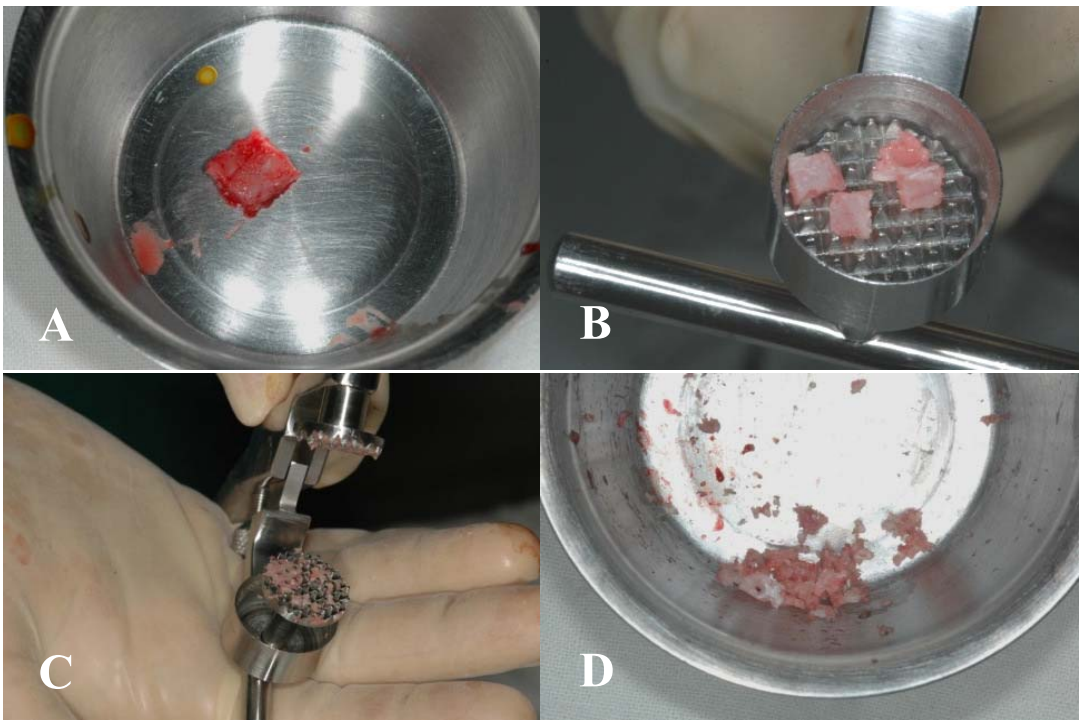

Figure 32. The 2 bicortical bone defect size was 10 X 10 mm (A). Harvested bone was placed in a well of bone morselizer (B). Bone was morselized between knurled titanium surfaces (C). Bone chips were removed from instrument diameter, before implantation (D).

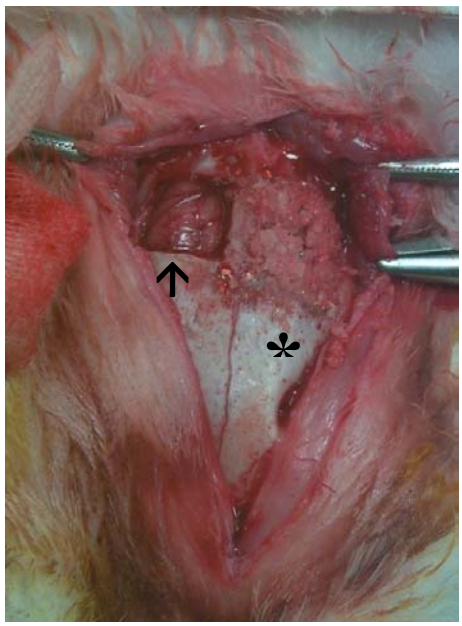

Figure 33. CSD alone (arrow) and autogenous bone chips (star) were implanted into the bone defect.

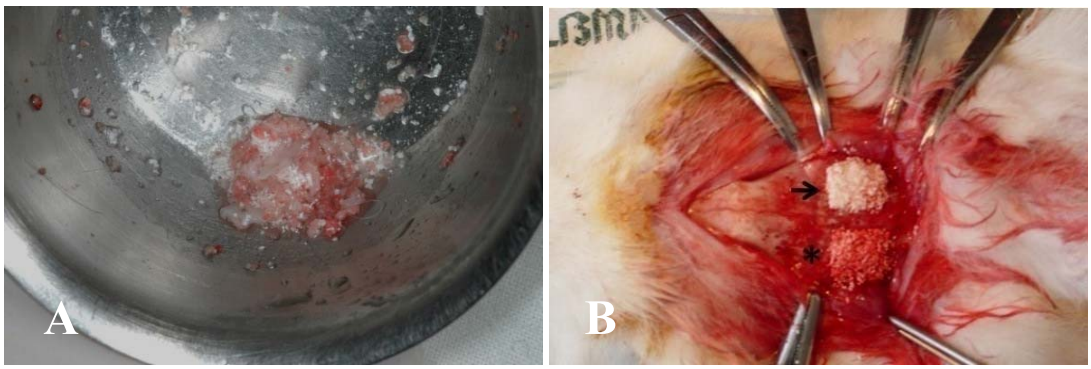

Figure 34. Composite DBB and autogenous bone chips at 1:1 ratio by weight (A) DBB alone (arrow) and composite of DBB and autogenous bone chips (star) were implanted into the bone defects (B).

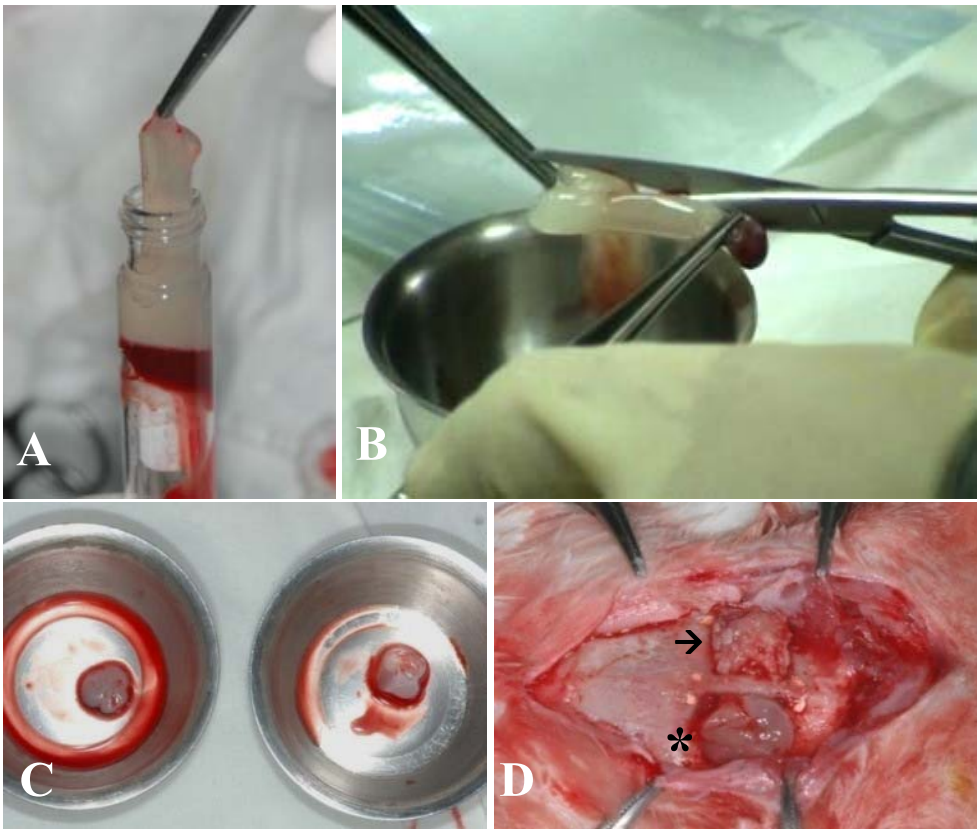

Figure 35. PRF was collected with straight non-toothed forceps (A). PRF clot was divided into 2 halves by iris scissors (B). Two halves of PRF clot (C). Autogenous bone chips were mixed with PRF (arrow) and PRF alone (star) were implanted into the bone defects (D).

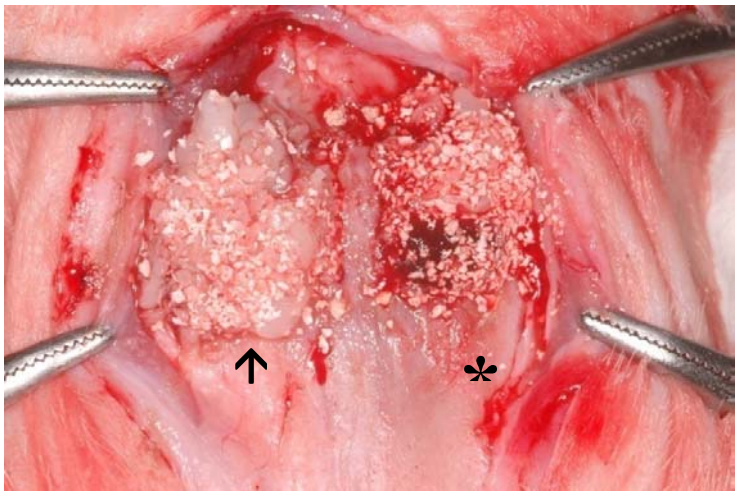

Figure 36. DBB mixed with PRF (arrow), DBB mixed with minced autogenous bone chips and PRF (star) were implanted into the bone defects.

3.3 Tissue processing

The animals were sacrificed with an overdose of pentobarbital sodium 200mg/ml intravenously via marginal ear vein 1.2-1.3 ml (Figure 37). Then calvarium was removed in one piece with fissure bur in a slow-speed micromotor under copious saline irrigation. The specimens were fixed in 10% formalin solution and submitted to radiographic and microscopic analysis for histomorphometric analysis.

Figure 37. The animal was sacrificed by pentobarbital administered via marginal ear vein.

3.4 Scanning electron microscopy (SEM) analysis

Two gel samples of PRF were immediately immersed in a sodium cacodylate-buffered formaldehyde–glutaraldehyde fixative for 24 hours at room temperature and post-fixed in 20% osmium tetroxide for 2 hours. Subsequently, samples were dehydrated by serial transfers in ascending concentrations of acetone (50–100%) and infiltrated with liquid carbon dioxide before the critical drying point. Finally, the samples were made electrically conductive by mounting on aluminum slabs with a silver point, followed by sputter coating with gold/palladium using the SPI-Module Sputter Coater & Carbon-Coater (SPI Supplies, Division of Structure Probe, Inc., West Chester, PA, USA) to a thickness of approximately 250A °. The above specimens were attached to an acrylic plate with glue tape (Figure 38). Finally, PRF clots were examined with a JSM-5800 scanning electron microscope (JEOL, JSM-5800LV, Tokyo, Japan) at The Scientific Equipment Center, Prince of Songkla University (Figure 39).

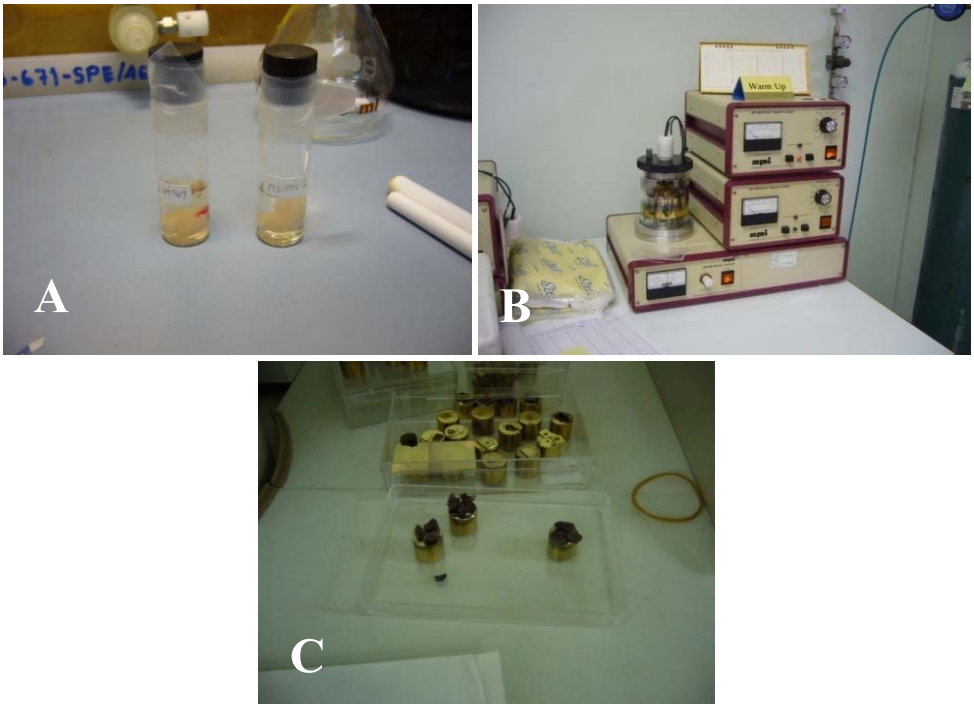

Figure 38. PRF clots were immersed in a sodium cacodylate- buffered formaldehyde–glutaraldehyde fixative (A). SPI-Module Sputter Coater & Carbon-Coater was used for the gold coating of scanning electron microscopy examination (B). The specimens were attached to an acrylic plate with glue tape (C).

Figure 39. JSM-5800LV Scanning electron microscope.

3.5 Radiographic method

Radiographs of the surgical region were obtained immediately post operative, 4 and 8 weeks post surgery. After sacrifice at 8 weeks, the specimens from the calvarial were radiographed. The radiographic method is shown in a flow chart (Figure 40). The animal was sedated with ketamine 25mg/kg and diazepam 5 mg/kg intramuscularly into the gluteal region before radiograph was taken. To obtain radiographic image of the rabbit calvarial defect, the animal was placed in the prone position. Kodak Ultra-Speed dental occlusal film (D-speed film) was placed into the parallel film holder device for parallel technique radiograph. Aluminum step wedge and 5X5 mm. aluminum foil were fixed on the film for calibrating in radiomorphometry process. Then the film was placed beneath the animal's head (Figure 41). The dental radiographic machine (Gendex, Gendex Co., IIIinois, USA) with short cone tube fixed with parallel film holder was used. The radiographs were exposed with 40-cm dff, 10 mA, 60kvp and 1.25 sec in every animal. The X-ray beam was perpendicular to the plane of the film.

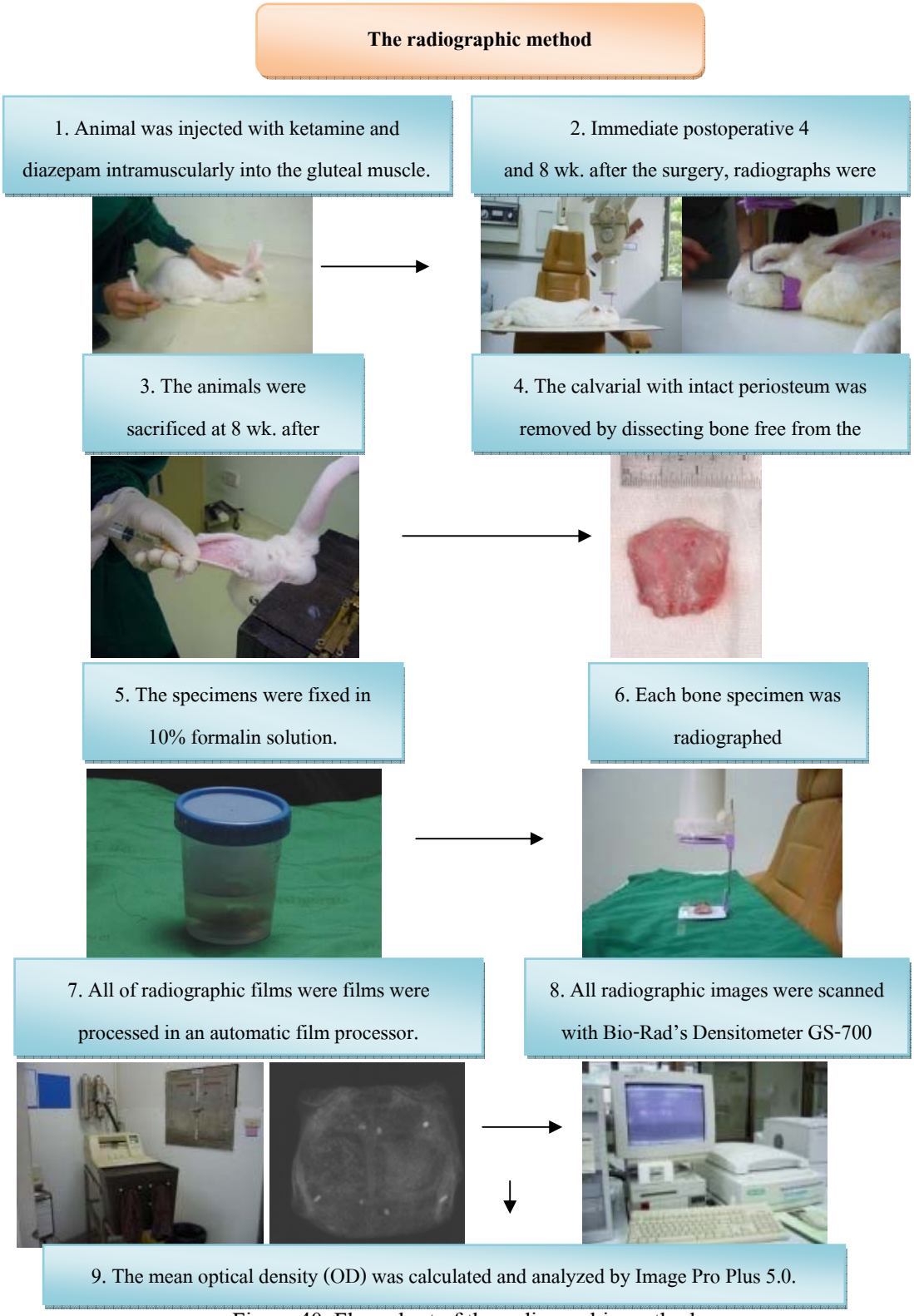

Figure 40. Flow chart of the radiographic method

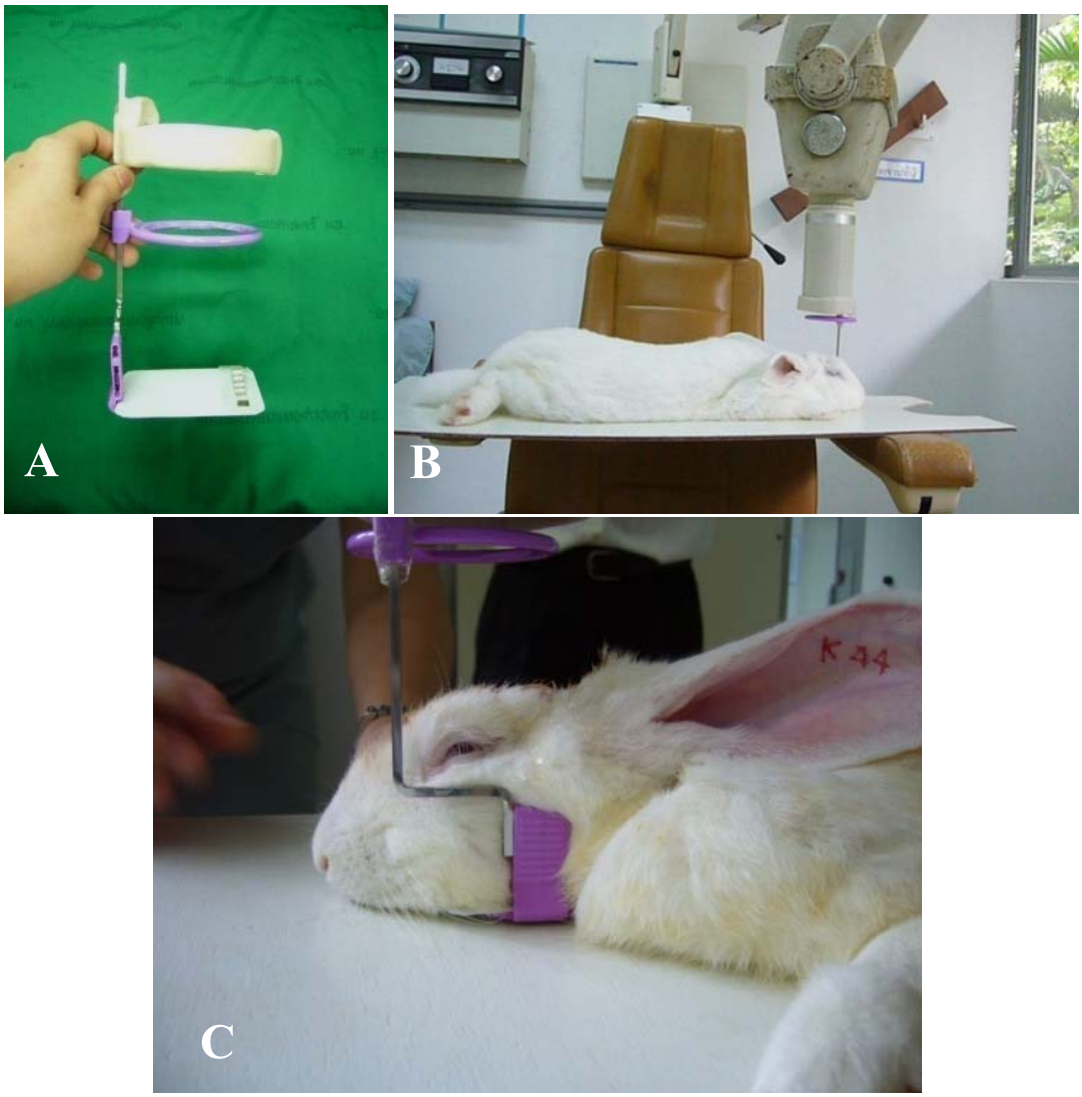

Figure 41. The parallel film holder device was used to obtain parallel technique radiograph, and fixed distance (A). The animal was placed in a prone position during radiographic procedure (B, C).

To obtain radiographic image of a bone specimen, a bone specimen was placed on a film and attached to the parallel film holder device for parallel technique radiograph. The parallel film holder device was developed from extension cone paralleling (XCP) to use in all of the radiographic examination (Figure 42). The dental radiographic machine (Gendex, Gendex Co., IIIinois, USA) with short cone tube fixed with parallel film holder was used. The radiographs were exposed with 40-cm dff, 10 mA, 50kvp and 0.42 sec in every specimen. The X-ray beam was perpendicular to the plane of the film.

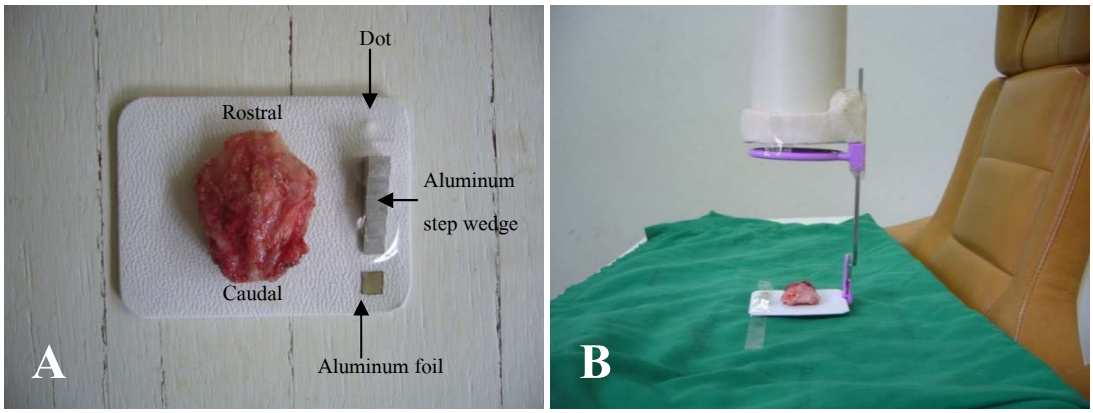

Figure 42. The bone specimen was placed on an x-ray film (A). The parallel film holder device was used for parallel technique radiograph (B).

All of radiographic films were taken by the same dental radiographic machine and then processed by an automatic film processor (Dent X 9000, Dent X/Logetronics GmbH, Kornberg, Germany) (Figure 43). Immediately after the radiographic procedure, each specimen was returned to fix in 10% formalin solution. All radiographic images were scanned into the computer with Bio-Rad's Densitometer GS-700 (BIO-RAD Laboratories Ltd, Hemel Hempstead, UK) to obtain digital radiographic images of the specimens (Figure 44). The digital radiographic images were transferred to a computer and assessed the bone density within 10x10 mm. bone defect. Then the native bone surrounding the defect of all specimens was measured (Figure 45). The digital radiographic images were blind assessed by one investigator. The mean optical density (OD) was calculated and analyzed by Image Pro Plus 5.0 (Media Cybernetics Inc., USA)

Figure 43. An automatic film processor (Dent X 9000, Dent X/Logetronics GmbH, Kornberg, Germany).

Figure 44. Bio-RAD GS-700 Imaging densitometer.

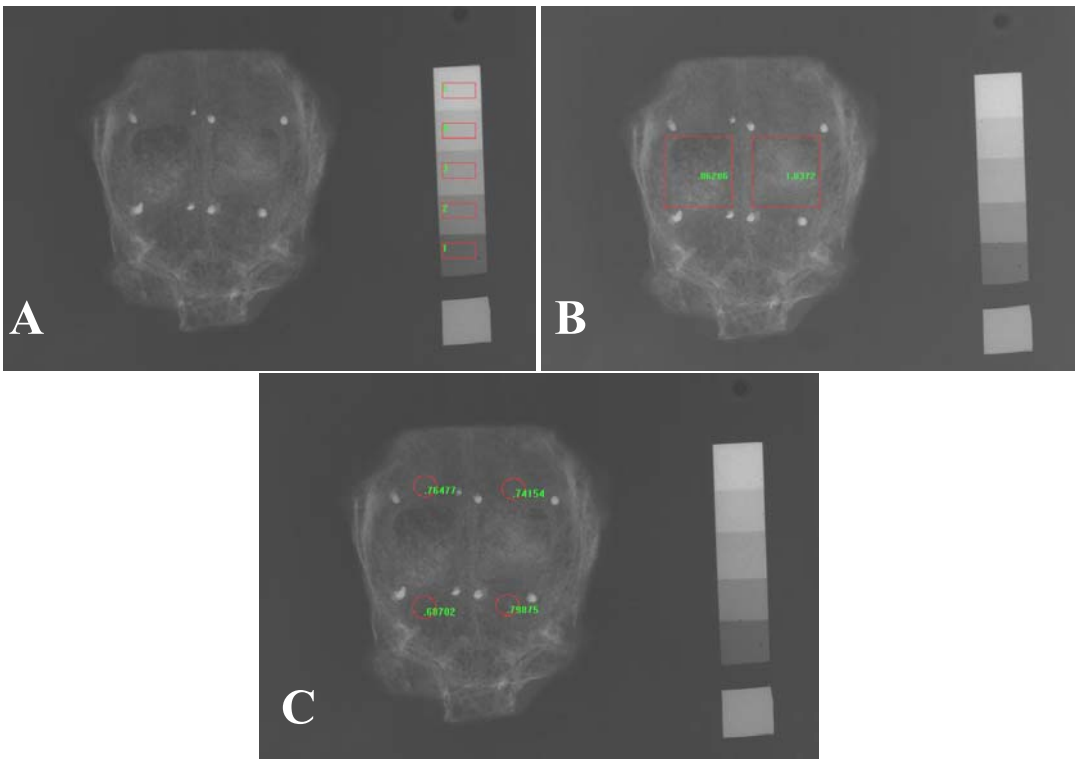

Figure 45. The mean optical density (OD) was calculated and analyzed by Image Pro Plus 5.0. First, the optical density of each step of the step-wedge was calibrated (A). The optical density within the bone defects of both sides were measured (B). The optical density of native bone surrounding the defects were measured (C).

3.6 Histotechnical preparation

Following radiography, three bur holes markers were made with a small round bur, one mm. from the edge of the defect on the left side of the periosteal side of each specimen (Figure 46).

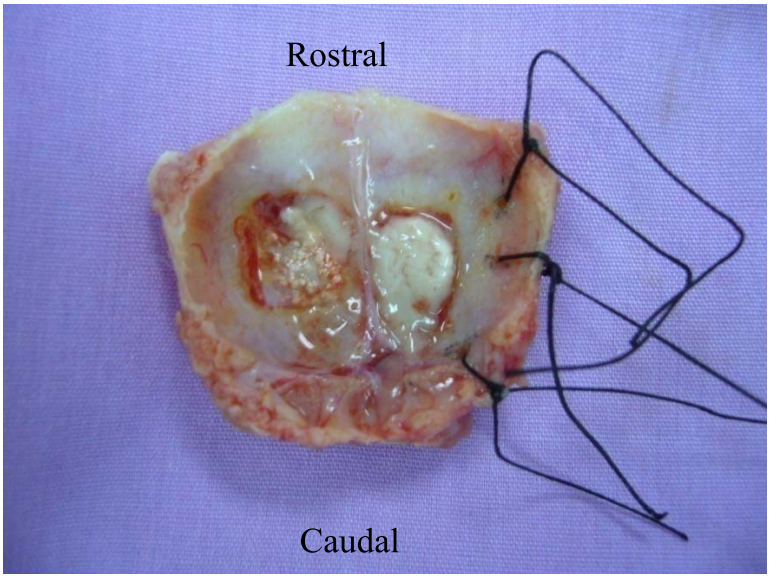

Figure 46. Each bone specimen was sutured with black silk into the prepared bur holes marker for identified the left side of the periosteal side of the specimen.

The calvarial specimens were decalcified in 10% formic acid which was subsequently changed every day for 3 weeks (Figure 47) and agitated at 160 rpm on an orbital shaker (KS 130 Basic Orbital Shaker, IKA Works, USA) (Figure 48). It is necessary to test for completion of decalcification before processing the tissue. Testing chemically for the end-point in decalcification is the only accurate method for determination of the complete removal of the calcium. The methods of needle-testing, flexibility, and x-ray have been extremely variable in results.[83] Decalcification was confirmed by the absence of a precipitation in the supernatant when a solution of saturated ammonium oxalate was added. Three mL of decalcification solution from the bottom of the specimen container was placed in a test tube and added 3 ml. of concentrated ammonium oxalate solution, then the tube was shook and left for 10 minutes. If after ten minutes there is any precipitate visible (slight cloudiness) there is still calcium present

and the specimen needs further decalcification (Figure 49). The end-point was achieved when a precipitation failed to appear upon the addition concentrated ammonium oxalate solution. Then the tissue was left in the same decalcifying solution for at least 48 hours longer and the test was repeated (Figure 50). This is necessary because the density of bone impedes the penetration of the reagent into the middle of the specimen.

Figure 47. Decalcification was performed by using acid decalcifying agent, 10% formic acid (A). 10% formic acid was changed daily day for 3 weeks (B).

Figure 48. The each calvarial specimen was decalcified in 10% formic acid and agitated at 160 rpm on an orbital shaker (KS 130 Basic Orbital Shaker).

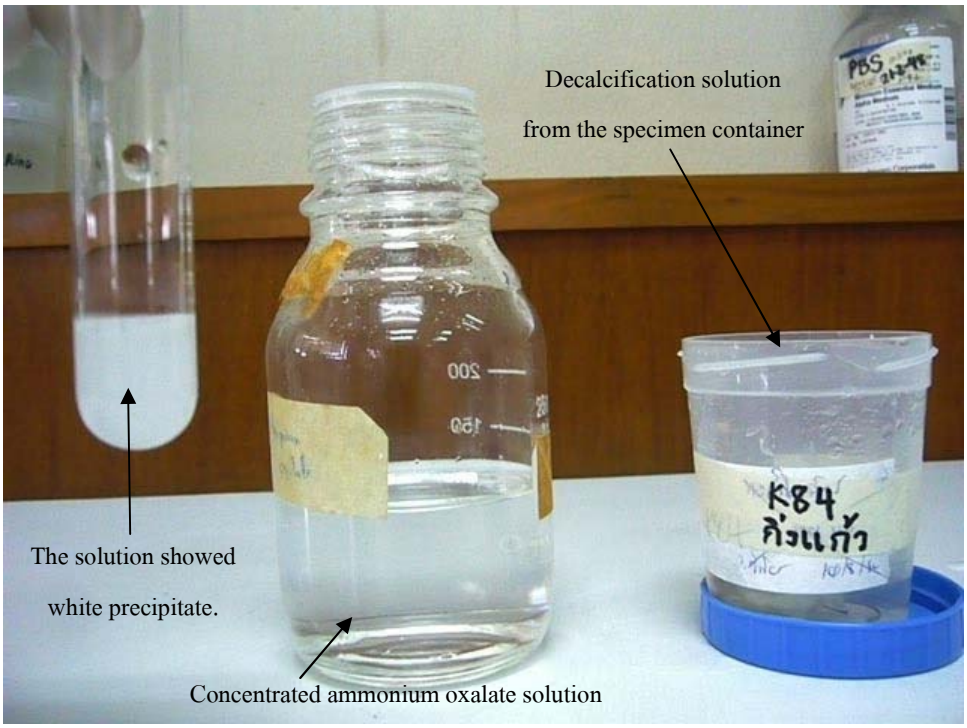

Figure 49. The remaining calcium in decalcifying tissue was tested with concentrated ammonium oxalate solution. The solution showed white precipitate (or cloudiness) when calcium was presented.

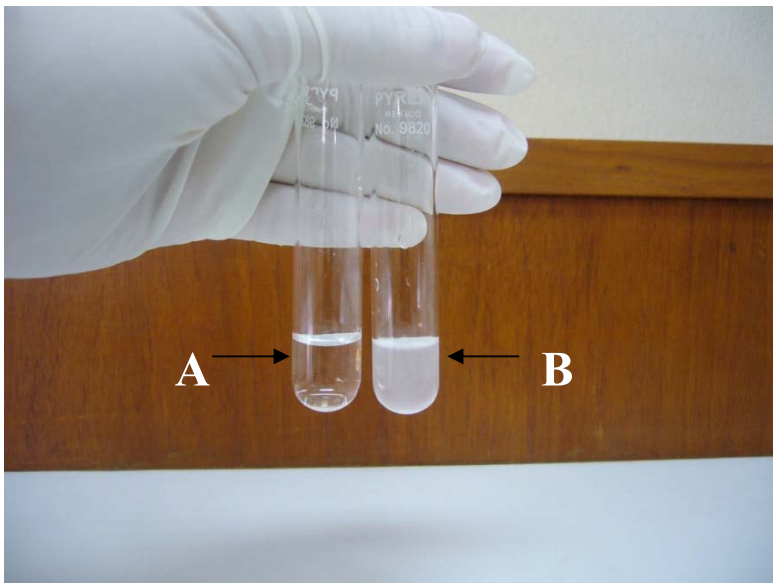

Figure 50. Clear solution without precipitation shows complete decalcification endpoint (A). The formation of a cloudy solution caused by precipitation of calcium oxalate indicated incomplete decalcification (B).

After complete decalcified, each bone specimen was divided into an upper, a middle and a lower part by a surgical blade No.22 , then placed into a disposable plastic cassette (Figure 51). An automatic tissue processor (Lipshaw automatic tissue processor model 2500A, Lipshaw, USA) was used to provide programs for fixing, dehydrating, clearing and paraffin impregnating (Figure 52). Serial sections of 5 µm were cut from each part using a microtome (Leica Model RM2135, Leica Microsystems, Germany), then stained with hematoxylin and eosin (H&E) and Masson's Trichrome using with an automated tissue staining (Shandon Linistain™ GLX Linear Stainer, Thermo Shandon Inc, USA.) (Figure 53). All slides were examined descriptively for detection of new bone formation, residual DBB particles, soft tissue element and inflammatory reactions by one calibrated examiner before histomorphometry analysis.

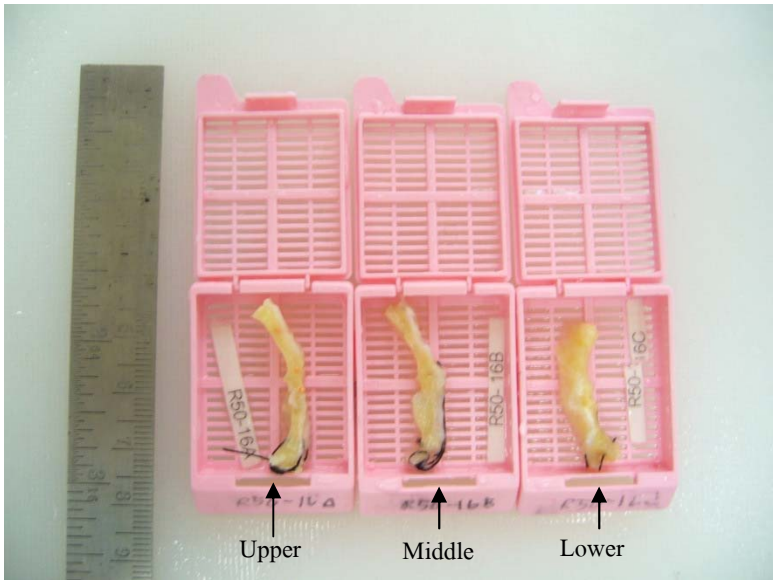

Figure 51. Each bone specimen was divided into an upper, a middle and a lower part, then placed into a disposable plastic cassette.

Figure 52. An automatic tissue processor (Lipshaw automatic tissue processor model 2500A).

Figure 53. Shandon Linistain™ GLX Linear Stainer.

3.7 Histomorphometric analysis

Computer-assisted histomorphometry was preformed in order to measure the amount of newly formed bone in the defect. The middle parts of the sections were used for histomorphometric analysis which had been done by the same examiner, all specimens were evaluated in a blinded, nonbiased using an image analysis system by measuring the percentages of newly deposited bone. The system consists of the followings:

1. An infinity corrected light microscope, Carl Zeiss model. Axiostar, with objective achromatic 5x and eyepiece 10x.
2. High resolution digital camera, Carl Zeiss model Axiocam mRC with adapter 0.63X for fit the field of view.
3. An image capture device (Axioversion)
4. A computer-based image processor for histomorphometry (Image Pro Plus™ 5.0 Media Cybernetic, Silver Springs, MD, USA)

The histologic images of the defect region were captured at X5 magnification using a light microscope (Axiostar, Carl Zeiss, Germany) coupled to an high resolution digital camera (Axiocam mRC, Carl Zeiss, Germany), connected to a PC computer (Figure 54). From each histologic cut, total fields were captured, covering the entire defect. Images of newly

formed bone were identified with a higher magnification and then label with a given color in each image. These were digitized and transferred into the computer software for image processing and analyzing the quantity fraction of the total area in the experimental and control sites. The percentage of bone area in the experimental and control bone defect were calculated (Figure 55).

$$\text{Percent bone area} = \frac{\text{Mineralized bone area X 100}}{\text{Total bone defect area}}$$

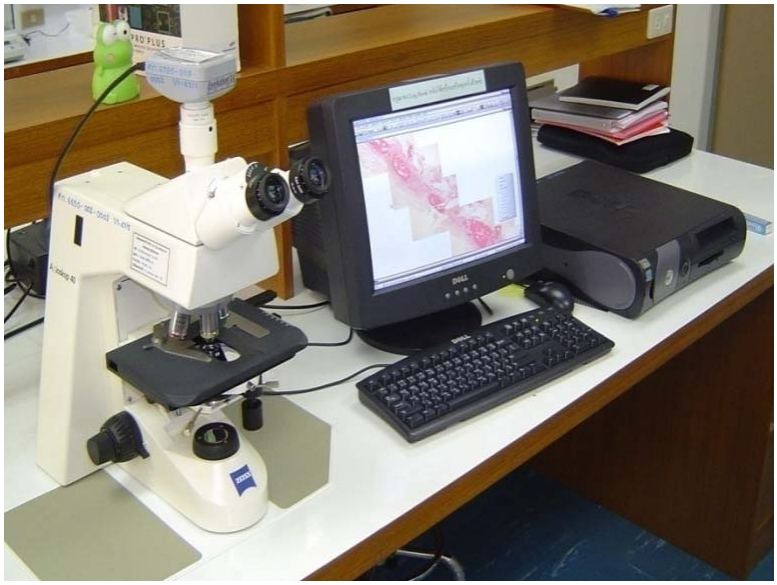

Figure 54. A microscope imaging system for histomorphometry analysis.

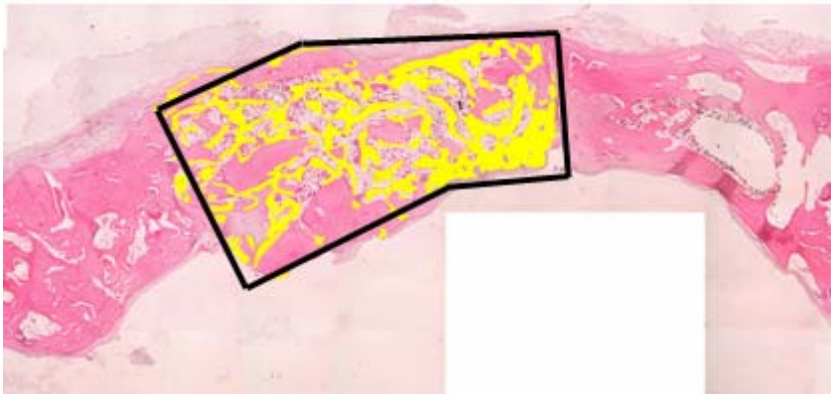

Figure 55. Histological slide stained with hematoxylin and eosin. The continuous (black) line contains the total bone defect. Newly formed bone (yellow) was marked in the defect.

3.8 Statistic analysis

Summary statistics (means ± SD) were calculated based on individual animal measurements. The radiomorphometry analysis and histomorphometry analysis assessments were made by a single investigator who was blinded to animal's group, thereby preventing bias. OD and percent bone area were measured 3 times separately to reduce the bias and then calculate the mean.

A descriptive and quantitative were performed by the same observer (K.P.) and thus were possibly impaired by memory. However, the quantitative analysis was performed 1 month after the descriptive. We believed that this time interval was long enough to reduce the potential memory bias to a negligible level. The difference in amount of radiographic bone density and percentage of new bone between the experimental and control sides were tested for normal distribution when distribution was normal, One-way analysis of variance and multiple comparison by Tukey HSD test ($p<0.05$) were used. The statistical analysis was performed using SPSS software (version 13.0, SPSS, Chicago, IL, USA). The significance level set at $p< 0.05$

Chapter 3

Results

1. Scanning electron microscopy (SEM) analysis

The SEM study yielded clear images of the elements that constituted the PRF clot, which had a scaffold appearance. It contained randomly arranged fibrillar elements, of homogeneous thickness throughout their length, with platelet cell elements arranged among them (Figure 56). The platelets did not show the typical morphology of their resting state but rather showed morphologic signs of the activated state, ovoid platelet cell elements with exocytosis phenomena (Figure 57).

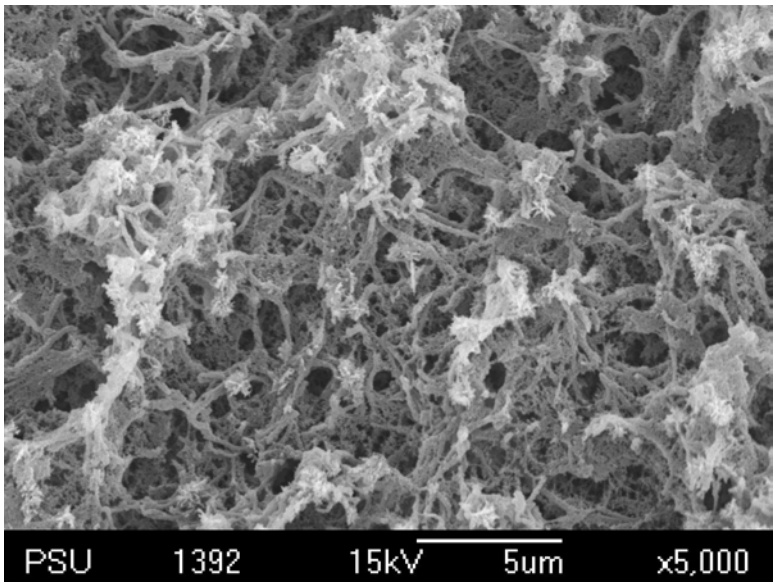

Figure 56. Scanning electron microscopy of rabbit PRF. Platelet cell elements can be observed trapped among fibrillar elements, original magnification, X 5,000.

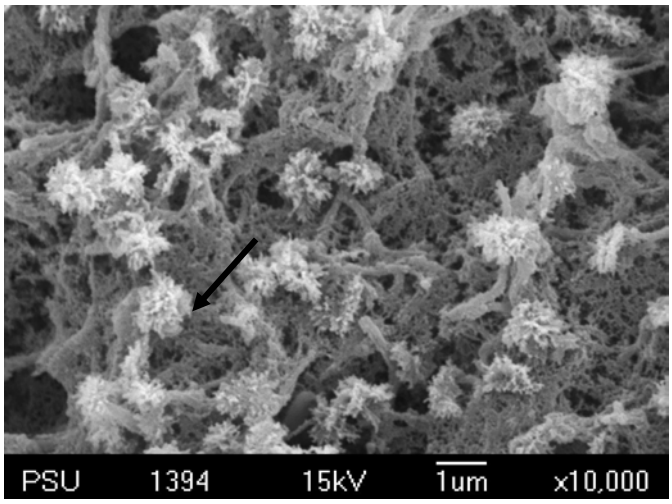

Figure 57. Scanning electron microscopy of rabbit PRF. The activated platelet (arrow) was illustrated by these cells, original magnification, X 10,000.

2. Clinical observation

All animals well tolerated with the surgical procedure and the anesthesia. They recovered rapidly after surgery without any evidence of wound infection or wound dehiscence. There was no accidental death of rabbit throughout the study period. After full recovery, they were able to eat the pellet food and drink water ad libitum (Figure 58). After euthanasia and epiperiosteal exposure of the calvaria no infection of the hard and soft tissues was detectable. The underlying brain and dura were kept intact.

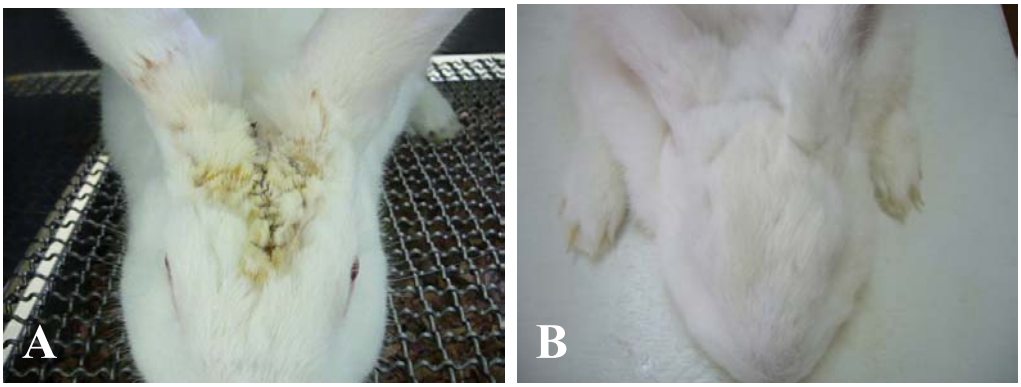

Figure 58. Examination at 1 week postoperatively, there was no wound dehiscence, exposure of the bone grafting materials or infection (A). All of the experimental animals had good wound healing before sacrifice at 8 week after the surgery (B).

3. Gross morphological evaluation

The macroscopically examination showed the graft blended into the surrounding host bone and denser in test groups (group 3 and group 4) than control groups (group 1 and group 2), respectively**. In group 1** (CSD alone Vs. Autogenous bone chips), the CSD side was occupied with soft fibrous tissue in all 5 specimens. The surface of the defect area was flat and soft in consistency. But the bone defect edge was projected into the defect with bone-like tissue projection which was dense and bone-like hardness in consistency. The filled surface of defect was under the margin of surrounding host bone. The autogenous bone chips side was filled with dense bone-like tissue in all specimens. The defect area had flat surface (Figure 59). **In group 2** (Composite DBB+autogenous bone chips (1:1) Vs. DBB alone), the composite DBB+autogenous bone chips side (1:1) was filled with bone-like tissue and DBB particles blended with the margin. The DBB alone side was filled with bone-like tissue at the defect edge but soft at the central part of the defect. The DBB particles presented homogenously in the whole area of bone defects with hard consistency. The consolidation of the composite DBB+autogenous bone chips (1:1) was denser than the DBB alone (Figure 60). **In group** 3 (CSD+PRF Vs. Autogenous bone chips+PRF), the CSD+PRF side was occupied with soft fibrous tissue. The defect area had flat surface, not dense, but the bone defect edge was extended with dense bone-like tissue. The CSD+PRF side were occupied with bone-like tissue in 4 specimens entire the defect with bone-like hardness in consistency. The CSD+PRF side presented of bone-like tissue including in the central area of the defect and displayed similar level of the surrounding host bone. The autogenous bone chips+PRF side was filled with very dense bone-like tissue. However one specimen had flat surface. In 4 specimens, the thicknesses at the central part of the defect were approximately 2-3 mm. The volume of bone-like tissue in the autogenous bone chips+PRF side was much greater and denser than the CSD+PRF side (Figure 61-62). The size of bony defect in the autogenous bone chips+PRF side was much smaller than the CSD+PRF side. The defect margin of the autogenous bone chips+PRF side was blended into the surrounding host bone better than the CSD+PRF side. **In group 4** (Composite DBB+ autogenous bone chips (1:1)+PRF Vs. DBB+PRF), The volume of bone-like tissue in the composite DBB+ autogenous bone chips (1:1)+PRF side was much greater and denser than the DBB+PRF side. The DBB particles were still observed in both the composite DBB+ autogenous

bone chips (1:1)+PRF side and the DBB+PRF side. The consolidation of the composite DBB+autogenous bone chips (1:1)+PRF was better than the DBB+PRF (Figure 63). The defect area was prominent and the thickness was 0.5-2.0 mm. at the central part of the defect in all of 5 specimens. The defect area of the DBB+PRF side had flat surface in 2 specimens and the thickness was 0.5-2.0 mm. at the central part of the defect in 3 specimens.

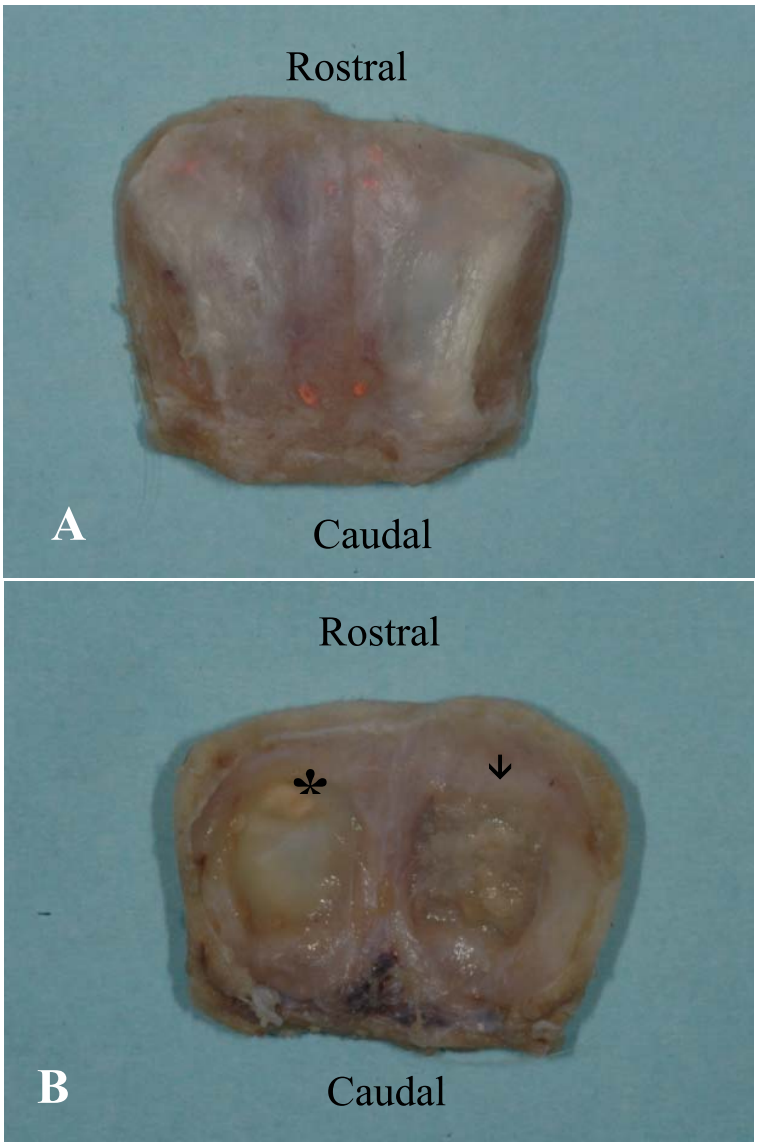

Figure 59. In group 1, the specimen of rabbit calvarium at 8 weeks postoperatively. On the periosteal side (outer side) of the rabbit calvarium, the periosteum was still remained and attached to the bone (A). On the endocranium side (inner side) of the rabbit calvarium (B), the autogenous bone chips side (arrow) and the CSD side (star).

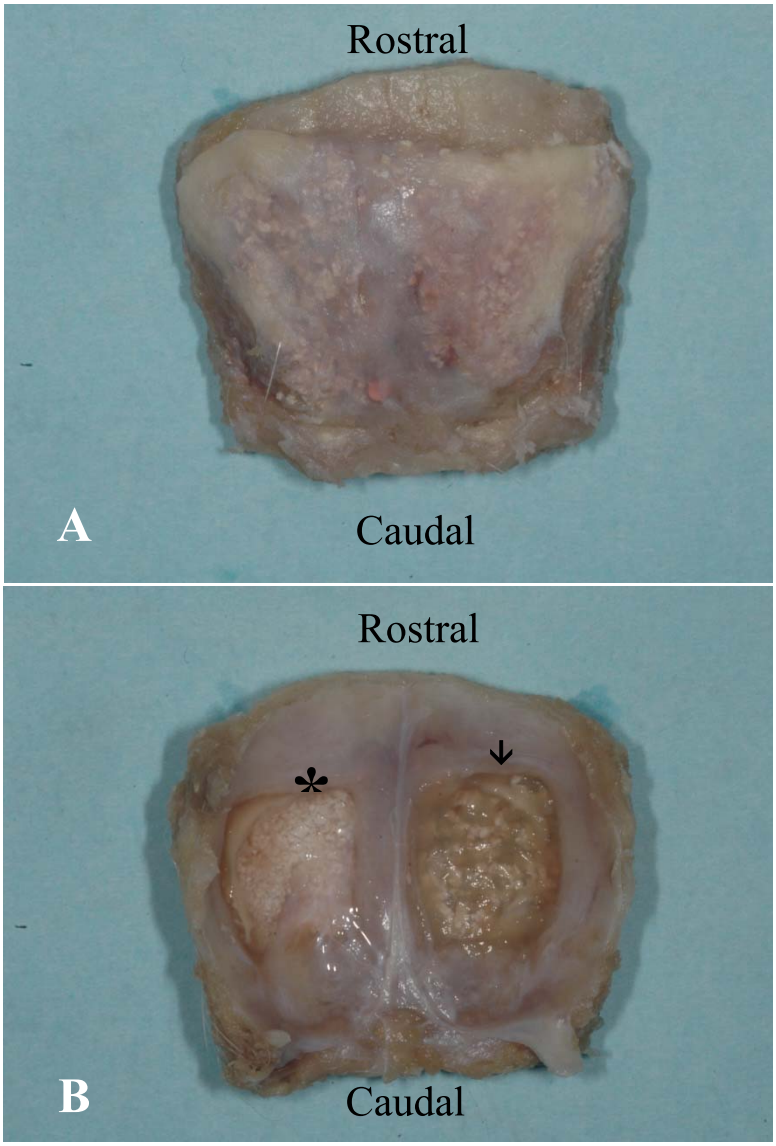

Figure 60. In group 2, specimen of rabbit calvarium at 8 weeks postoperatively. On the periosteal side (outer side) of the rabbit calvarium, the periosteum still remained and attached to the bone (A). On the endocranium side (inner side) of the rabbit calvarium, the composite DBB+ autogenous bone chips (1:1) (arrow) and the DBB side (star).

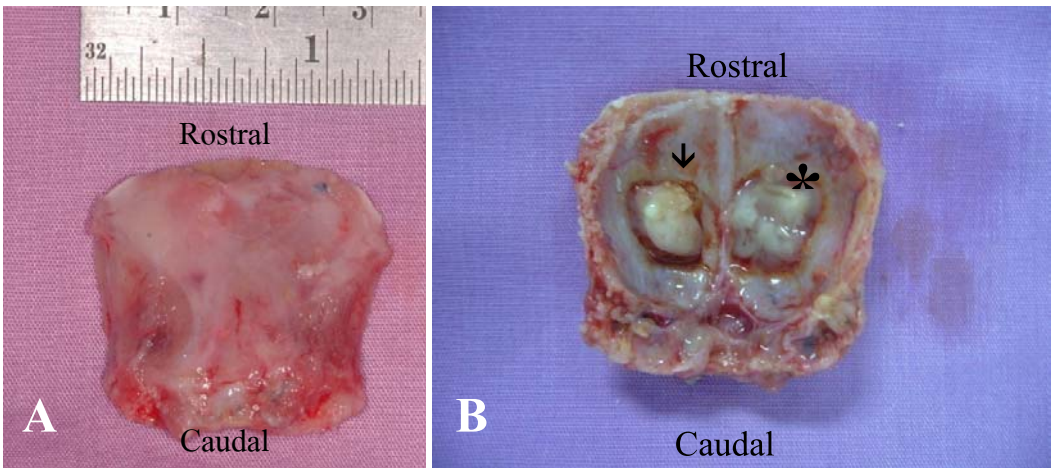

Figure 61. In group 3, the specimen of rabbit calvarium at 8 weeks postoperatively. On the periosteal side (outer side) of the rabbit calvarium, the periosteum still remained and attached to the bone (A). On the endocranium side (inner side) of the rabbit calvarium (B), the autogenous bone chips+PRF side (arrow) and the CSD+PRF side (star).

Figure 62. The cross section of the defect area showed volume of bone-like tissue in the autogenous bone chips+PRF side (arrow) which was much greater than the CSD+PRF side (star).

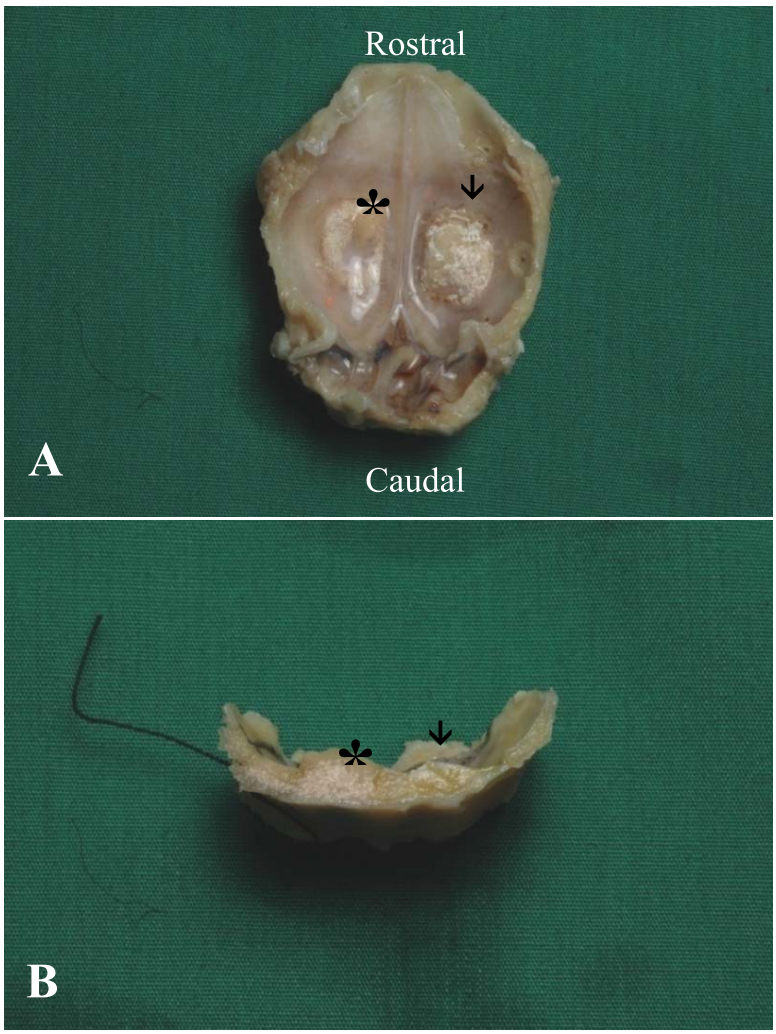

Figure 63. In group 4, specimen of rabbit calvarium at 8 weeks postoperatively. On the endocranium side (inner side) of the rabbit calvarium, the composite DBB+ autogenous bone chips (1:1)+PRF side (arrow) and the DBB+PRF side (star).

The gutta-percha marker around bone defect at both site were observed in all specimens. The gutta-percha marker was shown as biocompatible material because there was no sign of infection at the marker area. These markers were helpful for locating the bone defect margin, although, the bone original defect margins of both sites could be observed in all specimens (Figure 64).

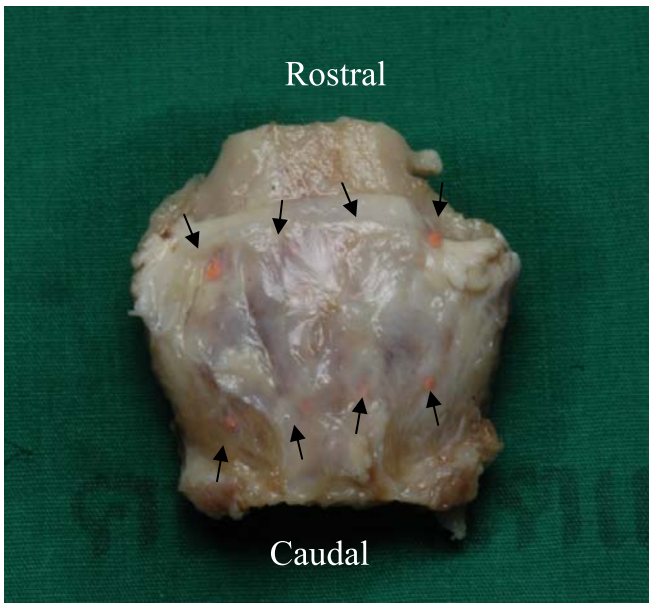

Figure 64. Specimen of rabbit calvarium at 8 weeks postoperatively. Eight arrows indicated the gutta-percha number at the corner of the defect margin. The periosteum was still remained and attached to the bone.

4. Radiographic evaluation

Radiographs of the surgical region were obtained immediately post operative, 4 and 8 weeks after the surgery and after sacrifice at 8 weeks postoperatively.

4.1 Radiographic features

Control group: In group 1 (CSD alone Vs. Autogenous bone chips), the CSD side was showed homogenous radiolucent area over nearly entire bony defect. The upper and lower parts of the defect were replaced with radiopaque mass, and its density was similar to that of normal bone. The autogenous bone chips side showed radiopaque mass of bone chip with varying sizes and densities. Homogenous radiopaque areas were apparent near the margins of the defects with similar density to that of normal bone (Figure 65). **In group 2** (Composite DBB+autogenous bone chips (1:1) Vs. DBB alone), a well-delineated of radiopaque area of a bone defect was seen. The bone defects were filled with the distinct radiopaque granules of DBB. The density of DBB alone side presented more radiopaque than the composite

DBB+autogenous bone chips (1:1) side (Figure 66). Test group: **In group 3** (CSD+PRF Vs. Autogenous bone chips+PRF), the CSD+PRF side showed homogenous radiolucent area in the central part of bony defect. The homogenous radiopaque area was found around the edge of the defect with similar density to a normal bone. The autogenous bone chips+PRF side showed more radiopaque than the CSD+PRF side and both sides of group 1 and group 2. The size of bony defect was much smaller than the CSD+PRF side and both sides of group 1 (Figure 67). **In group 4** (Composite DBB+autogenous bone chips (1:1)+PRF Vs. DBB+PRF), The DBB+PRF side showed more radiopaque than the composite DBB+ autogenous bone chips (1:1)+PRF side. The defect margin of the composite DBB+autogenous bone chips(1:1)+PRF side blended into the surrounding host bone better than the DBB+PRF side (Figure 68). The gutta-percha markers were observed in all specimens.

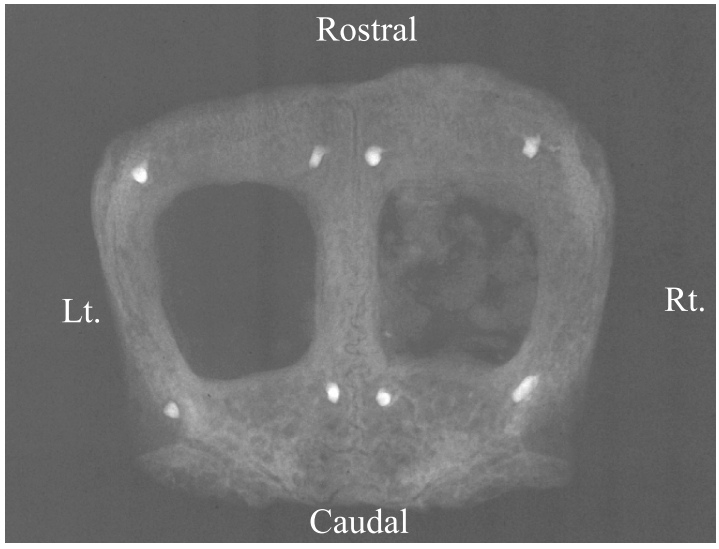

Figure 65. Photograph of the occlusal film of the rabbits' calvarium. The autogenous bone chip was at the right side, the ingrowth of bone from the defect margin was seen, as well as the radiopacity of the grafting materials and the critical size defect was at the left side, clear homogenous radiolucent area was seen. The defect margins of both sides were presented, the critical size defect side had more intact and sharp demarcation defect margin than those of autogenous bone chip side.

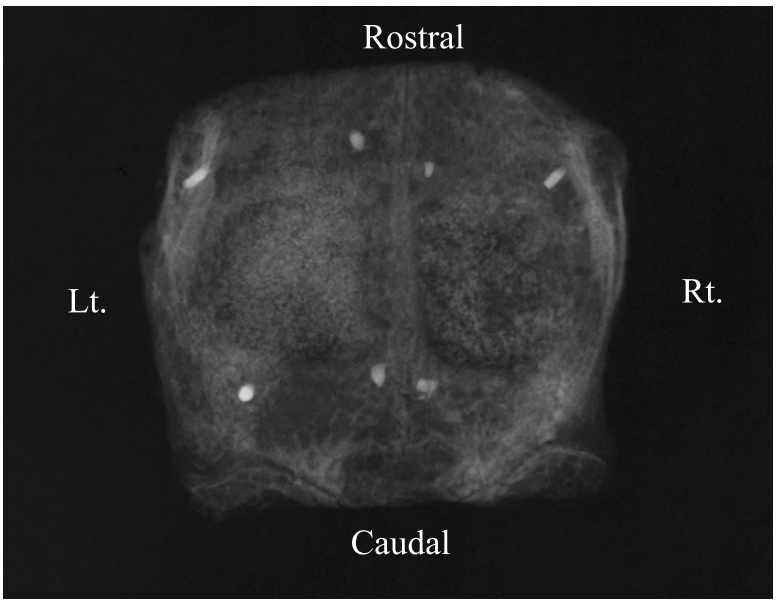

Figure 66. Photograph of the occlusal film of the rabbits' calvarium. The composite DBB+autogenous bone chips (1:1) was at the right side and the DBB alone was at the left side. The defect margins of both sides were observed but not intact.

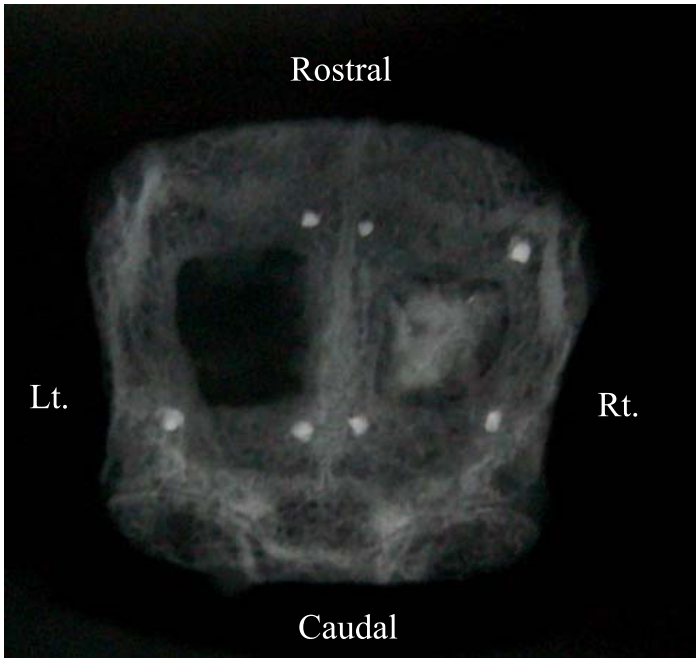

Figure 67. Photograph of the occlusal film of the rabbits' calvarium. The autogenous bone chips+PRF was at the right side and the CSD+PRF was at the left side. There was a greater opacity in grafts in the autogenous bone chips+PRF side than in grafts in the CSD+PRF.

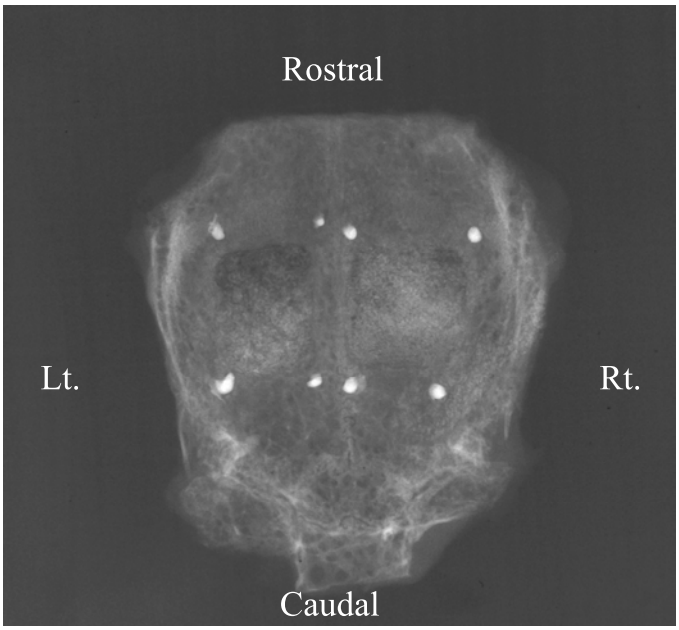

Figure 68. Photograph of the occlusal film of the rabbits' calvarium. The DBB+PRF was at the right side and the composite DBB+ autogenous bone chips (1:1)+PRF was at the left side.

4.2 Radiomorphometry analysis

Detailed computer-assisted analysis of the roentgenograms is presented in Table 9. At 8 weeks postoperatively, mean optical density (OD) of control group, the CSD (0.114±0.062), the autogenous bone chips (0.356±0.027), the composite DBB+autogenous bone chips proportion 1:1 (0.906±0.046), the DBB alone (1.066±0.052). Mean OD of test group, the CSD+PRF (0.294±0.062), the autogenous bone chips+PRF (0.596±0.189), the composite DBB+autogenous bone chips proportion 1:1+PRF (0.810±0.154), the DBB+PRF (1.178±0.167). At baseline, mean OD of native bone was measured (0.736±0.079).

Mean OD of the CSD was the lowest (0.114±0.062). There were statistically significant differences between CSD and all other groups ($p<0.05$). A significant increase in mean OD was seen when the CSD+PRF (0.294±0.062) was compared with the CSD ($p<0.05$). However, there was no significant difference between the CSD+PRF, the autogenous bone chips (0.356±0.027) and the autogenous+PRF (0.596±0.189) ($p>0.05$). There were only the autogenous bone chips +PRF and the composite DBB+autogenous bone chips proportion 1:1+PRF showed the optical density similar to native bone (0.736±0.079), no significant

difference were observed ($p>0.05$).

The DBB were filled into the defects of the composite DBB+autogenous bone chips(1:1) (0.906±0.046), the DBB alone (1.066±0.052), the composite DBB+autogenous bone chips proportion 1:1+PRF (0.810±0.154) and the DBB+PRF (1.178±0.167) groups. Mean OD of these groups are higher than native bone. The marked increase in mean OD were observed because the high opacity of these DBB particles. The results showed a significant increase in mean OD by as much as 10-60% when compared with native bone ($p<0.05$), except for the composite DBB+autogenous bone chips (1:1) +PRF group ($p>0.05$). The adjuvant effect of PRF to the composite DBB and autogenous bone chips (1:1) was slightly decrease in mean OD when compared with the composite DBB+autogenous bone chips (1:1). However, no significant difference was seen ($p>0.05$). There was also no significant difference in mean OD between the DBB alone and the DBB+PRF ($p>0.05$).

Table 9. The data of radiomorphometric (optical density) in group 1, group 2, group 3 and group 4 and native bone respectively.

Group			**Mean optical density (Mean±SD)**
Control groups	Group 1	CSD alone (N=5)	0.114±0.062 [b]
		Autogenous bone chips (N=5)	0.356±0.027 [ab]
	Group 2	Composite DBB+Autogenous bone chips(1:1) (N=5)	0.906±0.046 [ab]
		DBB alone (N=5)	1.066±0.052 [ab]
Test groups	Group 3	CSD + PRF (N=5)	0.294±0.062 [ab]
		Autogenous bone chips + PRF (N=5)	0.596±0.189 [a]
	Group 4	Composite DBB+ Autogenous bone chips(1:1)+PRF (N=5)	0.810±0.154 [a]
		DBB+PRF (N=5)	1.178±0.167 [ab]
Native bone (N=40)			0.736±0.079 [a]

a = significantly different from CSD alone ($p<0.05$)

b = significantly different from native bone ($p<0.05$)

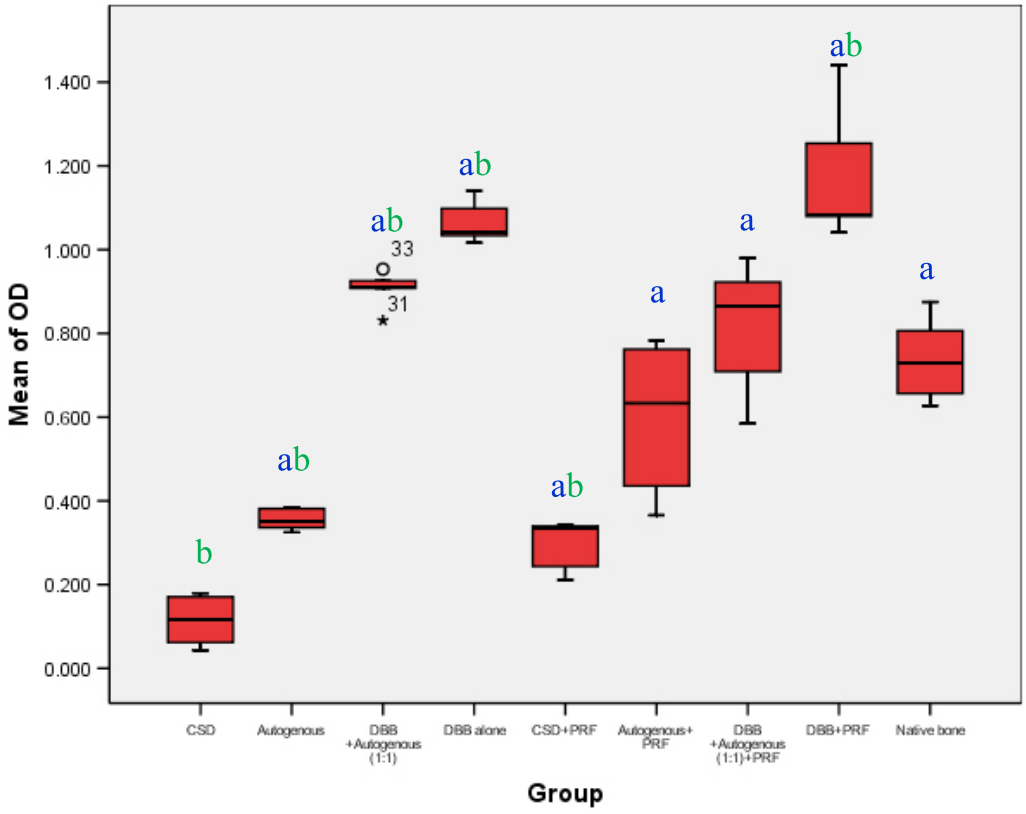

Figure 69. Mean optical density of rabbit's calvarium specimen, values of mean OD are displayed. a = significantly different from CSD alone ($p<0.05$), b = significantly different from native bone ($p<0.05$).

5. Histology

5.1 Histology observation

Control group: In group 1 (CSD alone Vs. Autogenous bone chips), the CSD side, the defect was filled with loose connective tissue and there was very rarely of newly formed bone projected from the defect edge (Figure 70). The autogenous bone chips side, the defects were completely bridged by a combination of newly formed mineralized bone and well-incorporated bone graft. The newly formed bone consisted of woven, parallel-fibered lamellar bone. Most of the bone chips were non-vital, particularly the larger pieces (Figure 71). In group 2 (Composite DBB+autogenous bone chips (1:1) Vs. DBB alone), the composite DBB+autogenous bone chips (1:1) side was filled with complete bone bridging along the defect, presented of generalized newly formed bone throughout the defect. New bone incorporated well

with the autogenous bone chips and the DBB particles (Figure 72). The DBB alone side was filled with the particles and newly formed bone projected from the defect edge and periosteal, extending centripetal and incorporated well with the particles but no new bone was found at the central part of the defect. All of the DBB particles were missing (Figure 73). The newly forming bone or woven bone was in the direct apposition to the DBB particles and there was no fibrous capsule layer detectable between them. Multinucleated giant cell was not found at the border of DBB particles.

Test group: In group 3 (CSD+PRF Vs. Autogenous bone chips+PRF), one of 5 specimens of the CSD+PRF side was filled with loose connective tissue and there was very rare newly formed bone projected from the defect edge. Four of 5 specimens of CSD+PRF side were filled with complete bridging woven bone along the defect (Figure 74). The new bone formation near the defect edges presented small areas of remodeling, stressed by the reversal lines and osteon-like structures (Figure 75-76). The autogenous bone chips+PRF side, the defects were completely bridged by a combination of newly formed mineralized bone and well-incorporated bone graft (Figure 77). The newly formed bone consisted of woven and lamellar bone. The old bone chips were visualized and exhibited new bone formation on their surfaces. Also, some remodeling was noted in the grafted bone, marked by the presence of the reversal lines and osteon-like structures (Figure 78-79). In group 4 (Composite DBB+autogenous bone chips (1:1)+PRF Vs. DBB+PRF), The composite DBB+autogenous bone chips (1:1)+PRF was filled with complete bone bridging along the defect, presented of generalized newly formed bone throughout the defect. New bone incorporated well with the autogenous bone chips and the DBB particles which were missing during histology process (Figure 80-82). DBB+PRF side was filled with the particles and newly formed bone projected from the defect edge and periosteal, extending centripetal and incorporated well with the particles. The newly forming bone or woven bone was direct apposition to the DBB particles. All of the DBB particles were missing. Multinucleated giant cell was not found at the border of DBB particle (Figure 83-85).

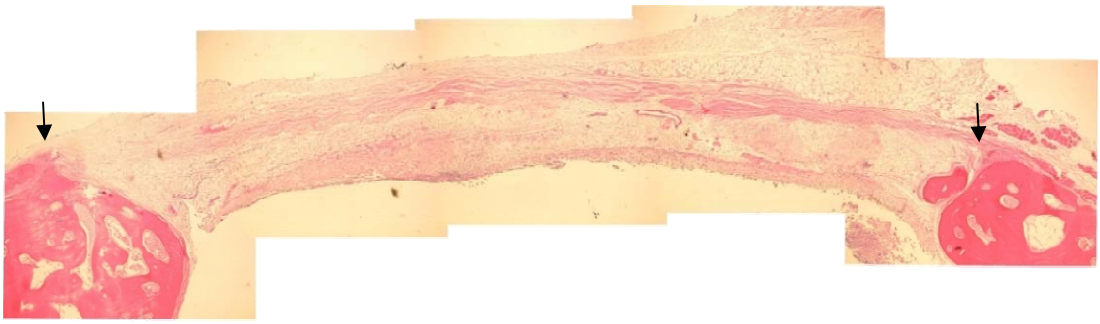

Figure 70. Coronal histological section through the calvarium showing the middle part of the defect of the critical size defect group after 8 weeks. (Specimens stained with Hematoxylin and Eosin, original magnification x5). Arrows indicate the margin site of defects prepared initially.

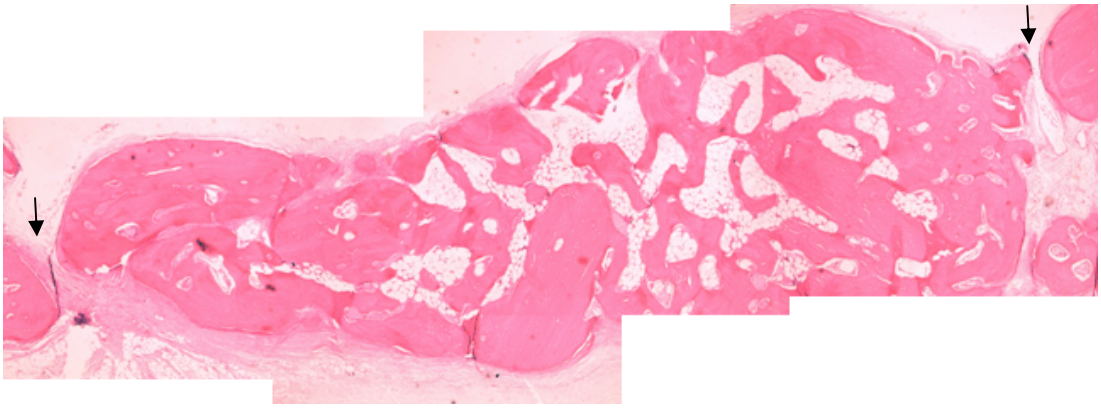

Figure 71. Coronal histological section through the calvarium showing the middle part of the defect of the autogenous bone chips group after 8 weeks. (Specimens stained with Hematoxylin and Eosin, original magnification x5). Arrows indicate the margin site of defects prepared initially.

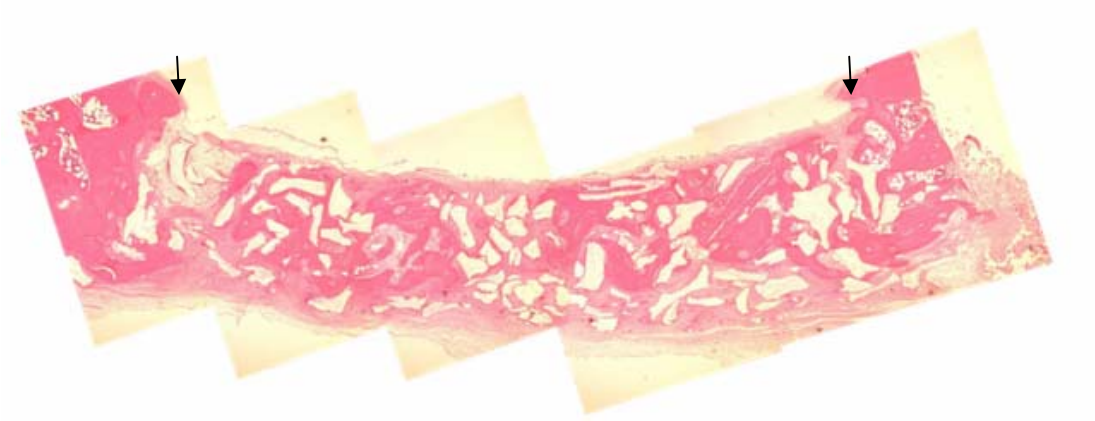

Figure 72. Coronal histological section through the calvarium showing the middle part of the defect of the composite DBB+autogenous bone chips proportion 1:1 group after 8 weeks. (Specimens stained with Hematoxylin and Eosin, original magnification x5). Arrows indicate the margin site of defects prepared initially.

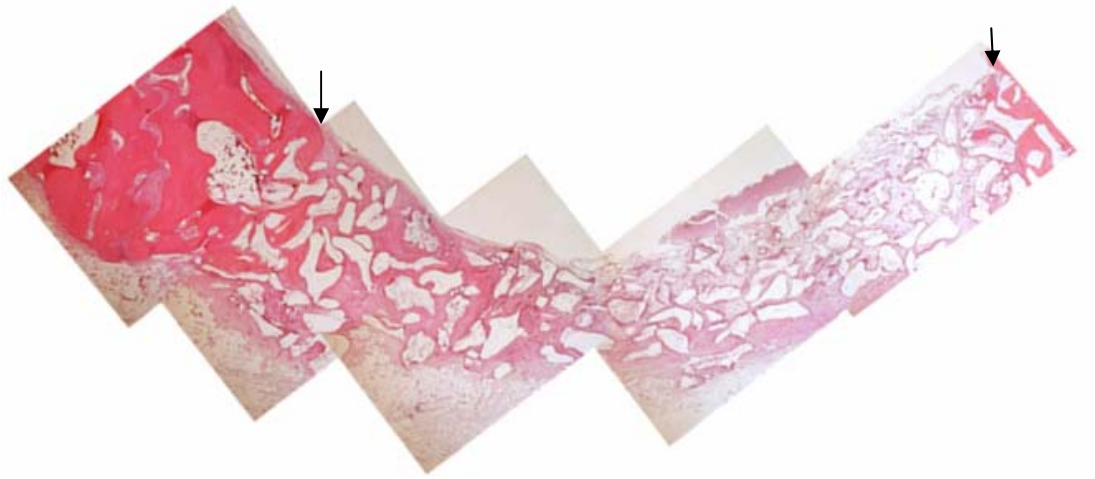

Figure 73. Coronal histological section through the calvarium showing the middle part of the defect of the DBB alone group after 8 weeks. (Specimens stained with Hematoxylin and Eosin, original magnification x5). Arrows indicate the margin site of defects prepared initially.

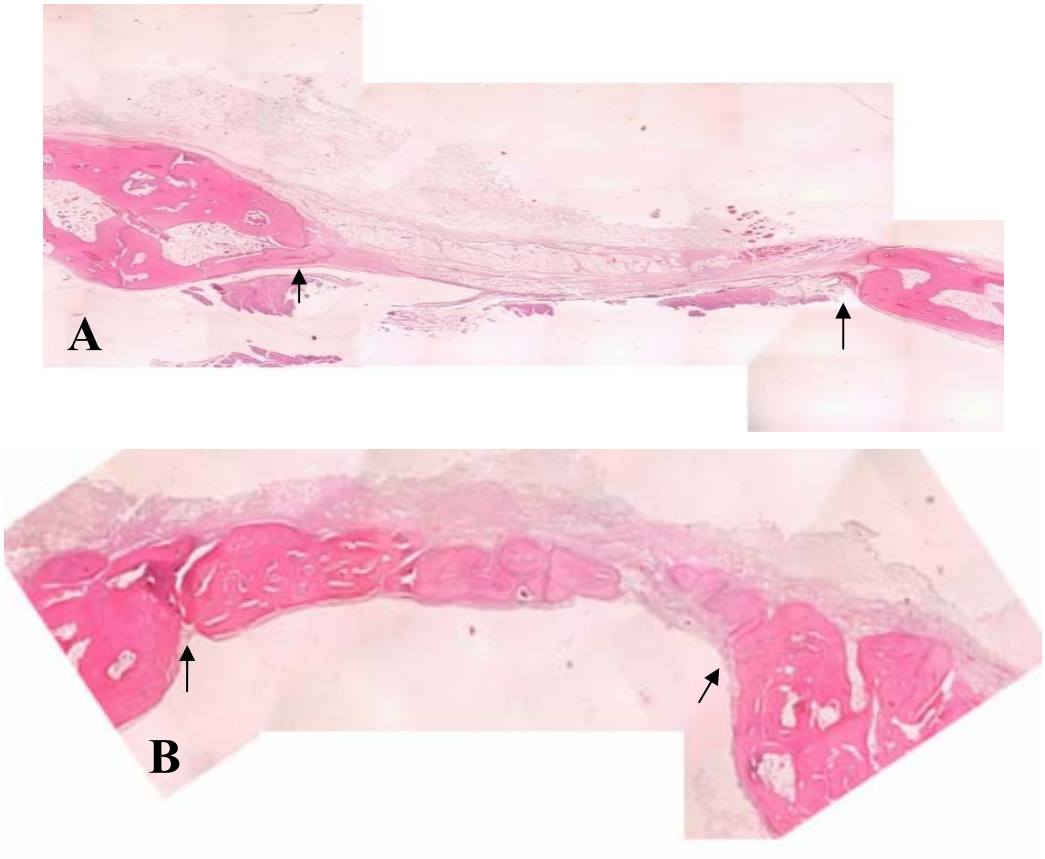

Figure 74. Coronal histological section through the calvarium showing the middle part of the defect of the CSD+PRF group after 8 weeks. One of 5 specimens of CSD+PRF side was filled with loose connective tissue between the defect margins (A). Four of 5 specimens of CSD+PRF side were filled with woven bone (B). (Specimens stained with Hematoxylin and Eosin, original magnification x5). Arrows indicate the margin site of defects prepared initially.

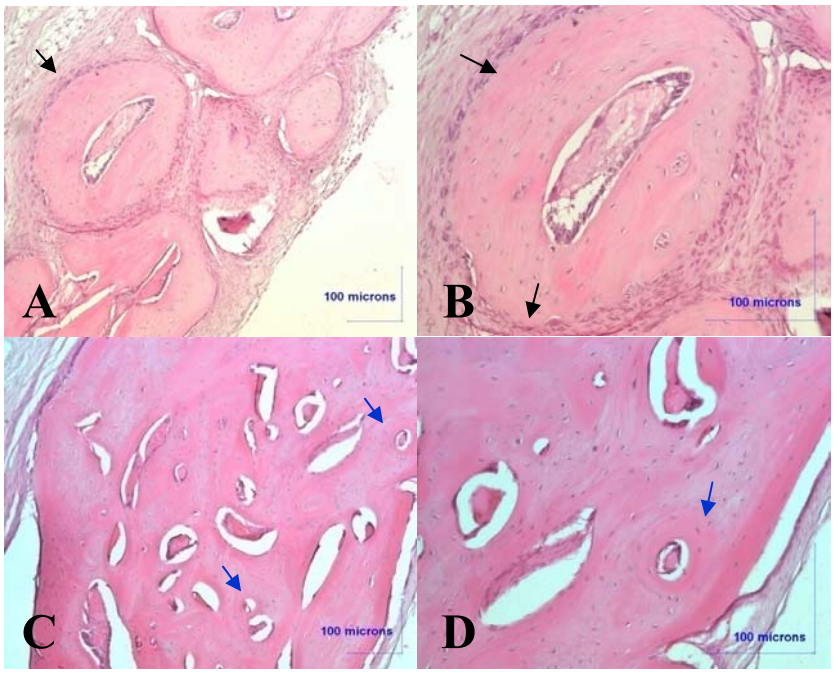

Figure 75. Specimen from the CSD+PRF group, demonstrating new bone formation in central part of the defect. Many osteoblasts rim (black arrows) were observed on the surface of the trabeculae of woven bone (original magnification x10 (A), original magnification x20 (B)). Demonstrating new bone formation near the defect edges. In some regions, the mineralized tissue was remodel into osteon-like structure (blue arrows) of the lamellar bone. (Specimens stained with Hematoxylin and Eosin, original magnification x10 (C), original magnification x20 (D)).

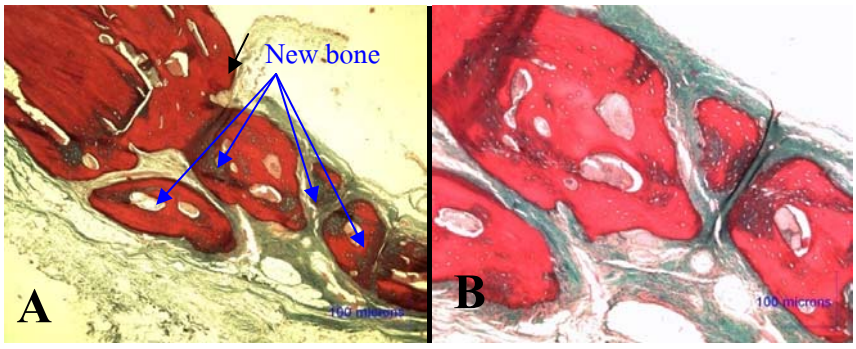

Figure 76. Specimen from the CSD+PRF group, demonstrating the newly formed bone projected from the defect edge. (Specimens stained with Masson's Trichrome stain, original magnification x5 (A), original magnification x10 (B)). Fibrous connective tissues stained green. Black arrows indicate the margin site of defects prepared initially.

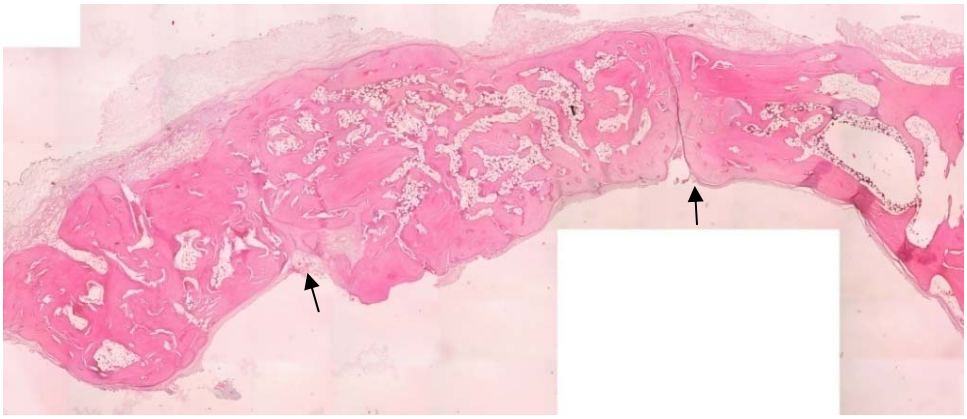

Figure 77. Coronal histological section through the calvarium showing the middle part of the defect of the autogenous bone chips +PRF group after 8 weeks. (Specimens stained with Hematoxylin and Eosin, original magnification x5). Arrows indicate the margin site of defects prepared initially.

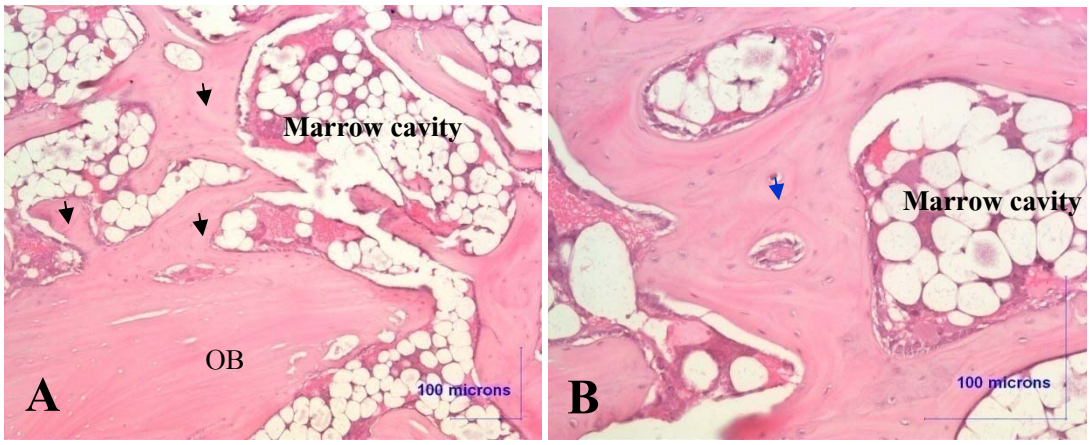

Figure 78. Specimen from the autogenous bone chips +PRF group, demonstrating the old bone chips (OB) are surrounded with woven bone (black arrows). In some regions, the mineralized tissue was remodel into osteon-like structure (blue arrows) of the lamellar bone. (Specimens stained with Hematoxylin and Eosin, original magnification x10 (A), original magnification x20 (B)).

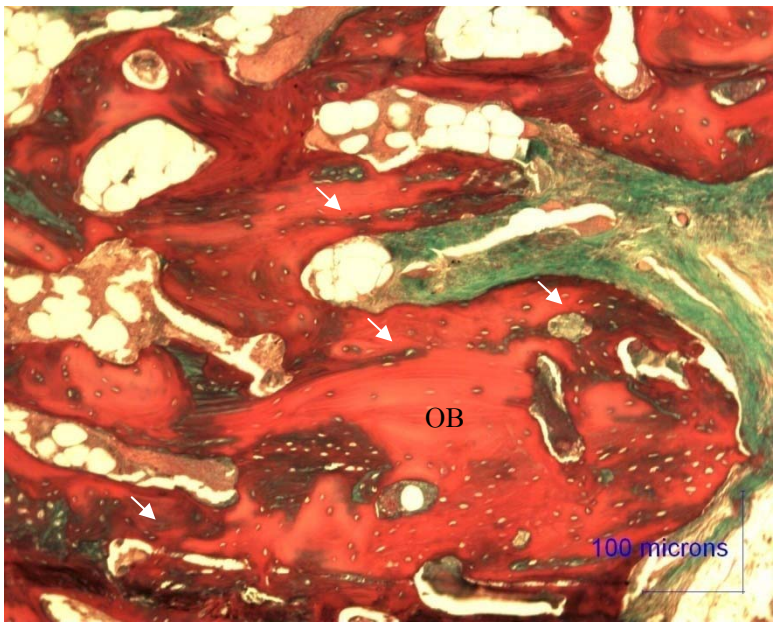

Figure 79. Specimen from the autogenous bone chips +PRF group, demonstrating a large amount of newly formed bone, connecting/bridging newly formed bone trabeculae. The old bone chips (OB) are surrounded by woven bone (white arrows). (Specimens stained with Masson's Trichrome stain, original magnification x10).

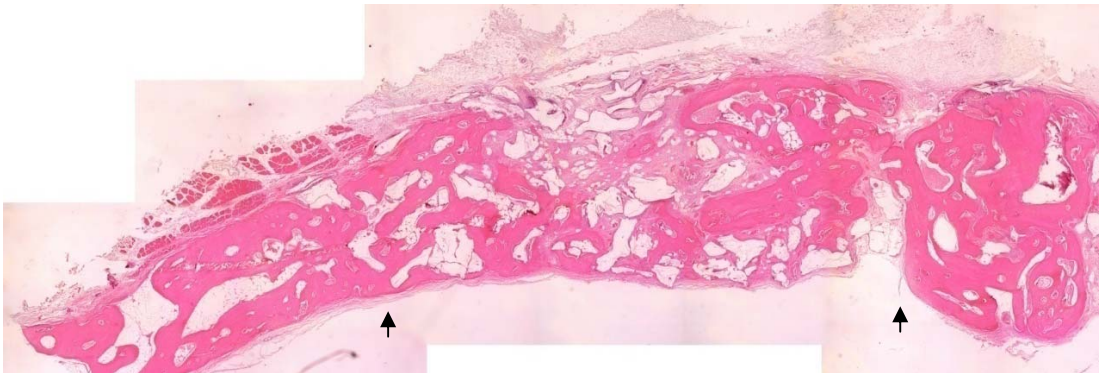

Figure 80. Coronal histological section through the calvarium showing the middle part of the defect of the composite DBB+autogenous bone chips (1:1)+PRF group after 8 weeks. (Specimens stained with Hematoxylin and Eosin, original magnification x5). Arrows indicate the margin site of defects prepared initially.

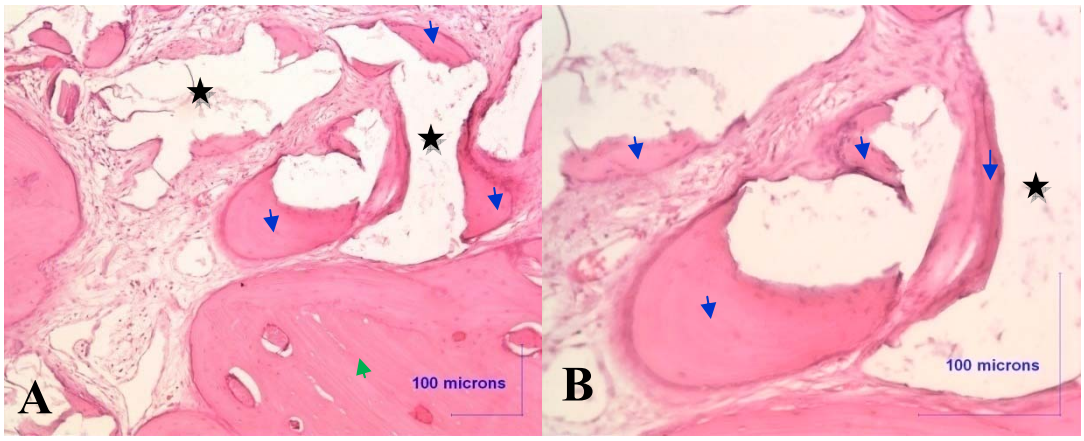

Figure 81. Specimen from the composite DBB+autogenous bone chips (1:1)+PRF group, demonstrating the increasing of new bone formation (blue arrows) around the DBB (stars), autogenous bone chips (green arrows), note the lack of inflammation (A). The DBB particles and new bone laid down along the surface of particles (B). (Specimens stained with Hematoxylin and Eosin, original magnification x10 (A), original magnification x20 (B)).

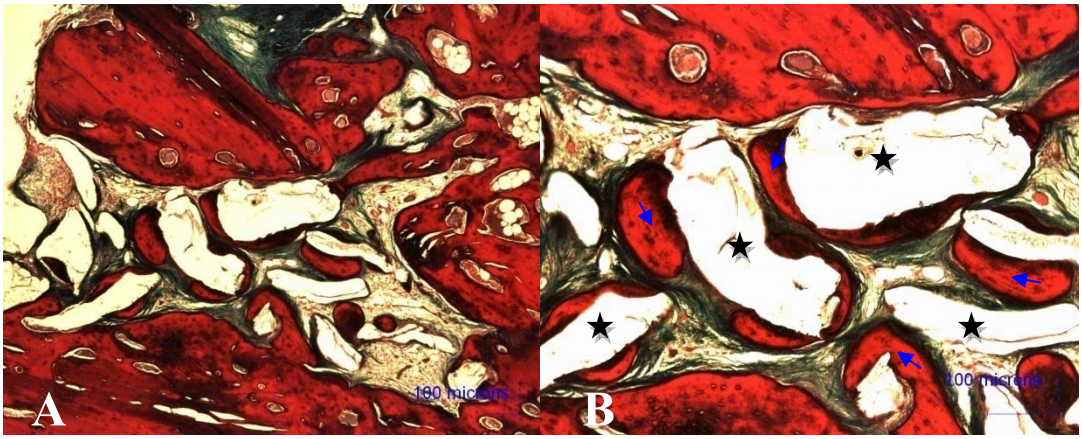

Figure 82. Specimen from the composite DBB+autogenous bone chips (1:1)+PRF group, demonstrating the new bone formation. At a higher magnification, there was close contact between the DBB particle (stars) and the new bone (blue arrows). (Specimens stained with Masson's Trichrome stain, original magnification x5 (A), original magnification x10 (B)).

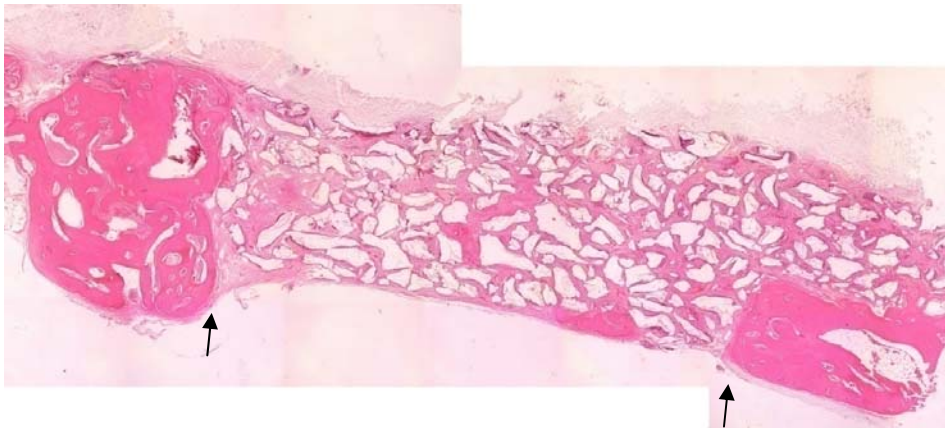

Figure 83. Coronal histological section through the calvarium showing the middle part of the defect of the DBB+PRF group after 8 weeks. (Specimens stained with Hematoxylin and Eosin, original magnification x5). Arrows indicate the margin site of defects prepared initially.

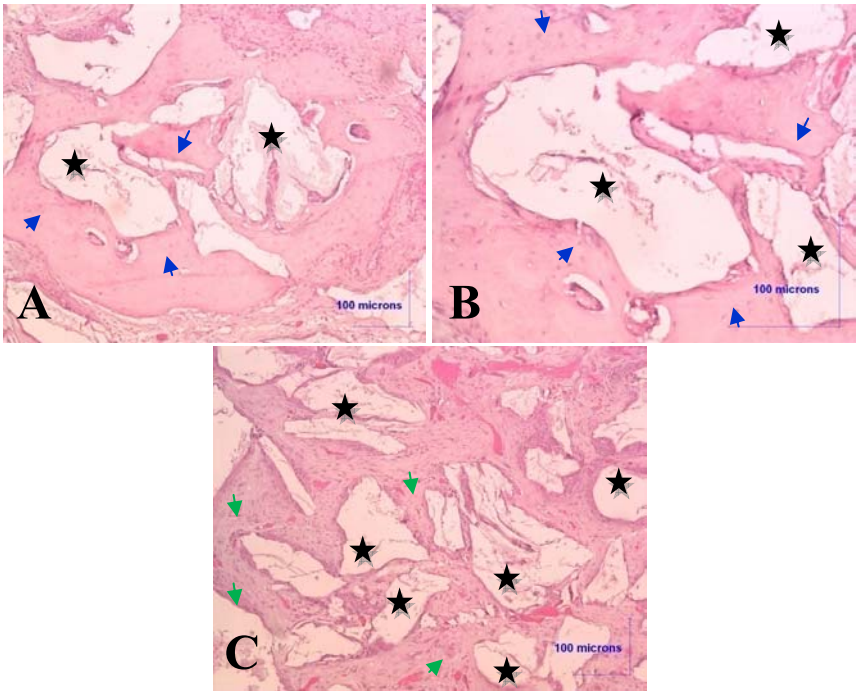

Figure 84. Specimen from the DBB+PRF group, demonstrating the increasing of new bone formation (blue arrows) around the DBB particles (stars) nearly the defect edge, note the lack of inflammation (A,B). Demonstrating extensive fibrous connective tissue (green arrows) around the DBB particles (stars) with minimal bony ingrowth in central part of the defect (C). (Specimens stained with Hematoxylin and Eosin, original magnification x10 (A, C), original magnification x20 (B)).

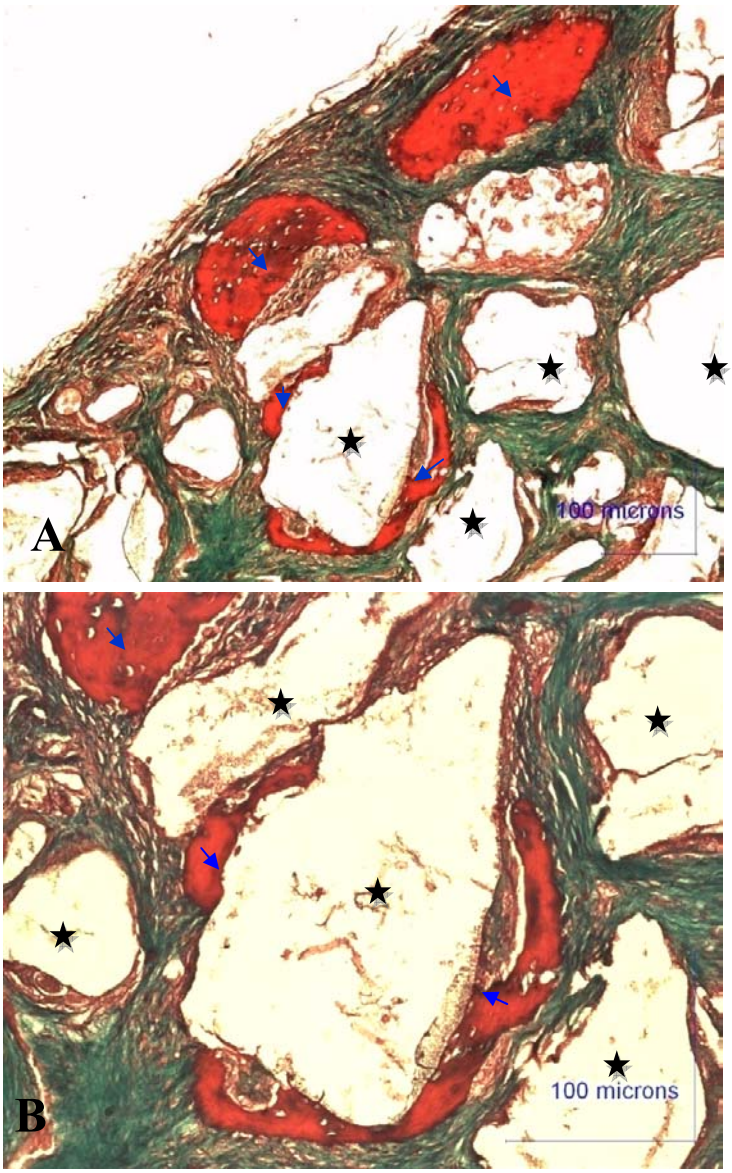

Figure 85. Specimen from the DBB+PRF side, demonstrating the newly formed bone (blue arrows) in close contact with the surface of the DBB (stars). (Specimens stained with Masson's Trichrome stain, original magnification x10 (A), original magnification x20 (B)).

5.2 Histomorphometry analysis

The histomorphometric analysis demonstrated mean new bone formation that presented in the percentage of new bone area (% new bone area) ±SD (Table 10), at 8 weeks postoperatively. The percent of new bone area of the autogenous bone chips+PRF group was

the highest (38.031± 4.231) and significant different from the CSD group (7.155±5.860) ($p<0.05$).The percentage of new bone area was increase when adjuvants PRF to autogenous bone chips. The result showed increase by as much as 25.84% when compared with the autogenous bone chips group and 162.85% when compared with the CSD group. However, there was no significant difference between the autogenous bone chips+PRF group (38.031± 4.231), autogenous bone chips (30.223±16.722) and the CSD+PRF group (18.807±9.272) ($p>0.05$). The results showed a significant increase in % new bone area of the composite DBB+autogenous bone chips (1:1)+PRF group (22.633±3.605) when compared with the CSD group (7.155±5.860) ($p<0.05$). However, there was no significant differences between the composite DBB+autogenous bone chips (1:1)+PRF group (22.633±3.605), the CSD+PRF group (18.807±9.272), the autogenous bone chips group, the composite DBB+autogenous bone chips (1:1) group (20.929±6.169), the DBB group (14.441±2.741) and the DBB+PRF group (13.067±3.643) ($p>0.05$).

Table 10. The data of histomorphometric analysis the percentage of new bone area in group 1, group 2, group 3 and group 4, respectively

Group			**% New bone area (Mean±SD)**	
Control groups	Group 1	CSD alone	7.155± 5.860	
		Autogenous bone chips	30.223±16.722	
	Group 2	Composite DBB+Autogenous bone chips (1:1)	20.929 ± 6.169	
		DBB alone	14.441± 2.741	
Test groups	Group 3	CSD + PRF	18.807±9.272	
		Autogenous bone chips + PRF	38.031±4.231	a
	Group 4	Composite DBB+ Autogenous bone chips(1:1) +PRF	22.633±3.605	a
		DBB+PRF	13.067±3.643	

a = significantly different from CSD alone ($p<0.05$).

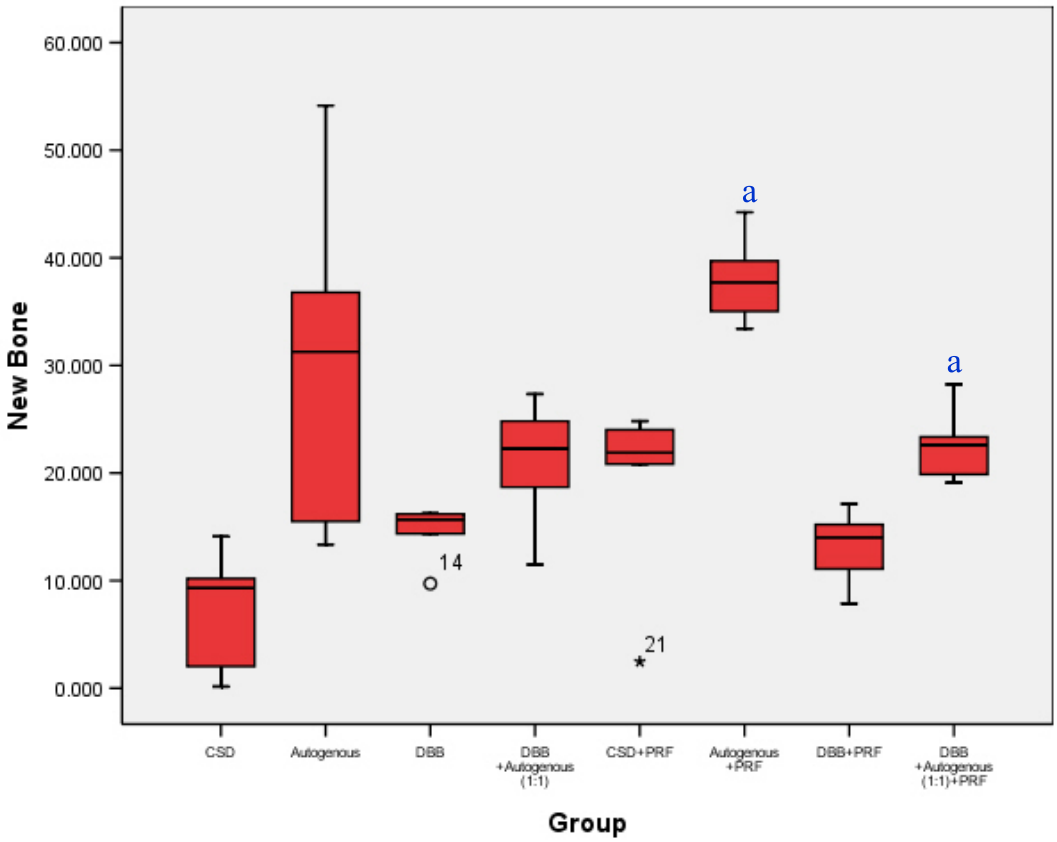

Figure 86. Percentage of new bone formation from histomorphometry analysis, a = significantly different from CSD alone ($p<0.05$).

Chapter 4

Discussion

1. The experimental model

The objective of this study was to assess the quality and quantity of new bone formation from the adjuvant of PRF to autogenous bone chip, DBB alone, composite DBB and autogenous bone chips, which applied to critical size rabbit calvarial defects. The experimental model used in this study was based on a model described by Pripatnanont et al[13, 78] which has been shown effective in evaluating the potential of material for enhancing bone formation at Prince of Songkla University setting. The rabbit also serves as an appropriate model for PRF investigations.

This model was selected by the following reasons: 1) a rabbit is widely used as an experimental animal because of cheap cost and easily to keep; 2) rabbits were readily available; 3) its hematologic status is similar to humans (ie, the platelets of human and rabbits have a similar ultrastructure and constituents[46] (Figure 87), rabbit blood has equal or higher levels of coagulation factors compared with humans[84](Table 11); 4) a rabbit is a useful model for preparation of platelet concentrates because it has a sufficient volume of blood.[46, 85] 5) the surgical procedure on the rabbit's calvarial bone is relatively simple to perform; 6) the physiological bone healing is similar to a human, but 3 times higher than human[86]; 7) the calvarial defect model has many similarities to the maxillofacial region, as anatomically the calvarium consists of two cortical plates with a region of intervening cancellous bone similar to the mandible[88] and physiologically, the cortical bone in the calvarium resembles an atrophic mandible[88] 8) the preparation of the tissue specimens is easy; 9) the parameters can be simply and accurately measured in each specimen; 10) the rabbit calvarial defect, compared with other experimental bone defects, is a suitable model for studying bone regenerative materials because of its effective accessibility and no fixation required[15]; 11) the histologic bone specimen is small therefore it has been helpful for analyzing bone formation in the same histologic slide; 12) a rabbit is easily manipulated and better ethically accepted for experiment than other animals such as a goat, a sheep, a dog, a monkey.

In this study, calvarial defects, previously proven to be good models for investigation the effect of bone graft material were used[89, 90] and it contains modest amounts of

bone marrow, and the defect size of 10x10 mm corresponds to "the critical size defect" (CSD) that will not heal during the animal's lifetime.[90] Investigations of the ability of bone graft materials to obtain complete bone healing of a defect necessitate use of a CSD to exclude spontaneous bony regeneration of the defect. The calvarial bone and the facial bone are pure membranous bone. Morphologically and embryologically, the calvarial develops from a membranous precursor and thus resembles the membranous bone of the face. The biologic inertness of the skull as compared to other bone can be attributed to poor blood supply and relatively deficiency of bone marrow. The middle meningeal artery provides the main cranial blood supply. Healing of calvarial defects can occur from defect edges, the underlying dura mater, or the overlying periosteum. The major part of the healing process came from the periosteal and the defect edges in both autogenous and material grafts.

Bone healing time in a rabbit, Robert et al[91]reported that the resorption and reversal phase was approximately 1 week in rabbits, while the duration of bone formation phase was about 5 weeks. Previous investigations had shown that most osteogenic remodeling of the autogenous bone graft in a rabbit model occurred within the first 6-8 weeks postsurgery.[91-95] Thus, we evaluated the animals at 8 weeks, which represented the entire resorption and deposition phases. Above all, two critical sized defects were used in the same animal therefore in this way a control and an experiment could be carried out in the same animal, with the same surgical procedure and also, the same condition of the healing process.

Evaluation of the healing process of critical-size calvarial osteotomy defects can be performed by gross specimen assessment, radiographic techniques, histologic evaluations and histomorphometry analysis. Radiographic evaluation has the potential advantages of being less costly and time consuming than the ''gold standard'' protocol of histologic analysis. Pryor et al[96] suggested that radiographic evaluation of bone fill in calvarial osteotomy defects yielded a low level of accuracy. Evaluation of bone formation in animal models aiming at treatment recommendations for clinical application should not solely be based on radiographic analysis, but should be confirmed by using histologic observations.

The precise identification of the former defect borders is necessary for adequate radiographic and histologic evaluations. Gutta-percha marking was therefore made at the corner of each defect. However, no difficulty was observed in identifying the original edges in

the present study because of the short observation period. The gutta-percha marking seems more useful for studies involving a longer observation period.

Table 11. The comparison of the normal platelet counts of a rabbit and a human.

Whole blood platelet count (per cu.mm.)	
Rabbit	Human
450,000[82]	150,000 - 350,000[97]
	150,000 - 400,000[98-100]
	150,000 - 450,000[101]

2. Technological concepts and evolution of platelet-rich fibrin (PRF)

Repair of large bony defect requires the surgical transfer of bone from donor to the wound site, which is considered to be the clinical "gold standard". However, such procedures can increase patient morbidity, and donor sources are finite. Ideal bone substitutes should be strong, malleable, osteoconductive, osteoinductive, resorbable, inexpensive, and easy to use intraoperatively, while promoting cell adhesion, proliferation, and differentiation.[102-104] During the last decades, the scientific developments from cellular and molecular biology and the progressive understanding of wound healing and tissue regeneration processes have stimulated the research and development of novel multidisciplinary fields like regenerative medicine and tissue engineering. Additionally, the field of medicine is advancing rapidly towards the development of less invasive procedures and accelerates treatments that generally reduces morbidity while enhances functional recovery. These simple and cost-efficient procedures may have a potential impact in reducing the economic costs for standard medical treatments. The development of PRF is one of that new development. [20, 22-25]

Researchers in oral and maxillofacial surgery continuously strive to improve on current bone-grafting techniques and provide a faster and denser bony regenerate. Growth factors are a realistic way to improve and expedite both soft tissue and bony wound healing. The

emergence and application of PRF have revolutionized the field of regenerative medicine in part due to the repair capacities of the growth factors secreted by the platelets.

2.1 Morphological characterization of PRF

This study used SEM technique to characterize a PRF clot. The microscopic images clearly demonstrate that the PRF is composed of two components: a fibrillar material with striated band which is similar to fibrin filaments, and a cellular component containing platelet cells that are essential for the soft/hard tissue regeneration. The platelets do not show the typical morphology of their resting state but rather morphologic signs of their activation: ovoid platelet cell elements with exocytosis phenomena (Figure 55-56). Platelet cells with exocytic vesicles on their surfaces are seen which indicate the stage of activated platelet.[105] However, the microscopic images of rabbit PRF had slight differences from human PRF. The fibrin filaments in human PRF were better formed and organized than rabbit PRF (Figure 87). This observation is of great interest, because it demonstrates that platelet activation is possible not only during the formation of a blood clot in vivo but also in a blood clot formed in vitro. Platelets contain angiogenic, mitogenic, and vascular growth factors in their granules.[106, 10721, 22] Platelets have a physiologic store of VEGF, which can be released when they are activated, secreted, or aggregated.[106] TGF-β_1 and TGF-β_2 have been shown to inhibit bone resorption, osteoclast formation, and osteoclast activity, as well as to trigger rapid maturation of collagen in early wounds. [108, 109] PDGF increases the population of wound healing cells and recruits other angiogenic growth factors to the wound site.[109] It is therefore a reasonable hypothesis that increasing the concentration of platelets in a bone defect may lead to improved healing.

In addition, the PRF clot also provides a matrix scaffold for the recruitment of tissue cells to an injured site. Specifically, fibrin is the end product of the coagulation cascade, an excellent matrix which has been used to deliver various human cells to a wound in suspension. It has been shown to be a natural ingrowth matrix for fibroblasts and endothelial cells and it is a flexible platform.[110] Fibrin in conjunction with fibronectin acts as a provisional matrix for the influx of monocytes, fibroblasts and endothelial cells.[111] Besides growth factors and chemotactic

factors, an appropriate extracellular matrix is also necessary for angiogenesis. Fibrin has been reported to induce angiogenesis directly.[112] If fibrin itself is sufficient to induce angiogenesis, it must perform at least two functions: 1) provide a three-dimensional matrix that supports cell migration, and 2) express selective chemotactic and chemokinetic activity such that endothelial cells migrate into fibrin clot.[111] In a recent in vitro study, it demonstrated that a low soluble form of rhBMP-2 that was physically entrapped in a fibrin matrix showed prolonged retention.[113] This prolonged rhBMP-2 presence in vitro has been correlated to in vivo with an enhanced efficacy in the repair of critical size defects in rat calvaria.[113] Therefore, fibrin is a suitable candidate as a delivery system for growth and differentiation factors.

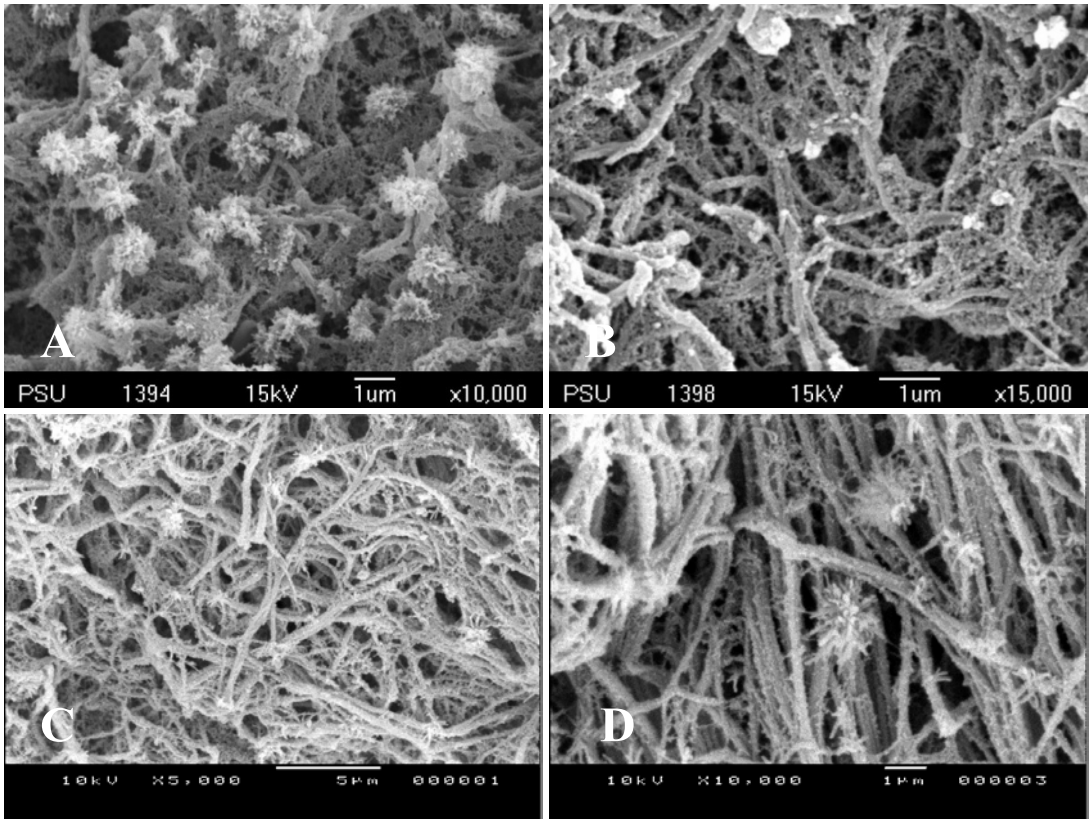

Figure 87. Scanning electron microscopy of rabbit PRF (A, B) and human PRF (C, D)

2.2 The differences between fibrin adhesives, PRP and PRF

Fibrin adhesives and PRP use a bovine thrombin and calcium chloride to commence the last stage of coagulation and sudden fibrin polymerization. The speed of this reaction is dictated by the use of these surgical additives, and their hemostatic function implies a

quasi-immediate setting and therefore significant quantities of thrombin. This mode of polymerization will considerably influence the mechanical and biologic properties of the final fibrin matrix.[114] PRF has the characteristic of polymerizing naturally and slowly during centrifugation. And the thrombin concentrations acting on the collected autologous fibrinogen are almost physiologic because there is no bovine thrombin addition.[20]

Because the life span of a platelet in a wound and the direct influence of its growth factors is less than 5 days[115], a pronounced effect of PRP would be expected to occur especially in the early stage of bone healing[84]. PRF had a lower cytokines concentration (and thus a weaker effect than PRP). Results from Dohan et al[20, 116] mainly assume that the immune and platelet cytokines are enmeshed in the fibrin network, so called are intrinsic cytokines. Intrinsic cytokines have bigger biologic action than cytokines released on the healing site (extrinsic cytokines). The key point is to understand why the quantity of cytokines is not important in a biologic in vivo system. Cytokines are used and destroyed very quickly in a healing wound. The synergy between cytokines and their support (the fibrin matrix) has much more important than any other parameters. A physiologic fibrin matrix such as PRF will have different effects from a fibrin glue or PRP.

2.3 The preparation of PRF

The preparation of PRF followed the PRF protocol of Dohan et al.[20] Blood sample was taken without anticoagulant in 10-mL tube. Our pilot study suggested that blood collection could be performed less than 10 ml for minimal injury to the animal. We found that 8 ml. of whole blood was sufficient for preparation of PRF (Figure 88). Blood processing with a centrifuge for PRF allowed the composition of a structured fibrin clot in the middle part of the tube. PRF clot was in a gel formed that was easy to apply to the surgical defects (Figure 89).

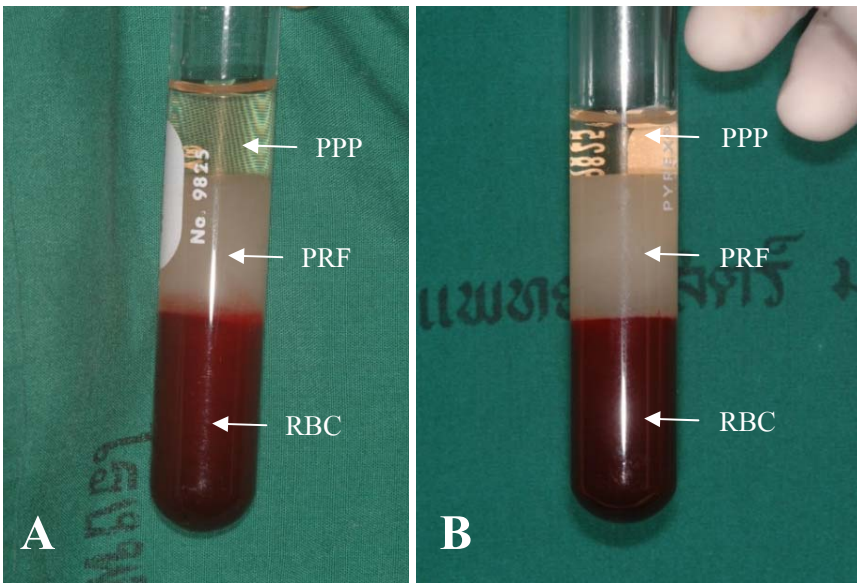

Figure 88. PRF preparation was obtained from 10 ml of whole blood (A). Preparation of PRF from 8 ml of whole blood (B).

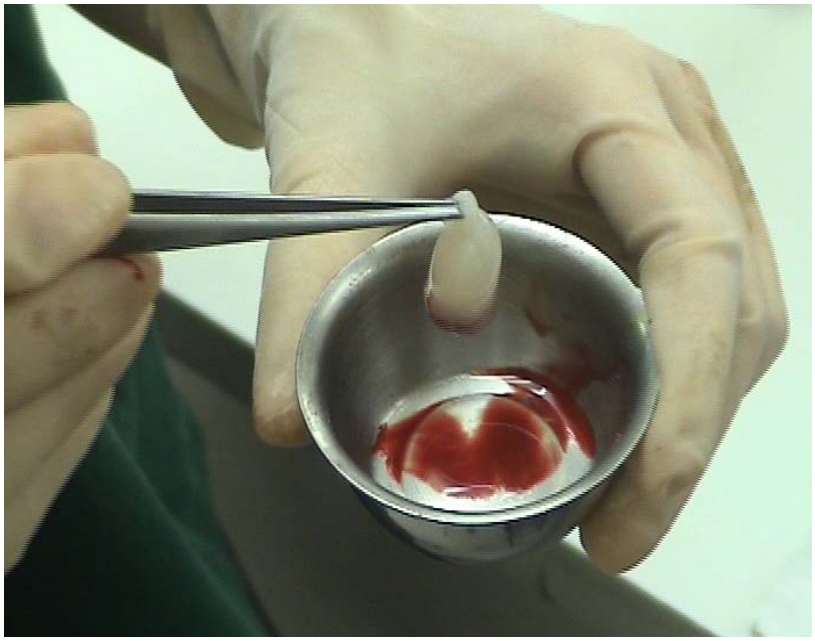

Figure 89. PRF clot was collected from the middle part of the tube in a gel form.

The preparation time for the PRF was simple and took only 10 minutes, because it can be prepared by not using without biochemical blood handling, used 1 centrifugation and no additional instrument was required. While the preparation time for the PRP was approximately 20 to 40 minutes.[21, 34, 36, 37, 47, 50, 57, 117-119] Preparation technique of PRF, which we adopted in this study

and clinical report[120] was simple and easy to do during the operation. There were no complications from the blood draw and PRF preparation. Approximately 3 ml of PRF could be obtained from 8 ml of whole blood, and it was sufficient to be mixed into the particles of autogenous bone chips or bone substitute materials. The success of this technique entirely depends on the speed of blood collection and transfer to the centrifuge. If the duration required to collect blood and launch centrifugation is overly long, failure will occur.

2.4 PRF when used alone

The macroscopically examination showed the combining of PRF with CSD, CSD+PRF side was occupied with bone-like tissue in 4 of 5 specimens with bone-like hardness in consistency, while all of 5 specimen of the CSD side were occupied with soft fibrous tissue. So the results obtained with radiomorphometry analysis showed a significant increase in the mean OD in the CSD+PRF group (0.294±0.062) when compared with the CSD group (0.114±0.062) ($p<0.05$). In addition, histomorphometry analysis of the CSD+PRF group (18.807±9.272) showed increased % new bone area 157.89% over the CSD group (7.155 ±5.860), but this was no statistically difference ($p>0.05$). When PRF was mixed with other grafting materials, the results were also inconclusive.

A recent human study demonstrated that PRF alone used for filling the cystic cavity of the maxilla, two and a half months later, the osseous defect was replaced by a dense and cortical bone instead of the average 10 months naturally. The use of PRF allowed acceleration of the physiologic phenomena.[24]

PRF clot was divided into 2 halves that we have mentioned before, because the volume of one half of PRF was suitable for each defect. One half of PRF was placed into the CSD in one side and the other half was mixed with autogenous bone chips and placed in the contra lateral side. Separation was not precise but the use was random. Although it can not be guaranteed the equal quantity of growth factors of the two half, it can be assumedly.

2.5 Combining PRF with autogenous bone or bone substitute materials

The emergence of novel biomaterials is having an enormous impact on medicine and dentistry. Researchers have looked for ways to enhance the quality of bone substitute materials, including the addition of autogenous bone, the addition of growth factors[51] or the use of guided tissue regeneration membranes. However, if the patient is not compromised, then autologous bone grafts are still the most commonly used material for treating bony defects, especially of the craniofacial region. In recent years, researchers have looked for ways to enhance healing of autologous bone grafts by adding individual growth factors or PRF.[20, 22-25]

The combination of PRF with autogenous bone or bone substitute materials are opening the door to novel therapeutic alternatives and improving preexisting ones, increasing the versatility of bone substitute materials. PRF acts as a biologic adhesive to hold the particles together, making manipulation of the bone grafting material much easier. It is very interesting to note that, when PRF was mixed with the grafts, subsequent radiographic bone graft consolidation seemed to result in enhancing bone graft healing.

In this study, the macroscopically examination showed the combining PRF with autogenous bone, the volume of bone-like tissue in autogenous bone chips+PRF side was much greater and denser than the CSD, the CSD+PRF and the autogenous bone chips groups. The results obtained from radiomorphometry analysis showed a significant increase in the mean OD in the autogenous bone chips+PRF group (0.596±0.189) when compared with the CSD group ($p<0.05$). However, there was no significant difference between the autogenous bone chips, the autogenous bone chips+PRF and the CSD+PRF groups ($p>0.05$). Note that the grafted bone of the autogenous bone chips+PRF group showed similar optical density to the native bone (0.736±0.079), no significant difference was seen ($p>0.05$). The results obtained with histomorphometry analysis demonstrated % new bone area of the autogenous bone chips+PRF group (38.031±4.231) exhibited highest amount of new bone and showed increase by as much as 25.84% when compared with the autogenous bone chips group (30.223±16.722). However, there was no significant difference between the autogenous bone chips group and the autogenous bone chips+PRF group ($p>0.05$). The amount of new bone may not significantly increase but the density of bone in the autogenous bone chips+PRF group was close to the native bone. This study

suggests that PRF combination with autogenous bone graft is effective in wound healing and bone remodeling of autogenous bone graft.

Information on possible effects of PRF is previously based on clinical reports. Choukroun et al[25] evaluated the potential of PRF in combination with freeze-dried bone allograft (FDBA) to enhance bone regeneration in sinus floor elevation. Nine sinus floor augmentations were performed. In 6 sites, PRF was added to FDBA particles (test group), and in 3 sites FDBA without PRF was used (control group). Four months later for the test group and 8 months later for the control group, bone specimens were harvested from the augmented region during the implant insertion procedure. The histologic similarity observed between these 2 groups (FDBA alone and FDB+PRF) was implied that PRF shorten the healing period in sinus floor augmentation in 4 months instead of 8 months. Moreover, the quantities of newly formed bone were equivalent in these 2 groups.

Phurisat and Pripatnanont[120] reported the clinical support of using PRF adjuncts to bone grafting material in sinus lift grafting. Four patients underwent sinus lift bone grafting and simultaneous implant placement with composite graft. The composite graft comprised of autogenous bone chips, deproteinized bovine bone (Bio-Oss®) and PRF. Clinical and radiographic examinations showed good results in newly formed bone. The size of bony window created at the lateral wall of the maxillary sinus for access was reduced and replaced by dense cortical bone. Radiographs showed homogeneity of bone grafting area with surrounding bone and an absent of previous sinus floor demarcation was noted. Sensi-/Densitometer (Densonorm 21 eco, Pehamed, Germany) showed high opacity at immediate postoperative and the density was decreased at four months postoperatively which implied that bone was remodeled with time. Based on these previous studies, the purpose of our study was to combine the use of PRF and DBB. We theorized that PRF, through its angiogenic properties, would lead to an improved revascularization and faster consolidation of the graft when combined with an osteoconductive material.

In this study, excellent bone-like tissue and DBB particles were observed in both sides of the composite of DBB+autogenous bone chips (1:1) group and the composite of DBB+autogenous bone chips (1:1)+PRF group. The volumes of bone-like tissue of these groups were much greater and denser tissue than DBB and DBB+PRF groups. The radiomorphometry

analysis results showed a significant increase in the mean OD in the composite of DBB+autogenous bone chips (1:1)+PRF group (0.810±0.154) when compared with the CSD group (0.114±0.062), the CSD+PRF group (0.294±0.062), and the autogenous bone chips group (0.356±0.027) ($p<0.05$). The marked increase in mean OD were observed because the high opacity of these DBB particles. It was noted that the grafted bone of the composite of DBB+autogenous bone chips (1:1)+PRF group showed similar optical density to the native bone (0.736±0.079), no significant difference were seen ($p>0.05$). There was also no significant differences in mean OD among the composite of DBB+autogenous bone chips (1:1)+PRF group (0.810±0.154), the composite of DBB+autogenous bone chips (1:1) group (0.906±0.046), the autogenous bone chips+PRF group (0.596±0.189), the DBB alone group (1.066±0.052) and the DBB+PRF group (1.178±0.167) ($p>0.05$). The results obtained from histomorphometry analysis showed a significant increase in % new bone area of the composite of DBB+autogenous bone chips (1:1)+PRF group (22.633±3.605) when compared with the CSD group (6.235±5.012) ($p<0.05$). However, there was no significant difference among the composite of DBB+autogenous bone chips (1:1)+PRF , the CSD+PRF, the autogenous bone chips, the composite of DBB+autogenous bone chips (1:1), the DBB alone and the DBB+PRF groups ($p>0.05$). This result failed to show statistically significant increase in bone formation with the addition of PRF to DBB radiologically or histomorphometrically in critical sized defects in the rabbit cranium.

The percentage of new bone area of the DBB alone group (14.441±2.741) and the DBB+PRF group (13.067±3.643) were less than the CSD+PRF group (18.807±9.272) ($p<0.05$). However, there was no significant difference. The histology observation in the CSD+PRF group showed the graft collapsed. While the DBB alone and the DBB+PRF groups were able to maintain the space, no graft collapsed and DBB particles served as the space-maintaining defect fillers (Figure 90). Therefore the use of PRF with grafts consisting of 100% DBB should be considered only in respect to the improvement of handling quality (containment) of the particulate graft material and providing the space-maintaining.

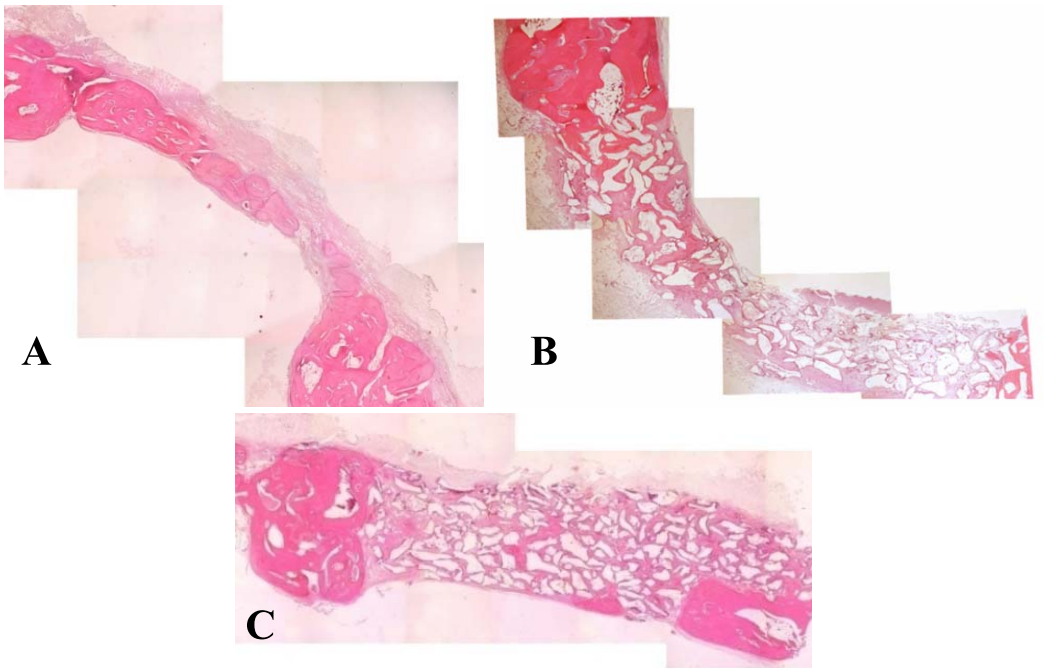

Figure 90. Coronal histological section through the calvarium showing defect from the middle part of the CSD+PRF group (A), the DBB alone group (B) and the DBB+PRF group (C) after 8 weeks. (Specimens stained with Hematoxylin and Eosin, original magnification x5).

In this study, the addition of PRF to autogenous bone chips in the rabbit cranial defect showed the greatest histomorphometric new bone area. Autogenous bone grafts heal through a mechanism whereby the body replaces the nonviable grafted bone with viable new bone. Therefore, the positive effect of PRF seems to be a result of the survival of osteoblasts, osteocytes and preosteoblasts present in autologous bone grafts. The rationale behind using PRF is that activation of a large number of platelets at the time of graft placement releases a bolus of various growth factors. This can be explained by the mechanism of the growth factors within PRF. The PRF contained growth factors PDGF, TGF and IGF[22] that act on healing capable cells to increase their numbers (mitogenesis) and stimulate angiogenesis but they are not osteoinductive. Therefore, they are dependent on the presence of osteogenetic cells.

Additionally, bone substitute materials may also improve the kinetic properties of PRF enabling a more slowly release of the stored growth factors. One potential field of interest is the incorporation of PRF in bone grafting technology. This development is extremely relevant in different surgical fields including orthopaedic and maxillofacial surgery and oral

implantology. For example, in oral implantology, dentists find difficult and challenging the manipulation and application of some bone augmentation materials such as DBB, Bio-Oss®, tricalcium phosphate (TCP) and even autogenous bone. By combining selected biomaterials with scaffold-like PRF, it is possible to improve the handling and adaptation of the matrix to the injured tissue because fibrin acts as a biologic glue to hold together the matrix particles. This may have implications for some specific dental surgeries like sinus lift bone grafting.

The hypothesis tested in this study that the addition of PRF to autogenous bone chips in a critical size defect of the rabbit's calvarial shows a significant increase in new bone formation and bone density, had to be accepted. But the addition of PRF to DBB shows a significant increase in new bone formation and bone density, had to be rejected.

2.6 Safety associated with PRF method

PRF was initially developed in dry glass tubes as early as 2000. In the medical field, the conventional PRF protocol has continued to be performed in these dry glass tubes. In a dental office, the problem is different. Dentists are not initially educated to perform blood harvests. Therefore, the use of plastic tubes has been recommended to avoid tube breaking, cutting and contaminations during these quite exceptional handlings in a dental office. This evolution indeed applies in all fields, because the main manufacturers only sell plastic tubes now. However, with plastic tubes alone, PRF can not be obtained. The contact with silica is necessary to start the polymerization process. The silica behaves as a clot activator. To produce PRF, either dry glass tubes or glass-coated plastic tubes must be used.[121] The silica microparticles coating these tubes represent a quite impossible risk of cytotoxicity, in contrast bovine thrombin (used to prepare PRP and fibrin glue)[19, 21] which may generate immune side effects.[122-124] PRF was developed to avoid this thrombin-related risk.

3. Deproteinized bovine bone (DBB)

DBB derived from heat treatment at 1200 $^{\circ}$C (DBB) was used in our study. Electron microscopic evaluation shows that this material has a structural configuration similar to

human bone.[5, 78] The particle size of the materials ranged from 0.25 to 1 mm in diameter, which is small, as indicated by Pallesen et al[125] who demonstrated that small (0.5 to 2 mm^3) particles of autogenous bone produced more bone substitution than larger (10 mm^3) particles.

The radiographic results indicated that the DBB alone and DBB+PRF groups had higher ODs than the other groups, because most of the radio-opaque particles remained. Although OD is an indicator of opacity, it cannot discriminate between new bone formation and DBB particles. In the specimens were filled with DBB, the regenerated bone was characterized by the direct apposition of new bone formation to the DBB particles. The newly formed bone tissue showed the centripetal of bone in growth. In the past DBB treated by heat treatment was widely used as bone substitute because its structure is similar to human bone and many studies claimed its properties of osteoconduction and biocompatibility to human body. Even though this study used DBB, treated by heat at 1200°C, the histology result showed the osteoconductive property and biocompatibility of this material. Histologic assessment revealed that DBB is a biocompatible, osteoconductive grafting material with no sign of foreign body reaction and severe inflammation in conjunction with its application.

In addition, the calvarial defect in the rabbit was relatively shallow in terms of its depth, and it is not exactly oral bone. These may be limiting factors in terms of applying the results derived from this study to a case involving a clinically larger bone defect. Therefore, further investigations are required using the clinically large bone defect model. Within the limits of this study, the volume of collected blood samples for PRF preparation was recorded but a growth factor assay was not performed which is an obvious drawback. The optimal level of platelet concentration for bone grafts is not known and may like other variables, influence the results. Nevertheless, the biological effects of different levels of growth factors, including any possible differences resulting from different relative growth factor levels in the PRF preparations, the complete characterization of the platelet released factors and proteins, the amount of PRF needed to achieve the intended biological effects are unknown, and are worthy of further investigation. However, the finding of our study showed activated platelets in the PRF clot. Platelets have a physiologic store of growth factors, which can be released when platelets are activated, secreted, or aggregated.[106] Therefore it can be postulated that PRF enhances wound healing and new bone formation by increased concentration of activated platelets.

Chapter 5

Conclusion

PRF, an autologous source of growth factors especially PDGF and TGF-β, influences bone regeneration. PRF can be prepared by simple technique, minimal cost and minimal invasive. This autologous product eliminates concerns about immunogenic reactions and disease transmission. The addition of PRF to the autogenous bone chips in a critical size defect of the rabbit's calvarial defects conferred significant benefit for the quality and quantity of new bone formation. But the addition of PRF to deproteinized bovine bone did not gain benefit for the quality and quantity of new bone formation. PRF may be useful for enhancing bone regeneration in the situation that containing osteogenic cells in situ. Further study in clinical setting may help to prove this postulation.

PRF represents a new biotechnology for the stimulation and acceleration of bone regeneration. This study indicates that the PRF is a promising biomaterial for the enhancement of bone regeneration. Author believes this technology may be a new exciting development in the next few decades. To succeed, some of the current challenges need to be addressed including the complete characterization of the platelet released factors and determining the intra-individual biological reasons that make PRF more effective than others and designing novel interactions with biomaterials than might increase the versatility of the technology. These efforts point to a future where tailored PRF will be used for each specific dental and medical purposes.

Reference

1. Lane JM, Yasko AW, Tomin E, Cole BJ, Waller S, Browne M, et al. Bone marrow and recombinant human bone morphogenetic protein-2 in osseous repair. ***Clin Orthop Relat Res*** 1999(361): 216-27.
2. Giannoudis PV, Dinopoulos H, Tsiridis E. Bone substitutes: an update. ***Injury*** 2005; 36 Suppl 3: S20-7.
3. Piattelli M, Favero GA, Scarano A, Orsini G, Piattelli A. Bone reactions to anorganic bovine bone (Bio-Oss) used in sinus augmentation procedures: a histologic long-term report of 20 cases in humans. ***Int J Oral Maxillofac Implants*** 1999; 14(6): 835-40.
4. Sartori S, Silvestri M, Forni F, Icaro Cornaglia A, Tesei P, Cattaneo V. Ten-year follow-up in a maxillary sinus augmentation using anorganic bovine bone (Bio-Oss). A case report with histomorphometric evaluation. ***Clin Oral Implants Res*** 2003; 14(3): 369-72.
5. Mangano C, Scarano A, Perrotti V, Iezzi G, Piattelli A. Maxillary sinus augmentation with a porous synthetic hydroxyapatite and bovine-derived hydroxyapatite: a comparative clinical and histologic study. ***Int J Oral Maxillofac Implants*** 2007; 22(6): 980-6.
6. Fukuta K, Har-Shai Y, Collares MV, Lichten JB, Jackson IT. Comparison of inorganic bovine bone mineral particles with porous hydroxyapatite granules and cranial bone dust in the reconstruction of full-thickness skull defect. ***J Craniofac Surg*** 1992; 3(1): 25-9.
7. Berglundh T, Lindhe J. Healing around implants placed in bone defects treated with Bio-Oss. An experimental study in the dog. ***Clin Oral Implants Res*** 1997; 8(2): 117-24.
8. Klinge B, Alberius P, Isaksson S, Jonsson J. Osseous response to implanted natural bone mineral and synthetic hydroxylapatite ceramic in the repair of experimental skull bone defects. ***J Oral Maxillofac Surg*** 1992; 50(3): 241-9.
9. Schlickewei W, Riede UN, Yu J, Ziechmann W, Kuner EH, Seubert B. Influence of humate on calcium hydroxyapatite implants. ***Arch Orthop Trauma Surg*** 1993;112(6):275-9.
10. Hammerle CH, Chiantella GC, Karring T, Lang NP. The effect of a deproteinized bovine

bone mineral on bone regeneration around titanium dental implants. ***Clin Oral Implants Res*** 1998; 9(3): 151-62.

11. Wetzel AC, Stich H, Caffesse RG. Bone apposition onto oral implants in the sinus area filled with different grafting materials. A histological study in beagle dogs. ***Clin Oral Implants Res*** 1995; 6(3): 155-63.
12. Schlegel KA, Fichtner G, Schultze-Mosgau S, Wiltfang J. Histologic findings in sinus augmentation with autogenous bone chips versus a bovine bone substitute. ***Int J Oral Maxillofac Implants*** 2003; 18(1): 53-8.
13. Pripatnanont P, Nuntanaranont T, Vongvatcharanon S. Proportion of deproteinized cancellous bovine bone and autogenous bone in bone formation of rabbit's calvarial defect. ***Asian J. Oral Maxillofac Surg*** 18 (3, supplement) 50, 2006
14. Springer IN, Acil Y, Kuchenbecker S, Bolte H, Warnke PH, Abboud M, et al. Bone graft versus BMP-7 in a critical size defect-cranioplasty in a growing infant model. ***Bone*** 2005; 37(4): 563-9.
15. Ahn SH, Kim CS, Suk HJ, Lee YJ, Choi SH, Chai JK, et al. Effect of recombinant human bone morphogenetic protein-4 with carriers in rat calvarial defects. ***J Periodontol*** 2003; 74(6): 787-97.
16. Zimmermann G, Moghaddam A, Reumann M, Wangler B, Breier L, Wentzensen A, et al. TGF-beta1 as a pathophysiological factor in fracture healing. ***Unfallchirurg*** 2006.
17. Lind M. Growth factor stimulation of bone healing. Effects on osteoblasts, osteomies, and implants fixation. ***Acta Orthop Scand Suppl*** 1998; 283: 2-37.
18. Lind M, Deleuran B, Thestrup-Pedersen K, Soballe K, Eriksen EF, Bunger C. Chemotaxis of human osteoblasts. Effects of osteotropic growth factors. ***Apmis*** 1995; 103(2): 140-6.
19. Gibble JW, Ness PM. Fibrin glue: the perfect operative sealant? ***Transfusion*** 1990; 30(8): 741-7.
20. Dohan DM, Choukroun J, Diss A, Dohan SL, Dohan AJ, Mouhyi J, et al. Platelet-rich fibrin (PRF): a second-generation platelet concentrate. Part I: technological concepts and evolution. ***Oral Surg Oral Med Oral Pathol Oral Radiol Endod*** 2006; 101(3): e37-44.

21. Marx RE, Carlson ER, Eichstaedt RM, Schimmele SR, Strauss JE, Georgeff KR. Platelet-rich plasma: Growth factor enhancement for bone grafts. ***Oral Surg Oral Med Oral Pathol Oral Radiol Endod*** 1998; 85(6): 638-46.

22. Dohan DM, Choukroun J, Diss A, Dohan SL, Dohan AJ, Mouhyi J, et al. Platelet-rich fibrin (PRF): a second-generation platelet concentrate. Part II: platelet-related biologic features. ***Oral Surg Oral Med Oral Pathol Oral Radiol Endod*** 2006; 101(3): e45-50.

23. Dohan DM, Choukroun J, Diss A, Dohan SL, Dohan AJ, Mouhyi J, et al. Platelet-rich fibrin (PRF): a second-generation platelet concentrate. Part III: leucocyte activation: a new feature for platelet concentrates? ***Oral Surg Oral Med Oral Pathol Oral Radiol Endod*** 2006; 101(3): e51-5.

24. Choukroun J, Diss A, Simonpieri A, Girard MO, Schoeffler C, Dohan SL, et al. Platelet-rich fibrin (PRF): a second-generation platelet concentrate. Part IV: clinical effects on tissue healing. ***Oral Surg Oral Med Oral Pathol Oral Radiol Endod*** 2006; 101(3): e56-60.

25. Choukroun J, Diss A, Simonpieri A, Girard MO, Schoeffler C, Dohan SL, et al. Platelet-rich fibrin (PRF): a second-generation platelet concentrate. Part V: histologic evaluations of PRF effects on bone allograft maturation in sinus lift. ***Oral Surg Oral Med Oral Pathol Oral Radiol Endod*** 2006;101(3): 299-303.

26. Mawatari M, Higo T, Tsutsumi Y, Shigematsu M, Hotokebuchi T. Effectiveness of autologous fibrin tissue adhesive in reducing postoperative blood loss during total hip arthroplasty: a prospective randomised study of 100 cases. ***J Orthop Surg*** (Hong Kong) 2006; 14(2): 117-21.

27. Nakamura H, Matsuyama Y, Yoshihara H, Sakai Y, Katayama Y, Nakashima S, et al. The effect of autologous fibrin tissue adhesive on postoperative cerebrospinal fluid leak in spinal cord surgery: a randomized controlled trial. ***Spine*** 2005; 30(13): E347-51.

28. Thorn JJ, Sorensen H, Weis-Fogh U, Andersen M. Autologous fibrin glue with growth factors in reconstructive maxillofacial surgery. ***Int J Oral Maxillofac Surg*** 2004; 33(1): 95-100

29. Huh JY, Choi BH, Zhu SJ, Jung JH, Kim BY, Lee SH. The effect of platelet-enriched

fibrin glue on bone regeneration in autogenous bone grafts. ***Oral Surg Oral Med Oral Pathol Oral Radiol Endod*** 2006; 101(4): 426-31.

30. Froum SJ, Wallace SS, Tarnow DP, Cho SC. Effect of platelet-rich plasma on bone growth and osseointegration in human maxillary sinus grafts: three bilateral case reports. ***Int J Periodontics Restorative Dent*** 2002; 22(1): 45-53.

31. Carlson NE, Roach RB, Jr. Platelet-rich plasma: clinical applications in dentistry. ***J Am Dent Assoc*** 2002; 133(10): 1383-6.

32. Thor A, Franke-Stenport V, Johansson CB, Rasmusson L. Early bone formation in human bone grafts treated with platelet-rich plasma: preliminary histomorphometric results. ***Int J Oral Maxillofac Surg*** 2007; 36(12): 1164-71.

33. Han J, Meng HX, Tang JM, Li SL, Tang Y, Chen ZB. The effect of different platelet-rich plasma concentrations on proliferation and differentiation of human periodontal ligament cells in vitro. ***Cell Prolif*** 2007; 40(2): 241-52.

34. Robiony M, Polini F, Costa F, Politi M. Osteogenesis distraction and platelet-rich plasma for bone restoration of the severely atrophic mandible: preliminary results. ***J Oral Maxillofac Surg*** 2002; 60(6): 630-5.

35. Raghoebar GM, Schortinghuis J, Liem RS, Ruben JL, van der Wal JE, Vissink A. Does platelet-rich plasma promote remodeling of autologous bone grafts used for augmentation of the maxillary sinus floor? ***Clin Oral Implants Res*** 2005; 16(3): 349-56.

36. Weibrich G, Kleis WK. Curasan PRP kit vs. PCCS PRP system. Collection efficiency and platelet counts of two different methods for the preparation of platelet-rich plasma. ***Clin Oral Implants Res*** 2002; 13(4): 437-43.

37. Oyama T, Nishimoto S, Tsugawa T, Shimizu F. Efficacy of platelet-rich plasma in alveolar bone grafting. ***J Oral Maxillofac Surg*** 2004;62(5):555-8.

38. Landesberg R, Moses M, Karpatkin M. Risks of using platelet rich plasma gel. ***J Oral Maxillofac Surg*** 1998;56(9):1116-7.

39. Muntean W, Zenz W, Finding K, Zobel G, Beitzke A. Inhibitor to factor V after exposure to fibrin sealant during cardiac surgery in a two-year-old child. ***Acta Paediatr*** 1994; 83(1): 84-7.

40. Banninger H, Hardegger T, Tobler A, Barth A, Schupbach P, Reinhart W, et al. Fibrin glue in surgery: frequent development of inhibitors of bovine thrombin and human factor V. ***Br J Haematol*** 1993; 85(3): 528-32.

41. Landesberg R, Burke A, Pinsky D, Katz R, Vo J, Eisig SB, et al. Activation of platelet-rich plasma using thrombin receptor agonist peptide. ***J Oral Maxillofac Surg*** 2005; 63(4): 529-35.

42. Cmolik BL, Spero JA, Magovern GJ, Clark RE. Redo cardiac surgery: late bleeding complications from topical thrombin-induced factor V deficiency. ***J Thorac Cardiovasc Surg*** 1993; 105(2): 222-7; discussion 27-8.

43. Sarfati MR, Dilorenzo DJ, Kraiss LW, Galt SW. Severe coagulopathy following intraoperative use of topical thrombin. ***Ann Vasc Surg*** 2004; 18(3): 349-51.

44. Park JJ, Cintron JR, Siedentop KH, Orsay CP, Pearl RK, Nelson RL, et al. Technical manual for manufacturing autologous fibrin tissue adhesive. ***Dis Colon Rectum*** 1999; 42(10): 1334-8.

45. Landesberg R, Roy M, Glickman RS. Quantification of growth factor levels using a simplified method of platelet-rich plasma gel preparation. ***J Oral Maxillofac Surg*** 2000; 58(3): 297-300; discussion 00-1.

46. Kim ES, Park EJ, Choung PH. Platelet concentration and its effect on bone formation in calvarial defects: an experimental study in rabbits. ***J Prosthet Dent*** 2001; 86(4): 428-33.

47. Okuda K, Kawase T, Momose M, Murata M, Saito Y, Suzuki H, et al. Platelet-Rich Plasma Contains High Levels of Platelet-Derived Growth Factor and Transforming Growth Factor-β and Modulates the Proliferation of Periodontally Related Cells In Vitro. ***J Periodontol*** 2003; 74(6): 849-57.

48. Gerard D, Carlson ER, Gotcher JE, Jacobs M. Effects of platelet-rich plasma on the healing of autologous bone grafted mandibular defects in dogs. ***J Oral Maxillofac Surg*** 2006; 64(3): 443-51.

49. Kim SG, Chung CH, Kim YK, Park JC, Lim SC. Use of particulate dentin-plaster of paris combination with/without platelet-rich plasma in the treatment of bone defects around implants. ***Int J Oral Maxillofac Implants*** 2002; 17(1): 86-94.

50. Aghaloo TL, Moy PK, Freymiller EG. Evaluation of platelet-rich plasma in combination with anorganic bovine bone in the rabbit cranium: a pilot study. ***Int J Oral Maxillofac Implants*** 2004; 19(1): 59-65.

51. Jung RE, Schmoekel HG, Zwahlen R, Kokovic V, Hammerle CH, Weber FE. Platelet-rich plasma and fibrin as delivery systems for recombinant human bone morphogenetic protein-2. ***Clin Oral Implants Res*** 2005; 16(6): 676-82.

52. Pryor ME, Polimeni G, Koo KT, Hartman MJ, Gross H, April M, et al. Analysis of rat calvaria defects implanted with a platelet-rich plasma preparation: histologic and histometric observations. ***J Clin Periodontol*** 2005; 32(9): 966-72.

53. Miranda SR, Nary Filho H, Padovan LE, Ribeiro DA, Nicolielo D, Matsumoto MA. Use of platelet-rich plasma under autogenous onlay bone grafts. ***Clin Oral Implants Res*** 2006; 17(6): 694-9.

54. Wiltfang J, Kloss FR, Kessler P, Nkenke E, Schultze-Mosgau S, Zimmermann R, et al. Effects of platelet-rich plasma on bone healing in combination with autogenous bone and bone substitutes in critical-size defects. An animal experiment. ***Clin Oral Implants Res*** 2004; 15(2): 187-93.

55. Mooren RE, Merkx MA, Bronkhorst EM, Jansen JA, Stoelinga PJ. The effect of platelet-rich plasma on early and late bone healing: an experimental study in goats. ***Int J Oral Maxillofac Surg*** 2007; 36(7): 626-31.

56. Schlegel KA, Zimmermann R, Thorwarth M, Neukam F-W, Klongnoi B, Nkenke E, et al. Sinus floor elevation using autogenous bone or bone substitute combined with platelet-rich plasma. ***Oral Surg Oral Med Oral Pathol Oral Radiol Endod*** 2007;104(3):e15-e25.

57. Aghaloo TL, Moy PK, Freymiller EG. Investigation of platelet-rich plasma in rabbit cranial defects: A pilot study. ***J Oral Maxillofac Surg*** 2002; 60(10): 1176-81.

58. Antoniades HN, Williams LT. Human platelet-derived growth factor: structure and function. ***Fed Proc*** 1983; 42(9): 2630-4.

59. Deuel TF, Huang JS. Platelet-derived growth factor. Structure, function, and roles in normal and transformed cells. ***J Clin Invest*** 1984; 74(3): 669-76.

60. Cochran DL, Rouse CA, Lynch SE, Graves DT. Effects of platelet-derived growth

factor isoforms on calcium release from neonatal mouse calvariae. ***Bone*** 1993; (1): 53-8.

61. Hughes FJ, Aubin JE, Heersche JN. Differential chemotactic responses of different populations of fetal rat calvaria cells to platelet-derived growth factor and transforming growth factor beta. ***Bone Miner*** 1992; 19(1): 63-74.

62. Celeste AJ, Iannazzi JA, Taylor RC, Hewick RM, Rosen V, Wang EA, et al. Identification of transforming growth factor beta family members present in bone-inductive protein purified from bovine bone. ***Proc Natl Acad Sci U S A*** 1990; 87(24): 9843-7.

63. Sporn MB, Roberts AB. Transforming growth factor-beta: recent progress and new challenges. ***J Cell Biol*** 1992; 119(5): 1017-21.

64. Okuda K, Nakajima Y, Irie K, Sugimoto M, Kabasawa Y, Yoshie H, et al. Transforming growth factor-beta 1 coated beta-tricalcium phosphate pellets stimulate healing of experimental bone defects of rat calvariae. ***Oral Dis*** 1995; 1(2): 92-7.

65. Okuda K, Murata M, Sugimoto M, Saito Y, Kabasawa Y, Yoshie H, et al. TGF-beta1 influences early gingival wound healing in rats: an immunohistochemical evaluation of stromal remodelling by extracellular matrix molecules and PCNA. ***J Oral Pathol Med*** 1998; 27(10): 463-9.

66. Hallman M, Lundgren S, Sennerby L. Histologic analysis of clinical biopsies taken 6 months and 3 years after maxillary sinus floor augmentation with 80% bovine hydroxyapatite and 20% autogenous bone mixed with fibrin glue. ***Clin Implant Dent Relat Res*** 2001; 3(2): 87-96.

67. Haas R, Donath K, Fodinger M, Watzek G. Bovine hydroxyapatite for maxillary sinus grafting: comparative histomorphometric findings in sheep. ***Clin Oral Implants Res*** 1998; 9(2): 107-16.

68. Maiorana C, Redemagni M, Rabagliati M, Salina S. Treatment of maxillary ridge resorption by sinus augmentation with iliac cancellous bone, anorganic bovine bone, and endosseous implants: a clinical and histologic report. ***Int J Oral Maxillofac Implants*** 2000; 15(6): 873-8.

69. Schwartz Z, Weesner T, van Dijk S, Cochran DL, Mellonig JT, Lohmann CH, et al.

ability of deproteinized cancellous bovine bone to induce new bone formation. ***J Periodontol*** 2000; 71(8): 1258-69.

70. Tadjoedin ES, de Lange GL, Bronckers AL, Lyaruu DM, Burger EH. Deproteinized cancellous bovine bone (Bio-Oss) as bone substitute for sinus floor elevation. A retrospective, histomorphometrical study of five cases. ***J Clin Periodontol*** 2003; 30(3): 261-70.

71. Spector M. Anorganic bovine bone and ceramic analogs of bone mineral as implants to facilitate bone regeneration. ***Clin Plast Surg*** 1994; 21(3): 437-44.

72. Kasabah S, Simunek A, Krug J, Lecaro MC. Maxillary sinus augmentation with deproteinized bovine bone (Bio-Oss) and Impladent dental implant system. Part II. Evaluation of deprotienized bovine bone (Bio-Oss) and implant surface. ***Acta Medica*** (Hradec Kralove) 2002; 45(4): 167-71.

73. Hurzeler MB, Quinones CR, Kirsch A, Gloker C, Schupbach P, Strub JR, et al. Maxillary sinus augmentation using different grafting materials and dental implants in monkeys. Part I. Evaluation of anorganic bovine-derived bone matrix. ***Clin Oral Implants Res*** 1997; 8(6): 476-86.

74. Murugan R, Panduranga Rao K, Sampath Kumar TS. Heat-deproteinated xenogeneic bone from slaughterhouse waste: Physico-chemical properties. ***Bull Mater Sci*** 2003; 26: 523.

75. Lin FH, Liao CJ, Chen KS, Sun JS. Preparation of a biphasic porous bioceramic by heating bovine cancellous bone with $Na_4P_2O_7.10H_2O$ addition. ***Biomaterials*** 1999; 20(5): 475-84.

76. Landi E, Tampieri A, Celotti G, Vichi L, Sandri M. Influence of synthesis and sintering parameters on the characteristics of carbonate apatite. ***Biomaterials*** 2004; 25(10): 1763-70.

77. Locardi B, Pazzaglia UE, Gabbi C, Profilo B. Thermal behaviour of hydroxyapatite intended for medical applications. ***Biomaterials*** 1993; 14(6): 437-41.

78. Pripatnanont P, Nuntanaranont T, Vongvatcharanon S, Limlertmongkol S. Osteoconductive effects of 3 heat-treated hydroxyapatites in rabbit calvarial defects. ***J Oral Maxillofac Surg*** 2007; 65(12): 2418-24.

79. Wang C, Duan Y, Markovic B, Barbara J, Rolfe Howlett C, Zhang X, et al. Proliferation and bone-related gene expression of osteoblasts grown on hydroxyapatite ceramics sintered at different temperature. ***Biomaterials*** 2004; 25(15): 2949-56.

80. Kose GT, Kenar H, Hasirci N, Hasirci V. Macroporous poly(3-hydroxybutyrate-co-3-hydroxyvalerate) matrices for bone tissue engineering. ***Biomaterials*** 2003; 24(11): 1949-58.

81. Boyan BD, Hummert TW, Dean DD, Schwartz Z. Role of material surfaces in regulating bone and cartilage cell response. ***Biomaterials*** 1996; 17(2): 137-46.

82. Flecknell PA. Anesthesia of common laboratory species : rabbits. ***Laboratory animal anesthesia***. 1996; 2nd edition , London ; Academic press limited: 182-90.

83. Morse A. Formic acid-sodium citrate decalcification and butyl alcohol dehydration of teeth and bones for sectioning in paraffin. ***J Dent Res*** 1945; 24(3): 143-53.

84. Butterfield KJ, Bennett J, Gronowicz G, Adams D. Effect of platelet-rich plasma with autogenous bone graft for maxillary sinus augmentation in a rabbit model. ***J Oral Maxillofac Surg*** 2005; 63(3): 370-6.

85. Dechichi P, Moura CC, Santana SI, Zanetta-Barbosa D. Histomorphometric analysis of rabbit calvarial bone: storage in saline solution versus storage in platelet-poor plasma. ***Int J Oral Maxillofac Implants*** 2007; 22(6): 905-10.

86. Roberts WE, Turley PK, Brezniak N, Fielder PJ. Implants: Bone physiology and metabolism. ***Cda J*** 1987; 15(10): 54-61.

87. Frame JW. A convenient animal model for testing bone substitute materials. ***J Oral Surg*** 1980; 38(3): 176-80.

88. Bays RA. Current concepts in bone grafting. ***Current Advances in Oral and Maxillofacial Surgery*** 1983; 4: 109.

89. Kleinschmidt JC, Marden LJ, Kent D, Quigley N, Hollinger JO. A multiphase system bone implant for regenerating the calvaria. ***Plast Reconstr Surg*** 1993;91(4):581-8.

90. Schmitz JP, Hollinger JO. The critical size defect as an experimental model for craniomandibulofacial nonunions. ***Clin Orthop Relat Res*** 1986(205): 299-308.

91. Roberts WE, Smith RK, Zilberman Y, Mozsary PG, Smith RS. Osseous adaptation to continuous loading of rigid endosseous implants. ***Am J Orthod*** 1984; 86(2): 95-111.

92. Watanabe K, Niimi A, Ueda M. Autogenous bone grafts in the rabbit maxillary sinus. ***Oral Surg Oral Med Oral Pathol Oral Radiol Endod*** 1999; 88(1): 26-32.

93. Albrektsson T. Repair of bone grafts. A vital microscopic and histological investigation in the rabbit. ***Scand J Plast Reconstr Surg*** 1980; 14(1): 1-12.

94. Albrektsson T, Linder L. Intravital, long-term follow-up of autologous experimental bone grafts. ***Arch Orthop Trauma Surg*** 1981; 98(3): 189-93.

95. Bogoch E, Gschwend N, Rahn B, Moran E, Perren S. Healing of cancellous bone osteotomy in rabbits--Part I: Regulation of bone volume and the regional acceleratory phenomenon in normal bone. ***J Orthop Res*** 1993; 11(2): 285-91.

96. Pryor ME, Susin C, Wikesjo UM. Validity of radiographic evaluations of bone formation in a rat calvaria osteotomy defect model. ***J Clin Periodontol*** 2006; 33(6): 455-60.

97. Berger S, Aledort LM, Gilbert HS, Hanson JP, Wasserman LR. Abnormalities of platelet function in patients with polycythemia vera. ***Cancer Res*** 1973; 33(11): 2683-7.

98. Thuente DD, Neely DE. Spontaneous medial rectus hemorrhage in a patient with acute myelogenous leukemia. ***J AAPOS*** 2002; 6(4): 257-58.

99. Ludwig D, Borsa JJ, Maier RV. Transjugular intrahepatic portosystemic shunt for trauma? ***J Trauma*** 2000; 48(5): 954-6.

100. Faraday N. Pro: Should Aspirin Be Continued After Cardiac Surgery in the Setting of Thrombocytopenia? ***J Cardiothorac Vasc Anesth*** 2006; 20(1): 112-13.

101. Schaub S, Dickenmann M, Cynke E, Bircher A, Steiger J. Prednisone-induced neutropenia after cadaveric kidney transplantation. ***Nephrol Dial Transplant*** 2002;17(6):1119-21.

102. Whang K, Healy KE, Elenz DR, Nam EK, Tsai DC, Thomas CH, et al. Engineering bone regeneration with bioabsorbable scaffolds with novel microarchitecture. ***Tissue Eng*** 1999; 5(1): 35-51.

103. Calvert JW, Marra KG, Cook L, Kumta PN, DiMilla PA, Weiss LE. Characterization of osteoblast-like behavior of cultured bone marrow stromal cells on various polymer surfaces. ***J Biomed Mater Res*** 2000; 52(2): 279-84.

104. Hutmacher DW. Scaffold design and fabrication technologies for engineering tissues--state of the art and future perspectives. ***J Biomater Sci Polym Ed*** 2001; 12(1): 107-24.

105. Rotllan E, Escolar G, Ordinas A, Bastida E. [Effect of PAF (platelet-activating factor) on hemostasis. Studies on endothelial cells and platelets]. ***Sangre (Barc)*** 1993; 38(2): 115-9.

106. Banks RE, Forbes MA, Kinsey SE, Stanley A, Ingham E, Walters C, et al. Release of the angiogenic cytokine vascular endothelial growth factor (VEGF) from platelets: significance for VEGF measurements and cancer biology. ***Br J Cancer*** 1998; 77(6): 956-64.

107. Maloney JP, Silliman CC, Ambruso DR, Wang J, Tuder RM, Voelkel NF. In vitro release of vascular endothelial growth factor during platelet aggregation. ***Am J Physiol*** 1998; 275(3 Pt 2): H1054-61.

108. Bonewald LF, Mundy GR. Role of transforming growth factor-beta in bone remodeling. ***Clin Orthop Relat Res*** 1990(250): 261-76.

109. Steenfos HH. Growth factors and wound healing. ***Scand J Plast Reconstr Surg Hand Surg*** 1994; 28(2): 95-105.

110. Yang YI, Seol DL, Kim HI, Cho MH, Lee SJ. Composite fibrin and collagen scaffold to enhance tissue regeneration and angiogenesis. ***Current Applied Physics*** 2007; 7(Supplement 1): e103-e07.

111. Clark RA. Fibrin and wound healing. ***Ann N Y Acad Sci*** 2001; 936: 355-67.

112. Knighton DR, Hunt TK, Thakral KK, Goodson WH, 3rd. Role of platelets and fibrin in the healing sequence: an in vivo study of angiogenesis and collagen synthesis. ***Ann Surg*** 1982; 196(4): 379-88.

113. Schmoekel H, Schense JC, Weber FE, Gratz KW, Gnagi D, Muller R, et al. Bone healing in the rat and dog with nonglycosylated BMP-2 demonstrating low solubility in fibrin matrices. ***J Orthop Res*** 2004; 22(2): 376-81.

114. Mosesson MW, Siebenlist KR, Meh DA. The structure and biological features of fibrinogen and fibrin. ***Ann N Y Acad Sci*** 2001; 936: 11-30.

115. Marx RE. Platelet-rich plasma: a source of multiple autologous growth factors for bone grafts. ***Tissue engineering***. Quintessence Publ Group 1999: 71–82.

116. Dohan DM, Choukroun J. PRP, cPRP, PRF, PRG, PRGF, FC ... How to find your way

in the jungle of platelet concentrates? ***Oral Surg Oral Med Oral Pathol Oral Radiol Endod*** 2007; 103(3): 305-06.

117. Pryor ME, Yang J, Polimeni G, Koo KT, Hartman MJ, Gross H, et al. Analysis of rat calvaria defects implanted with a platelet-rich plasma preparation: radiographic observations. ***J Periodontol*** 2005; 76(8): 1287-92.

118. Weibrich G, Kleis WK, Buch R, Hitzler WE, Hafner G. The Harvest Smart PRePTM system versus the Friadent-Schutze platelet-rich plasma kit. ***Clin Oral Implants Res*** 2003; 14(2): 233-9.

119. You TM, Choi BH, Li J, Jung JH, Lee HJ, Lee SH, et al. The effect of platelet-rich plasma on bone healing around implants placed in bone defects treated with Bio-Oss: A pilot study in the dog tibia. ***Oral Surg Oral Med Oral Pathol Oral Radiol Endod*** 2007.

120. Phurisat K, Pripatnanont P. Clinical application of platelet-rich fibrin (PRF) for sinus lift bone grafting: Preliminary case reports. ***1st International Bone and Dental Technology Symposium***; 2007. Nov 12-13; Thailand.

121. Dohan DM, Del Corso M, Charrier J-B. Cytotoxicity analyses of Choukroun's platelet-rich fibrin (PRF) on a wide range of human cells: The answer to a commercial controversy. ***Oral Surg Oral Med Oral Pathol Oral Radiol Endod*** 2007; 103(5): 587-93.

122. Lawson JH. The clinical use and immunologic impact of thrombin in surgery. ***Semin Thromb Hemost*** 2006; 32 Suppl 1: 98-110.

123. Ortel TL, Mercer MC, Thames EH, Moore KD, Lawson JH. Immunologic impact and clinical outcomes after surgical exposure to bovine thrombin. ***Ann Surg*** 2001; 233(1): 88-96.

124. Su Z, Izumi T, Thames EH, Lawson JH, Ortel TL. Antiphospholipid antibodies after surgical exposure to topical bovine thrombin. ***J Lab Clin Med*** 2002; 139(6): 349-56.

125. Pallesen L, Schou S, Aaboe M, Hjorting-Hansen E, Nattestad A, Melsen F. Influence of particle size of autogenous bone grafts on the early stages of bone regeneration: a histologic and stereologic study in rabbit calvarium. ***Int J Oral Maxillofac Implants*** 2002; 17(4): 498-506.

Appendix

Materials

1. Biological Material

1.1 Male New Zealand White rabbits

2. Tested Material

2.1 Deproteinized bovine bone derived (DBB) from heat treatment at 1200 °C, Metal and Material Technology Center, Thailand

3. Equipments and Instruments

3.1 Autoclave Hiclave™, Model HB-50, Hirayama Manufacturing Corp., Japan

3.2 Automated tissue staining, Shandon Linistain™ GLX Linear Stainer, Thermo Shandon Inc, USA

3.3 Automatic film processor, Dent X 9000, Dent X/Logetronics GmbH, Germany

3.4 Automatic tissue processor, Model 2500A, Lipshaw, USA

3.5 Bio-Rad's Densitometer, Model GS-700, BIO-RAD Laboratories Ltd, UK

3.6 Bone morselizer,

3.7 Dental radiographic machine, Gendex, Gendex Co., USA

3.8 Digital Camera, Panasonic Lumix Model DMC-FX3, Japan

3.9 Microtome, Leica Model RM2135, Leica Microsystems, Germany

3.10 Orbital shaker, Model KS 130 Basic, IKA Works, USA

3.11 Refrigerated Centrifuge, Labofuge Model 400 R, Heraeus, Germany

3.12 Scanning electron microscope, Model JSM-5800LV, JEOL LTD, Japan

3.13 Sputter Coater, SPI-ModuleTM, Model 11425, SPI supplies, USA

3.14 Weighing Measurement, Model BJ 12100G, Precisa Instruments AG, Switzerland

4. Disposable materials

4.1 Disposable extension tube, 18 inch approx 3.0 ml, Bever Medical Industries Co.,Ltd, Thailand

4.2 Disposable hypodermic needle, 18G X 1", Nipro Medical Corporation, Japan

4.3 Disposable hypodermic needle, 20G X 1", Nipro Medical Corporation, Japan

4.4 Disposable hypodermic needle, 21G X 1", Nipro Medical Corporation, Japan

4.5 Disposable hypodermic needle, 25G X 1", Nipro Medical Corporation, Japan

4.6 Disposable syringe 3 ml, Terumo® Syringe, Laguna, Philippines\

4.7 Disposable syringe 5 ml, Terumo® Syringe, Laguna, Philippines

4.8 Disposable syringe 10 ml, Terumo® Syringe, Laguna, Philippines

4.9 Pediatric solution infusion set, 60 drops per ml. per minute, Kawasumi Laboratories Co.,Ltd, Thailand

5. Chemical and reagents

5.1 Alcohol 70%, Cat No.IA807/39, Coholsahakarn, Thailand

5.2 Dextrose 5% in ¼ Sterile saline , General Hospital Products Public Co.,Ltd, Thailand

5.3 Diazepam 10 mg/2ml, The GOVT. PHARM. ORG., Thailand

5.4 Ketamine 50 mg/ml, Calypsol®, Gideon Richter Co.,Ltd, Hungary

5.5 Lidocaine HCL 2% with epinephrine 1:100,000 1.8 ml

5.6 Penicillin G Sodium 5,000,000 units/vial, General Drugs House Co.,Ltd, Thailand

5.7 Saline Irrigation (Sodium Chloride 900 mg.), General Hospital Products Public Co.,Ltd, Thailand

5.8 Sterile water 100 ml, General Hospital Products Public Co.,Ltd, Thailand

5.9 Thiopental sodium 1.0 g, Pentothal sodium®, Abbott Laboratories, Canada

6. Softwares

6.1 Image Pro Plus 5.0 (Media Cybernetics Inc., USA)

6.2 SPSS for windows, Version 14.0, Standard Software Package Inc., USA

Vitae

Name Miss Kingkaew Phurisat

Student ID 4910820001

Educational Attainment

Degree	Name of Institution	Year of Graduation
Doctor of Dental Surgery	Khon Kaen University	2003
Graduated diploma in Clinical Science (Oral and Maxillofacial Surgery)	Prince of Songkla University	2006

List of Publication and Proceeding

Poster Presentation

Phurisat K, Pripatnanont P. "Clinical application of platelet-rich fibrin (PRF) for sinus lift bone grafting: Preliminary case reports." in The 1st International Bone and Dental Technology Symposium, 2007, November 12th -13th, Bangkok, Thailand.